E.I.R. Bericht Nr. 28

Eidgenössisches Institut für Reaktorforschung,
Würenlingen, Schweiz

SUBCRITICAL REACTOR KINETICS AND REACTIVITY MEASUREMENTS *)

by

Tsahi GOZANI **)

Würenlingen, September 1962

*) This work was submitted in partial fulfillment of the requirements for the degree of D.Sc. in Physics at the E.T.H. in Zurich.

**) On leave from the Israel A.E.C.

DISCLAIMER

EIR-Bericht Nr. 28

EIR-Bericht Nr. 28

Eidg. Institut für Reaktorforschung Würenlingen
Schweiz

Subcritical Reactor Kinetics and Reactivity Measurements

by

Tsahi GOZANI

Würenlingen, September 1962

Preliminary Errata

Page	Location	Should be
Tables of Contents	4th line from below	AMPLITUDE
38	Numerator of Eq. 55	$\nu_q' - \nu_q$
61	12th line from above	degeneracy
66	denominator of Eq. 70a	$\nu_1 \Sigma_{f1} v_1(h_1^+, h_1) + \nu_2 \Sigma_{f2} v_2(h_1^+, h_2)$
71d	Fig.5	current (1) should have the value -0.11 at the interface
71d	Fig.5	current (2) should have the value -0.15 at the interface
71g	Fig.8	current (3) should have the value -9.08 at the interface
71g	Fig.8	current (4) should have the value -10.1 at the interface
82a	Fig.3 (b)	arrows should be reversed

TABLE OF CONTENTS

Abstract: Three kinetic methods measuring reactivity in the subcritical state by means of source-jerk, rod-drop and pulsed source, respectively, are the subject of discussion in this work. The main problems encountered in the use of these methods, e.g. local detection, harmonics effects, etc., are discussed from both the theoretical and experimental points of view.

The special role played by the three reactivities defined respectively as kinetic, static and dynamic is demonstrated using general transport theory. After reducing this to the multigroup model, additional important properties of delayed and prompt neutron distributions are shown. Using two group time dependent theory, numerical examples are given to show the importance of these properties in heavy water reactors.

With the help of the theoretical results, modification of the source-jerk and rod-drop techniques, aimed at lessening perturbing effects, are discussed.

These modified experimental methods have been successfully checked in the swimming-pool reactor SAPHIR and the heavy-water reactor DIORIT in Würenlingen. Some of the experiments are reported here.

KINETIK UNTERKRITISCHER REAKTOREN UND REAKTIVITAETSMESSUNGEN

Zusammenfassung: In der vorliegenden Arbeit werden drei kinetische Messmethoden zur Bestimmung der Reaktivität unterkritischer Systeme behandelt, nämlich die Quellsprungmethode, die Stabfallmethode und die Methode der gepulsten Quelle.

Die grundlegenden experimentellen und theoretischen Merkmale dieser Methoden werden besprochen, besonders diejenigen der Quellsprung- und Stabfallmethoden. Einflüsse von Harmonischen, die eine scheinbare Ortsabhängigkeit der Reaktivität zur Folge haben, werden an Hand von Beispielen aus der Ein- oder Zweigruppentheorie des unreflektierten oder reflektierten Systems erläutert. Diese Berechnungen, sowie umfangreiche experimentelle Ergebnisse aus der Literatur, lassen die Bedeutung der Harmonischen-Effekte deutlich werden.

Als nächstes wird gezeigt, dass die in kinetischen Experimenten tatsächlich gemessene Grösse, nämlich der Eigenwert der Grundwelle, in eindeutiger Weise jeder beliebigen Definition der Reaktivität zugeordnet werden kann. Diese Willkür im Begriff der Reaktivität hat ihren Grund in dem willkürlichen Gewichten der Neutronendichte. Von den vielen möglichen Gewichtsfunktionen verdienen drei besondere Beachtung, nämlich die kinetische, die statische und die dynamische Gewichtsfunktion. Es wird auf den bedeutenden Platz hingewiesen, welchen die statische Reaktivität auf Grund ihrer speziellen Eigenschaften einnimmt. Anschliessend wird die Theorie mathematisch entwickelt und vornehmlich auf das Mehrgruppenmodell angewendet. An Hand dieses Modells wird gezeigt, dass die verzögerten Neutronen ein für sie charakteristisches, eng verteiltes Eigenwertspektrum und dementsprechend ähnliche Eigenfunktionen (Oberwellen) aufweisen. Die Aehnlichkeit dieser verzögerten Eigenfunktionen mit der Grundwelle des fiktiv kritischen Reaktors wird durch verschiedene Reaktortypen demonstriert. Besondere Beachtung wird der möglichen Abweichung der prompten Neutronen-Oberwelle von der Grundwelle geschenkt, da diese meist übersehen wird. Auch wird gezeigt, dass die Generationszeit von Neutronen, deren Verteilung der prompten Oberwelle entspricht, stark vom Reaktortyp abhängt. Diese Grösse ist von grundlegender Bedeutung für Experimente mit gepulsten Neutronen, und es zeigt sich, dass ein nicht vernachlässigbarer Unterschied zwischen ihr und der Generationszeit der asymptotischen Grundwelle besteht, besonders in Schwerwasser-Reaktoren.

Auf Grund der Annahme, dass die Verteilung der verzögerten Neutronen derjenigen der asymptotischen Grundwelle entspricht, werden experimentelle Modifikationen der Quellsprung- und Stabfallmethoden vorgeschlagen. Es wird gezeigt, dass es auf diese Weise möglich ist, die systematischen Fehler, die von den Harmonischen der anfänglichen Neutronenverteilung herrühren, zu vermindern, indem man die Messresultate entweder von der Anfangsverteilung unabhängig macht ("shape method"), oder sie experimentell für Beimischungen von Harmonischen korrigiert ("amplitude method"). Vorteile und Nachteile dieser Methoden werden besprochen, unter besonderer Betonung der Anwendung auf Schwerwasser-Reaktoren. Die Theorie wird auf Experimente im schweizerischen Swimming Pool Reaktor SAPHIR und im Schwerwasser-Reaktor DIORIT angewendet.

CINETIQUE DES REACTEURS SOUS-CRITIQUES ET MESURES DE LA REACTIVITE

Sommaire: La discussion des trois méthodes cinétiques sous-critiques, utilisant respectivement le saut de source, la chute de barre et la source pulsée, fait l'objet du présent travail. On examine les aspects essentiels, tant théoriques qu'expérimentaux, des diverses méthodes, en particulier des techniques de saut de source et de chute de barre.

L'effet des harmoniques, qui cause une dépendance spatiale apparente de la réactivité, est soumis à une discussion; on l'illustre au moyen de modèles à un et deux groupes pour des systèmes nus et réfléchis. Ces calculs, ainsi que de très nombreux résultats expérimentaux donnés tant dans la littérature que dans le présent travail, mettent en évidence l'importance de l'effet des harmoniques.

On montre ensuite que la quantité effectivement obtenue lors de mesures cinétiques, à savoir la valeur propre cinétique de la distribution persistante, peut être rapportée de façon cohérente à n'importe quelle définition de la réactivité. Cet arbitraire du concept de réactivité est dû à une pondération arbitraire de la population de neutrons. On montre que parmi les nombreuses fonctions de pondération possibles, trois méritent une attention particulière: la fonction cinétique, la fonction statique et la fonction dynamique de pondération. Le rôle important joué par la réactivité statique, sa signification et ses propriétés spéciales font l'objet d'une discussion. On développe ensuite la théorie mathématiquement en l'appliquant principalement au modèle à groupes multiples. Ce modèle souple permet de démontrer que l'une des caractéristiques des neutrons retardés réside dans le spectre serré de leurs valeurs propres et des fonctions propres correspondantes ('sous-modes'). On montre la proche ressemblance des sous-modes des neutrons retardés avec le mode principal critique virtuel pour diverses configurations de réacteurs; on met l'accent sur la déviation possible du sous-mode des neutrons prompts par rapport au mode principal, qui est habituellement négligée. On examine la façon dont le temps de génération des neutrons distribués selon le sous-mode principal dépend de la configuration du réacteur, cette relation jouant un rôle essentiel dans les expériences de neutrons pulsés. On montre qu'il existe une différence non-négligeable entre ce temps de génération et celui du mode persistant, spécialement dans les réacteurs à eau lourde.

En utilisant la distribution des neutrons retardés pour représenter le mode persistant, on propose des modifications des techniques expérimentales du saut de source et de la chute de barre. On montre que ces modifications, qui sont indépendantes du flux initial (méthode de forme, "shape-method"), ou qui apportent une correction expérimentale à ce dernier (méthode de l'amplitude), reduisent effectivement l'erreur systématique due aux harmoniques. On discute les avantages et les limitations des deux méthodes du point de vue théorique, en accordant une considération particulière aux réacteurs à eau lourde; les deux méthodes ont été éprouvées lors d'expériences menées dans la pile piscine SAPHIR et le réacteur à eau lourde DIORIT à Würenlingen.

Chapter I

INTRODUCTION AND SUMMARY

The reactivity, ρ, is generally defined as the ratio of net production rate throughout the reactor to the total production rate. It serves as a measure of the deviation of the reactor from the critical state, in which the net production rate is just zero. The reactor is subcritical, critical or supercritical, according as $\rho<0$, $\rho=0$ or $\rho>0$ respectively.

Although the definition of reactivity is not unique, its determination is nevertheless a rather important task, because it characterizes, regardless of definition, the overall balance of the reaction rate in the system, and therefore represents a global constant of the reactor.

Knowledge of this global parameter may be used, through known relationships, to determine other parameters either of the reactor itself, or of an external sample (refs. 1, 6) . Most of these determinations are carried out near the critical state ($|\rho|<<1$ $), and no principal difficulty exists in performing the experiment and interpreting it. These methods cannot be extended to measurements of excess reactivity and worth of control rods, because those usually amount to several dollars, and period measurements can, for safety reasons, cover only a small part of the required range. Other methods, such as the compensation method, require knowledge of the interference effects of different perturbations, which is a rather difficult task to perform.

On the other hand, ability to determine large amounts of reactivity ($|\rho|>>1$) is vital to a reactor for reasons of routine operation, safety , and theoretical understanding.

The kinetic sub-critical techniques, like the Source-Jerk (S.J.) technique, the Rod-Drop (R.D.) technique and the Pulsed-Source (P.S.) technique can handle such problems, although they pose some experimental and theoretical difficulties.

These methods are based essentially on the transient response of the neutron density to a step change (R.D. and S.J.), or a delta change (P.S.) in time. In the R.D. method the negative reactivity to be measured (e.g. control rod worth) is inserted rapidly into a critical reactor. The amount of reactivity is then deduced from the ratio of initial to transient response of a suitable detector. In the S.J. method, a subcritical reactor is held at constant power by means of an extraneous source. The source is removed rapidly, and the reactivity of the subcritical state can be found from the ra-

tio of initial to transient response of a detector. In the P.S. method an extraneous delta source is applied to the subcritical reactor, whose negative reactivity is to be measured. Again, the transient response of a suitable detector is used for the reactivity measurement.

In addition to the very important fact of providing a means for measuring large negative reactivities, the above mentioned methods offer the following advantages:

a) The measurements are relatively rapid (particularly by means of P.S. and S.J. techniques).
b) They can be repeated in relatively short times, since they leave no long range traces behind (e.g. via the creation of photoneutrons).
c) The results are in principle more easily reproducible than those by other kinetic methods, since the measurements are carried out in a stable reactor.
d) Large amounts of reactivity can be measured without any danger, since the reactor is always subcritical.

The main drawbacks are:

a) A very abrupt change in count rate (due to the step or delta changes) may cause high counting losses in the initial part of the transients, and low statistical precision at later times.
b) The presence of harmonics due to the initial distribution introduces a fictitious space dependence into the measured reactivity.
c) Some difficulties are encountered in interpreting the experiments.

The three sub-critical kinetic methods, utilizing respectively the source-jerk, the rod-drop and the pulsed-source are the subject of discussion in the present work.

The essential experimental and theoretical features of the methods, in particular of the S.J. and R.D. methods, are discussed. The harmonics effect, which causes an apparent space dependence of the reactivity, is discussed and demonstrated by means of the one and two groups models for bare and reflected systems. This calculation, as well as plentiful experimental evidence contained both in the literature and in this work demonstrates the seriousness of the harmonics effect.

It is next shown that the quantity really measured in the kinetic measurements, namely the kinetic eigenvalue of the persisting dis-

tribution, can be related in a consistent manner to any desirable definition of reactivity. This arbitrariness in the concept of reactivity is caused by an arbitrary weighting of the neutron population. Among the many possible weight-functions three are shown to merit special attention: The kinetic function, the static function and the dynamic weight-function. The important rôle played by the static reactivity, its meaning and its special properties are discussed. The theory is then developed mathematically and applied mainly to the multigroup model. With this tractable model it is demonstrated that a characteristic feature of delayed neutrons is their closely spaced spectrum of eigenvalues and correspondingly similar eigenfunctions ('sub-modes'). The close resemblance of the delayed neutron sub-modes to the virtual critical main mode is shown for various reactor configurations. The possible deviation of the prompt neutron sub-mode from the main mode, which is usually overlooked is emphasized. The dependence on the reactor configuration of the generation time of neutrons distributed in the prompt sub-mode, which is an essential quantity for pulsed-neutron experiments is discussed. It is shown that a non-negligible difference exists between this generation time and that of the persisting mode, especially in heavy water reactors.

Using the delayed neutron-distribution as representative of the persisting mode, modifications of the experimental procedure of the S.J. and R.D. techniques are proposed. It is shown that these modifications, which are independent of the initial flux (the 'Shape-Method'), or correcting for it experimentally ('Amplitude-Method'), do indeed reduce the systematic error due to harmonics. The advantages and limitations of both methods are discussed, with special attention being paid to heavy water reactors, from the theoretical point of view, and are demonstrated by experiments conducted in the Swiss swimming-pool reactor SAPHIR and the heavy water reactor DIORIT.

Chapter II

REACTIVITY MEASUREMENT BY KINETIC METHODS

1. STATIC AND KINETIC METHODS FOR MEASUREMENT OF REACTIVITY

The methods by which reactivity is measured can be roughly divided into two categories: a) static methods
b) kinetic methods.

a) The static method is essentially a measurement in the stable state; either when the reactor is critical, for instance the compensation method (ref. 1 p.603, refs. 2-8) or in a subcritical stable state e.g. the subcritical multiplication method (refs. 8,9,10 (pp 11-16)).

The compensation method is based on maintaining criticality by counteracting any change in the reactivity by means of control rods or insertion of homogeneous poison. The first method, namely compensation by control rods, is very often used for relative calibration of control rods. The precision of this method depends either on the absence of interaction between the various components (i.e. shadowing effect cf. ref. 82) or on the degree to which these effects are known. Usually it is very difficult to calculate interaction effects, and for this reason the compensation of reactivity with local absorber is limited to the measurement of small amounts of reactivity. The compensation with an absorber distributed homogeneously throughout the reactor can be interpreted accurately. But it is very time consuming and not always feasible.

The subcritical multiplication method depends strongly on the knowledge of the harmonics content at the measuring point, which is introduced by the source that maintains the constant neutron flux in the subcritical reactor. Estimating the effect of harmonics in a real system is often very difficult.

b) Kinetic methods are based on a measurement of the time behaviour of a local neutron population, due to some change in the reactor.

These methods may be divided into three groups:

1) Measurement in the near critical state.
2) Measurement in the positive prompt critical region.
3) Measurement in far subcritical states.

The kinetic methods when applied to the near critical state (summarized in ref. 1), evidently measure only small amounts of reactivity. Their range in the supercritical domain is limited for obvious reasons of safety to $\rho \lesssim 0.3\ \$$. In the subcritical region a limitation is imposed by the very low sensitivity at negative reactivities greater than ~ 0.3 $ (see sec.3 and ref.11). These kinetic methods include the following techniques:

1. Stable reactor period (refs. 12, 13, 10, 14-16)
2. Pile oscillator (refs. 1, 17-19)
3. Rod-drop-bump method (square wave) (refs. 20, 21)
4. Trapezoid-wave (ref. 22, 21)
5. Electronic simulator (refs. 1, 23).

The positive prompt transient method is limited to a very few special reactors (refs. 24, 2, 25). Because of obvious safety reasons it cannot be used elsewhere.

Methods applicable to the far subcritical domain may, of course, be applied to near critical states. But their main advantage lies in their ability to yield measurements of large negative reactivities. In this group one includes the following methods:

1) The statistical method (refs. 26, 27)
2) Rod-Drop (or briefly R.D.) (refs. 20, 10, 28)
3) Source-Jerk (S.J.)(refs. 20, 19)
4) Pulsed-Source (P.S.) (refs. 30-32).

The initial state in all methods, except the R.D. method, is a subcritical state, the reactivity of which is to be measured. In an R.D. experiment the initial state is usually just critical. In all methods the final state is subcritical.

The statistical method, i.e. the Rossi-α method (ref. 26) is practical only when small amounts of negative reactivity are to be measured. The Rossi-α method gives accurate results in fast systems and can be extended to somewhat slower systems. Nevertheless this method is not considered practical for thermal reactors.

The three methods 2, 3 and 4 are used almost exclusively for the measurement of large negative reactivities (e.g. total worth of control rods, single or in banks, shut-down value etc.).

2. SPACE INDEPENDENT THEORY OF KINETIC MEASUREMENTS

Space independent kinetic theory is obtained if one assumes a detector distribution function $W(\vec{r},\vec{v})$. Then the average neutron population $\langle N(t)\rangle$ and precursor population $\langle C_i(t)\rangle$ where

$$\langle N(t)\rangle = \int W(\vec{r},\vec{v}) N(\vec{r},\vec{v},t)\, d\vec{r}d\vec{v}\,, \quad \langle C_i(t)\rangle = \int W(\vec{r},\vec{v}) C_i(\vec{r},\vec{v},t)\, d\vec{r}d\vec{v}\,, \tag{1}$$

satisfy rigorously the simple kinetic equations (for details see Chap.III,Sec.10):

$$\frac{d\langle N(t)\rangle}{dt} = \frac{\rho(t)-1}{\Lambda^*(t)}\langle N(t)\rangle + \sum_{i=1}^{\ell} \lambda_i \langle C_i(t)\rangle + \langle Q(t)\rangle \quad , \tag{2}$$

$$\frac{d\langle C_i(t)\rangle}{dt} = \frac{b_i(t)}{\Lambda^*(t)}\langle N(t)\rangle - \lambda_i \langle C_i(t)\rangle \qquad i = 1,2,\ldots,\ell\,. \tag{3}$$

with ℓ delayed neutron groups.

$\langle Q(t)\rangle$ - average external source term;

$\rho(t)$ - reactivity in dollar units defined as the ratio of average net production rate to the product of average production rate and $\beta(t)$;

$\Lambda^*(t) = \frac{\Lambda(t)}{\beta(t)}$ is the reduced generation time of neutrons;

$b_i(t) = \beta_i(t)/\beta(t)$, where $\beta_i(t)$ is the effective fractional yield of delayed neutrons, i.e. the average fractional precursor production;

$\beta = \sum_{i=1}^{\ell} \beta_i$.

For the sake of brevity, the symbol $\langle\ \rangle$, indicating average, will be dropped in the rest of this chapter.

The integral reactor parameters ρ, Λ^* and b_i are time dependent even if the destruction and production operators are time independent. This so-called internal time dependence disappears when the flux throughout the reactor is separable in space and time. This occurs when the flux in the whole reactor falls or rises with a unique time constant. Under these conditions the flux is said to have reached its persisting distribution (ref. 33, Chap. XII).

In the region of the persisting distribution, the three methods are formally described by the following conditions:
Rod-Drop (R.D.) experiment:

$$\rho(t) = \begin{cases} \rho_0 & t<0 \\ -\rho_1 & t\geq 0 \end{cases} \quad \text{also as a result:} \quad \Lambda^*(t) = \begin{cases} \Lambda_0^* & t<0 \\ \Lambda_1^* & t\geq 0 \end{cases} \quad b_i(t) = \begin{cases} b_{i0} & t<0 \\ b_{i1} & t\geq 0 \end{cases} \qquad (4)$$

Source jerk (S.J.) experiment:

$$\rho(t) = -\rho_1 = \text{const.} \qquad Q(t) = \begin{cases} Q(0) & t<0 \\ AQ(0) & t\geq 0 \end{cases} \qquad A<1 \qquad (5)$$

Pulsed-source (P.S.) experiments:

$$\rho(t) = -\rho_1 = \text{const.} \qquad Q(t) = \begin{cases} Q(0) & t<0 \\ Q(0)+P\delta(t) & t\geq 0 \end{cases} \qquad (6)$$

where P is the number of neutrons emitted per cm^3 by the source.

The response of kinetic equations 2 and 3 to the step and delta changes given by Eqs. 4,5 and 6 can be obtained either by means of a Laplace transformation or by direct substitution of Eqs. 4, 5 and 6 into the integral equation of reactor kinetics (refs. 34, 35). The results are expressed in terms of a Green's function $G_\rho(t)$ of the kinetic equations (with the help of the convolution symbol) as follows:

R.D.

$$\frac{N(t)}{N(0)} = \frac{\Lambda_1^*}{\Lambda_0^*}\left[1 + \rho_1(1-B)\int_0^t G_{\rho_1}(t)dt + G_{\rho_1}(t)(\Lambda_0^*-\Lambda_1^*) + \Delta W(t)*G_{\rho_1}(t)\right],$$

S.J.

$$\frac{N(t)}{N(0)} = 1 + \rho_1(1-A)\int_0^t G_{\rho_1}(t)dt, \tag{8}$$

P.S.

$$\frac{N(t)}{N(0)} = 1 + \Lambda_1^* \frac{P}{N(0)} G_{\rho_1}(t), \tag{9}$$

where:

$$N(0) = \begin{cases} -\dfrac{\Lambda_0^* Q(0)}{\rho_0} & \text{R.D.,} \\ -\dfrac{\Lambda_1^* Q(0)}{\rho_1} & \text{S.J. and P.S.,} \end{cases} \qquad \rho_0, \rho_1 < 0 \tag{10}$$

$$B = -\Lambda_0^* \frac{Q(0)}{N(0)}, \tag{11}$$

$$W(t) = \mathcal{L}^{-1}\left\{\sum_{i=1}^{\ell} \frac{b_i}{s+\lambda_i}\right\}, \quad (s \text{ is the Laplace transform variable}) \tag{12}$$

$$\Delta W(t) = \mathcal{L}^{-1}\left\{\sum_{i=1}^{\ell} \frac{b_{i0} - b_{i1}}{s+\lambda_i}\right\},$$

$$G\rho(t) = \mathcal{L}^{-1}\left\{\frac{1}{s[\Lambda^* + \bar{W}(s)] - \rho}\right\} = \sum_{\mu=0}^{\ell} A_\mu e^{\gamma_\mu t}. \tag{13}$$

$$A_\mu^{-1} = \Lambda^* + \sum_{i=1}^{\ell} \frac{b_i \lambda_i}{(\gamma_\mu+\lambda_i)^2}, \tag{14}$$

and γ_μ are the solutions of the inhour equation:

$$\rho = s\Lambda^* + s\bar{W}(s) = s\Lambda^* + \sum_{i=1}^{\ell} \frac{s\, b_i}{s+\lambda_i}. \tag{15}$$

The time-behaviour following rapid insertion of a control rod, Eq.7, or the fast removal of a source, Eq.8, are identical in the present model if A = 0, B = 0, and if Λ_0^* and $b_{\iota 0}$ are not affected by the reactivity change. The first condition can be fulfilled since an A, which differs from zero, can be regarded as a given background and may be subtracted. The second condition is fulfilled if the reactor is critical, for then the effect of any background source may be made negligibly small, and it consequently follows that B = 0. The third condition is also fulfilled to a fair degree of approximation. This is due to the fact that both Λ^* and β_ι are quantities which are based on production processes, while the change in ρ is usually achieved by changing the destruction rate. The effect of the reactivity insertion on $b_\iota = \beta_\iota/\beta$ is even smaller (see also IV, Sec.7).

Assuming the above mentioned conditions to be fulfilled and the background to be negligible (or automatically subtracted) in the P.S. case, one finds the following simplified relationships:

R.D. and S.J. $$\frac{N(t)}{N(0)} = 1 + \rho_1 \int_0^t G_{\rho 1}(t)dt, \qquad (16)$$

P.S. $$\frac{N(t)}{P} = \Lambda^* G_{\rho 1}(t). \qquad (17)$$

Of the $\iota + 1$ solutions of the inhour equation, the first describes the rapid response of the prompt neutrons, while the ι other solutions represent the behaviour of delayed neutrons, which is much slower. For negative reactivities all solutions are negative. This characteristic is common to Eqs.16 and 17. The main difference is the very small ratio of delayed to prompt neutrons in the response to P.S. when compared with the corresponding ratio in Eq.16.

These features are clearly shown by using the model of a single delayed neutron group:

$$N(t)/N(0) = -\frac{\rho}{1-\rho}\left\{\exp\left[-\frac{1-\rho}{\Lambda^*}t\right] - \frac{1}{\rho}\exp\left[\frac{\lambda\rho}{1-\rho}t\right]\right\} \quad \text{for R.D. and S.J.} \qquad (18)$$

$$N(t)/P = \exp\left[-\frac{1-\rho}{\Lambda^*}\,t\right] + \frac{\lambda\Lambda^*}{(1-\rho)^2}\exp\left[\frac{\lambda\rho}{1-\rho}\,t\right] \quad \text{for P.S..} \qquad (19)$$

In this model the ratio of prompt to delayed exponents is about 10^3 for a D_2O-reactor at -10 ¢. The same value is found for the ratio of relative delayed to prompt population in R.D. (and S.J.) to P.S.

Knowing N(0), the initial population, and measuring N(t), enables one to determine the reactivity in the R.D. and S.J. cases. In fact, it is not necessary to measure the decay curve in detail. It suffices to measure the population just after the jump when the delayed neutron population has not yet had enough time to change. Ideally one would like to measure the initial population of delayed neutrons, $N_d(0)$, (from eq.16):

$$\lim_{t\to 0}\frac{N_d(t)}{N(0)} = \lim_{s\to\infty}\left\{s\left[\frac{1}{s} + \frac{\rho}{s^2\left(0+\bar{W}(s)\right)-s\rho}\right]\right\} = \frac{1}{1-\rho}\,.$$

Therefore:

$$\frac{N(0) - N_d(0)}{N_d(0)} = -\rho. \qquad (20)$$

$N_d(0)$ could, in principle, be obtained by extrapolating the delayed population to time zero. The main advantage of this straightforward procedure is due to the fact that it does not involve any additional parameters. On the other hand, it does involve the use of a fast recorder (ref. 20) and the sometimes questionable extrapolation of the delayed neutron density to zero. In D_2O-reactors this extrapolation procedure may be entirely erroneous, since the prompt decay constant, γ_0, has a time constant of the order of the fastest delayed neutron group, γ_1. For example at -3 ¢ $\gamma_0 = -40$ and $\gamma_1 = -3{,}84$, and at -1 ¢ $\gamma_0 = -20$ and $\gamma_1 = -3{,}80$ sec^{-1}.

In order to overcome the difficulties, Schmid (ref. 29) proposed the convenient integral count method, which derives the reactivity from the relationship,

$$\frac{N(0)}{\int_0^\infty N(t)dt} = -\frac{\rho}{[\Lambda^* + \bar{W}(0)]} = -\frac{\rho}{[\Lambda^* + \sum_{i=1}^{6} b_i/\lambda_i]}\,. \qquad (21)$$

Other methods for deducing the reactivity from N(t)/N(0) can easily be found according to the experimental facility at hand (cf. ref. 36).

In a P.S. experiment one measures the population decay curve after injecting a neutron burst. Treating the delayed neutrons as background, the slope of this decay curve on a semilogarithmic scale for the population directly gives $\frac{1-\rho}{\Lambda^*}$ (cf. ref. 30).

The pulsed-source equipment is based on the nuclear reaction of charged particles (e.g. ionized D or T atoms and molecules). Pulsing the neutrons is achieved by either pulsing the ion source or periodical deflection of the ions away from the target. The delta function behaviour of the source is obtained by having a very narrow burst of, for instance, 1 to 5 μsec width, with very high intensity of neutrons, such as $10^6 - 10^{10}$ neutrons per burst (ref. 37).

Technically the rod-drop is achieved by dropping a single rod or a number of rods ("single or multiple scram"), which are accelerated by gravity, by air pressure, or by both. The source jerk can be achieved by various methods, cf. refs. 10, 20 or by rapid withdrawal of an antimony source from a beryllium envelope (ref. 38, 39). While the step in the source may be very fast, the rod-drop is never truly instantaneous. The drop may be said to be instantaneous, if the effective dropping time is short compared to the decay constant, (λ_2), of the fastest delayed neutron group.

The deviation from a true step function exhibited by $\rho(t)$ (ref. 40) or $Q(t)$ (e.g. if a pneumatic method is used, ref. 20) should be taken into account in solving the kinetic equations 2 and 3. The basic features will still be maintained, but the simple form of the solution is, of course, lost.

The non step-like behaviour can be treated exactly, when solving the equations on a digital computer (ref. 41). It may also be regarded as a source of error introduced into the ideal situation; the value of this error may be estimated approximately (ref. 42).

Another approach (ref. 43) is based on the fact that some time after the completion of the drop, which begins at time zero, the time-dependence of the population coincides with that of a step-function which occured at a later time t_1^* ($t_1^* > 0$). The time t_2 after which the population behavior is the same as the response to a shifted step-function, can be determined by experiment or by an exact solution of the problem. However, it is not very sensitive to details of $\rho(t)$, and therefore, once calculated for a certain case it can be used, or approximated rather easily, for other cases.

Knowing t_1, the moment the drop is finished, and t_2, one can determine t_1^* (see Fig. 1).

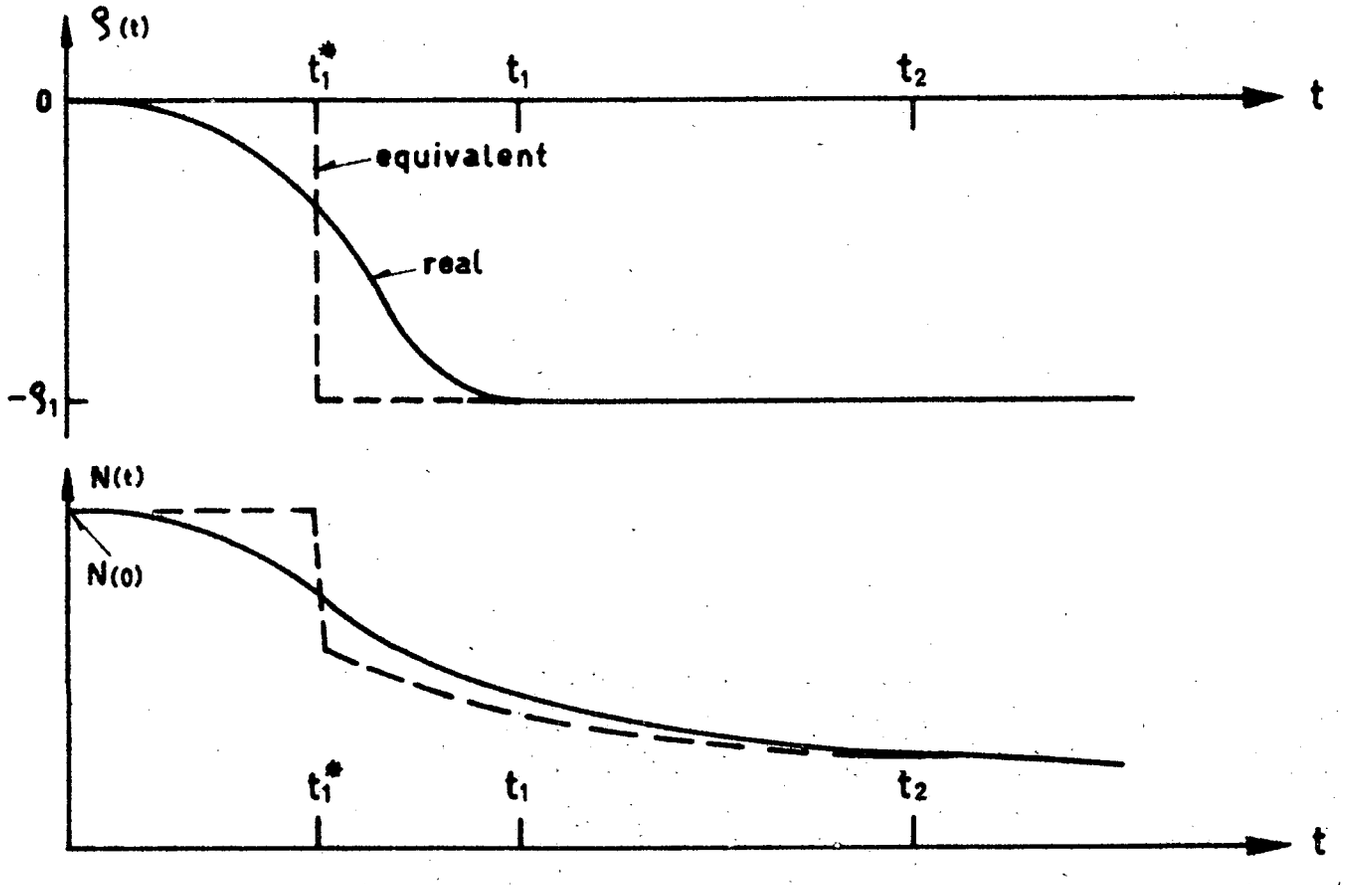

Fig. 1 Reactivity and power response to a non-instantaneous rod-drop.

To achieve this, one may use the Laplace transform of the kinetic equation (Eqs. 2,3) or their integral representation (ref. 35, p.30 with $\Lambda^* = 0$):

$$N(t) = \frac{1}{1-\rho(t)} \left[\int_0^t D(t-\tau) N(\tau) d\tau + N(0) W(t) \right] \qquad (22)$$

where:

$$D(t) = \sum_{i=1}^{\ell} b_i \lambda_i \, e^{-\lambda_i t} . \qquad (23)$$

Noting that $N(t_2) = N^*(t_2)$ (the asterisk denotes quantities related to the equivalent step-function) one gets:

$$\int_0^{t_2} D(t_2 - \tau) N(\tau) d\tau = \int_0^{t_2} D(t_2 - \tau) N^*(\tau) d\tau . \qquad (24)$$

Under the reasonable assumption that $t_2 << \Sigma b_i \lambda_i^{-1} = 13$ sec (for U^{235} fuel), one finds for $t \leqslant t_2$:

$$N(t) \cong \frac{N(0)}{1-\rho(t)} . \qquad (25)$$

After substitution of Eq. 25 into Eq. 24 one gets with some algebra, two equivalent transcendental equations for t_1^* in terms of ρ_1, t_1 and t_2:

$$W(t_2 - t_1^*) = \frac{1}{\rho_1} \left\{ 1 - (1-\rho_1) W(t_2) - \int_0^{t_2} D(t_2 - \tau) \frac{1-\rho_1}{1-\rho(\tau)} d\tau \right\} , \qquad (26)$$

$$W(t_2 - t_1^*) = \frac{1}{\rho_1} \left\{ W(t_2 - t_1) - (1-\rho_1) W(t_2) - \int_0^{t_1} D(t_2 - \tau) \frac{1-\rho_1}{1-\rho(\tau)} d\tau \right\} . \qquad (27)$$

3. LOCAL DETECTORS

The space independent kinetic equations (Eq. 2 and 3) were obtained by averaging the densities of neutrons and precursors over a detector distribution, $W(\vec{r},\vec{v})$. The reactivity thus defined is really global and represents the overall balance of the reaction rate in the reactor, provided such a global detector is at the experimenter's disposal.

Actually, however, the detectors are rather local and their energy response is nearly a Dirac delta function.

Following the procedure described in Sec. 2, such a detector distribution will furnish one with a reactivity which might depend strongly on the properties of the detector and in particular on its location. Such a situation obscures the main purpose of introducing the concept of reactivity, namely a global representation of the reactor.

To overcome this difficulty one can use the local measurement of the detector to determine some time characteristic of the reactor as a whole, e.g. the stable period, which is of course, independent of position. But now, instead of defining the reactivity with the aid of the actual detector distribution, and getting a local quantity, one can relate the stable period to some convenient hypothetical detector distribution (see Chap.III).

In this chapter the treatment will be limited to the most common reactivity concept, the static reactivity. The hypothetical detector distribution needed to achieve it is the adjoint static density function. By weighting with this function one obtains the static reactivity, the static (weighted) generation time and the static (weighted) effective delayed neutron fraction. These three global parameters are related to the kinetic eigenvalue, e.g. the stable period, through the inhour equation:

$$\rho_s = \Lambda_s^* w + \sum_{i=1}^{\ell} \frac{w b_{is}}{w + \lambda_i} , \qquad i = 1,\ldots,\ell. \qquad (28)$$

Thus in the present approach the local detector is used to deduce the global eigenvalue w, which is unique only after all memory effects due to initial conditions have died out. The ability to establish a unique time behavior throughout the reactor is an essential property of the chain reaction. Nevertheless, waiting until this behavior is achieved and then measuring the stable period is not practical in subcritical states; since one looses all sensitivity to reactivity. This is demonstrated in Table 1 below, where the persisting eigenvalue $w_{0,8}$, is tabulated as a function of the static reactivity ρ_s, ($\lambda_8 = 1.244 \cdot 10^{-2} sec^{-1}$).

TABLE 1

$-\rho_s$ ¢	12	10	8	6	4
$10^{-2} w_{o,s}$ sec^{-1}	1,2409	1,2403	1,2394	1,2377	1,2345

$-\rho_s$ ¢	2	1	0,8	0,6	0,4	0,2
$10^{-2} w_{o,s}$ sec^{-1}	1,2243	1,2009	1,1878	1,1637	1,1078	0,9145

In any case, none of the kinetic methods of subcritical reactivity measurements comply with the demand of measuring in the domain of the persisting density. Instead the R.D. and S.J. methods are based on a comparison of initial flux to some other flux after insertion of the control rod, or after removal of the source. The P.S. on the other hand, though not refering to any initial flux, depends upon the prompt mode, which is not necessarily equal to the persisting one.

The discussion of the last point is postponed until later (Chaps.III and IV), while the influence of harmonics on the R.D. and S.J. methods will be discussed more thoroughly in the next section and in Chap.V.

4. HARMONICS EFFECTS

In order to treat with sufficient rigor the time behavior of a reactor with either a removable external source or with a sink that may be inserted, at least two energy groups will be needed. This is due to the fact that the source emits fast neutrons, while the sink (e.g. control rod) absorbs thermal ones. Application of this model to a realistic configuration is highly impractical. On the other hand the one-energy group model surely overestimates the actual effect of the sink or source. For this reason one is on the 'safe' side when using a one group model for such a study. On the other hand, sufficient simplicity is retained to gain physical insight into the problem. Thus for the general discussion of harmonics a one-group model

will be adopted. It will be applied first to a reactor containing a point source and then to one with a delta sink. The main difference between the one group and the two-group model will be illustrated in Appendix II.

a) A bare homogeneous reactor with a source.

The kinetic equation governing this state is:

$$v(D\nabla^2-\Sigma)n(x,t) + vk(1-\beta)\Sigma n(x,t) + \sum_{i=1}^{\ell} \lambda_i c_i(x,t) + Q(x,t) = \frac{\partial n(x,t)}{\partial t},$$

$$v\beta_i k\Sigma n(x,t) - \lambda_i c_i(x,t) = \frac{\partial c_i(x,t)}{\partial t}, \quad i = 1,\ldots,\ell. \tag{29}$$

with the condition that the neutron and precursor densities vanish at the extrapolated boundaries, $\tilde{x}$:

$$n(\tilde{x},t) = c_i(\tilde{x},t) = 0.$$

In the equation above,

$n(x,t)$ - neutron density at space point x and time t,

$Q(x,t)$ - external source,

$c_i(x,t)$ - precursor density,

v,D,Σ,k - velocity of neutrons, thermal diffusion constant, absorption cross-section, and infinite multiplication constant, respectively.

The solution of the equations may be obtained by means of the expansions

$$n(x,t) = \sum_{q=o}^{\infty} T_q(t)n_q(x), \qquad c_i(x,t) = \sum_{q=o}^{\infty} T_q^i(t)n_q(t),$$

where: $\nabla^2 n_q = -B_q^2 n_q$,

and B_q^2 is the q-th geometrical eigenvalue of the system. The general solutions and those for slab geometry are given in Appendix I-1.

The initial density of the subcritical reactor due to the constant source $Q(x,0)$ is:

$$n(x,0) = \sum_{q=o}^{\infty} T_q(0)n_q(x) = -\Lambda^* \sum_{q=o}^{\infty} (Q_q(0)/\rho_q)n_q(x), \quad (\rho_q<0) \tag{30}$$

where: $Q_q(0) = \int Q(x,0)n_q(x)dx / \int n_q^2(x)dx$.

The harmonics contribution to the initial density is:

$$H(x,0) = -\Lambda^* \sum_{q=0}^{\infty} (Q_q(0)/\rho_q) n_q(x) + \Lambda^* (Q_0(0)/\rho_0) n_0(x) = \\ = -\Lambda^* \sum_{q=1}^{\infty} (Q_q(0)/\rho_q) n_q(x), \qquad (31)$$

since in this case the persisting mode just corresponds to the lowest geometrical eigenvalue.

The harmonics content of the density after instantaneous removal of the source is evidently smaller. For example, for the time integrated flux

$$H(x) = \Lambda^* [\Lambda^* + \bar{W}(0)] \sum_{q=1}^{\infty} (1/\rho_q)^2 Q_q(0) n_q(x). \qquad (32)$$

The higher modes are damped here faster than those in the initial density, due to the appearance of the factor $1/\rho_q^2$. The modal reactivity ρ_q increases rapidly with the modal index. Physically this behaviour is clear, since after the removal of the source, only the decaying precursors produced formerly by the source-neutrons are not distributed according to the persisting mode (ref. 39).

To demonstrate the deviation of the normalized initial density, $[n(x,0)]_{nor.}$, which is the basic reference function employed in the usual S.J. and subcritical multiplication techniques, from the persisting distribution of the state to be measured, Eq. A-I-12a was evaluated for a heavy water slab reactor. This reactor has a material buckling $B^2 = 4{,}101 \cdot 10^{-4} cm^{-2}$ (see configuration DI-1 A-V). It is made -10$ subcritical by reducing the extrapolated thickness from d = 155,1 cm to d = 115,6 cm. A plane source is placed at various positions x_0, thus introducing various amounts of harmonics. Fig.2(c), (e) and Fig.3(b) show $[n(x,0)]_{nor.}$ for a number of source locations. One sees immediately that the deviation from the persisting mode, sin $B_1 x$, is increasing as the source moves farther away from the center. A clearer indication of the deviation is provided by the ratio:

$$[n(x,0)]_{nor.} / \sin B_1 x = r(x,0), \qquad (33)$$

plotted in Figs. 2 (a),(b),(d) and Fig. 3 (a) curves 1.

This ratio actually gives the magnitude of the correction that should, in principle, be applied to normal S.J. experiments in order to cor-

Fig. 2 : c,e) Thermal neutron distribution in a slab reactor with plane source
a,b,d) 1. Harmonics content of the neutron density.
2. Harmonics content of the time integrated density.

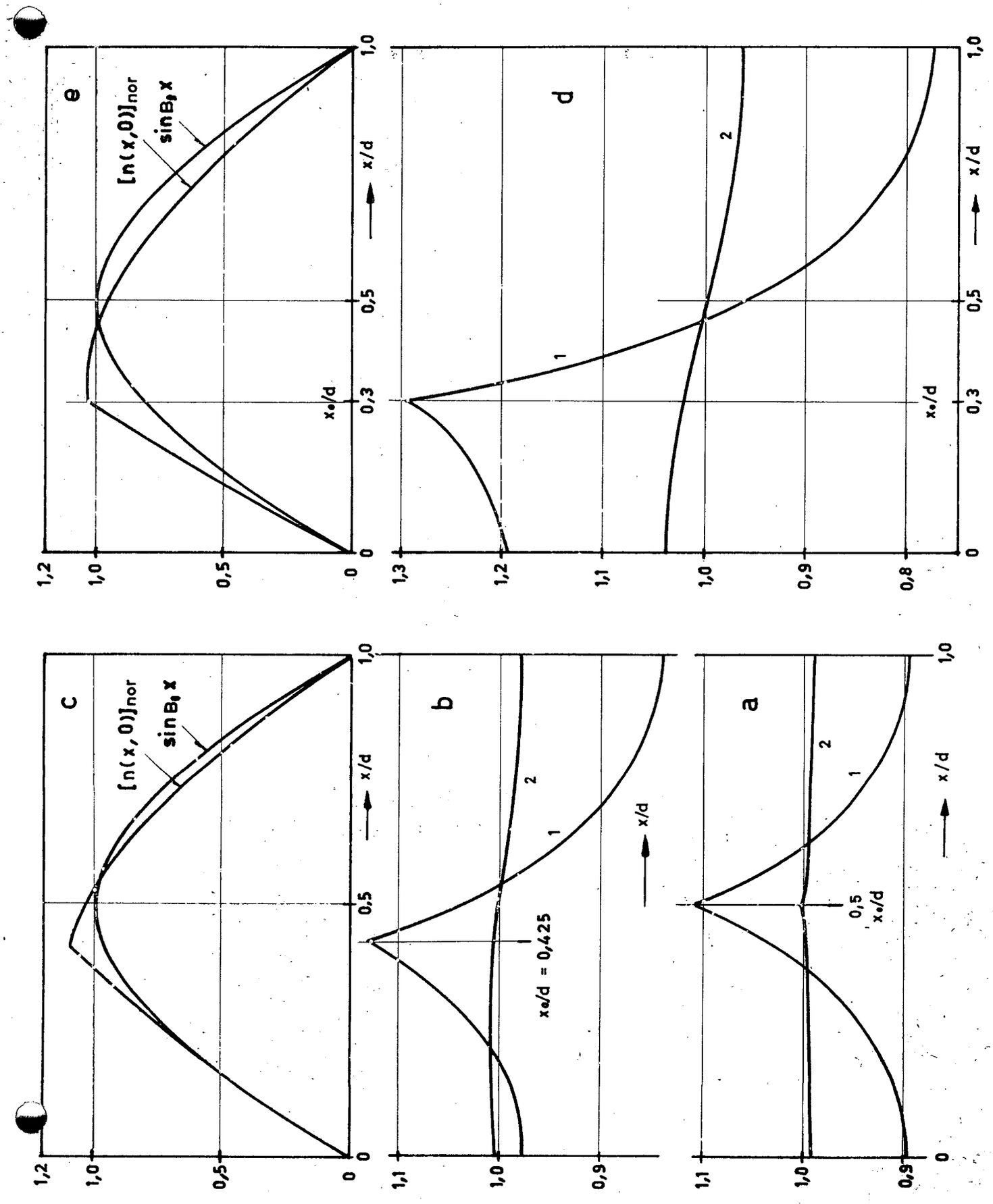

Fig.3 : Thermal neutron distribution in a slab reactor with plane source (a,b) and plane absorber (c).

curve 1) Harmonics content of the neutron density.
curve 2) Harmonics content of the time integrated density.

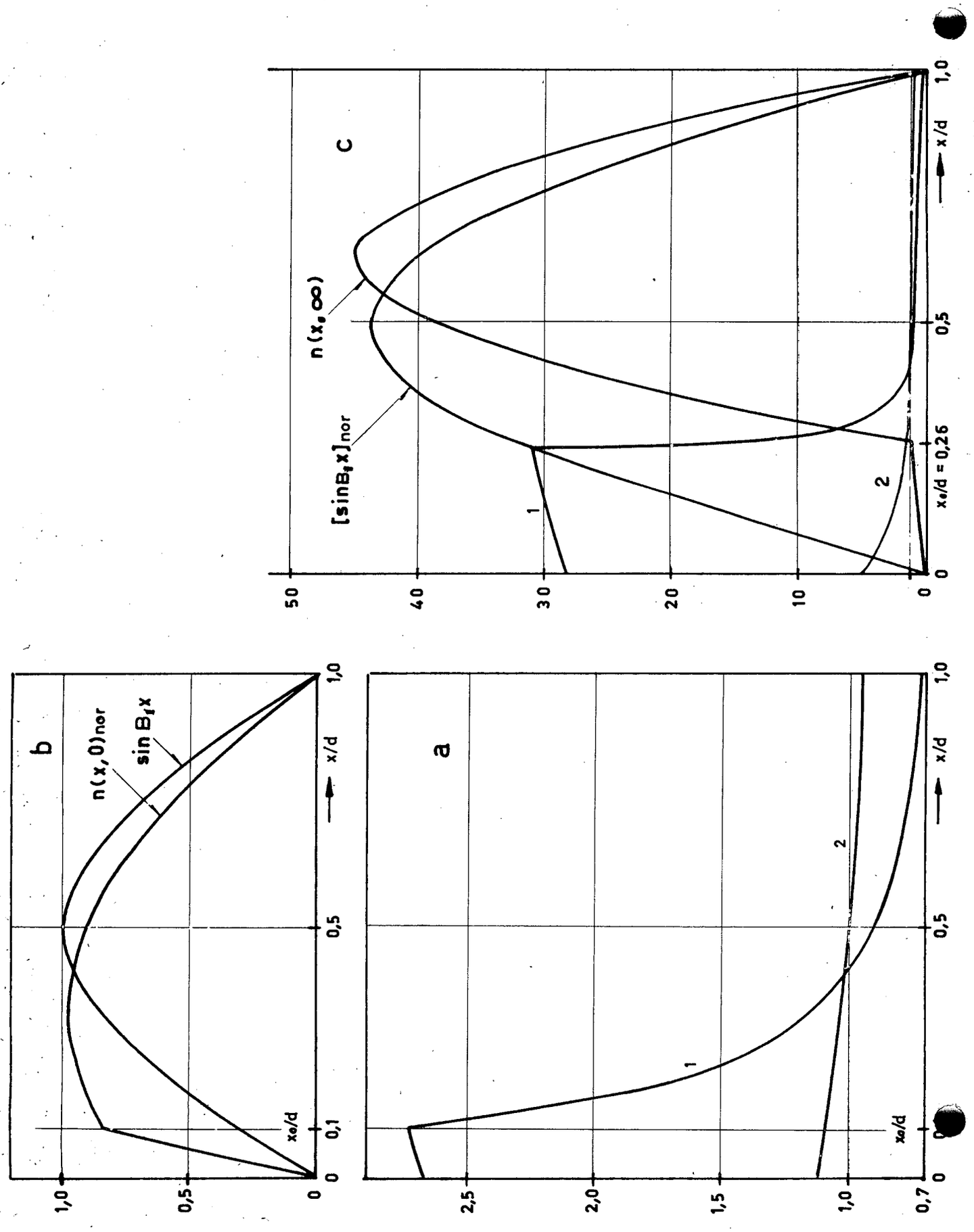

rect for harmonics. Since the time integrated density contains only an extremely small amount of harmonics (see e.g. the last Figs. curves 2), the above ratio, Eq. 33, directly gives (through Eq.21) the error introduced in the reactivity as measured by the integral count method. For example, if the removable source is in the center, one underestimates the reactivity by about 10 % if the detector is far away from the source. The reactivity will be overestimated by about the same amount, if the measurement is carried out in the center. Placing the source at about 1/3d, and measuring in its vicinity would cause an overestimate of about 30%, while measuring near the farther boundary will result in an underestimate of about 20% .

It should be clear that in a two group calculation the damping of higher modes is stronger. Furthermore, in the three dimensional case integration over the volume is more effective in suppressing the contribution of higher harmonics than in the one dimensional case. On the other hand, real reactors are usually more complex, and sometimes involve media with widely different parameters, which again give rise to considerable harmonics contamination.

b) Bare homogeneous reactor with a delta sink.

This configuration is intended to simulate a rod-drop experiment. Its evaluation (A-IV) is carried out by the method of orthogonal functions, applied by Auerbach (ref.44) to control statics.

After dropping the rod, the new persisting mode, $n(x,\infty)$ which is established after all higher harmonics have died out, is given by (A-IV, Eq.13):

$$n(x,\infty) = n(x_o,\infty)\gamma^*\Lambda^* \sum_{p=o}^{\infty} n_p(x_o)n_p(x)/\rho_p .$$

In a slab reactor with a plane absorber at x_o it becomes (A-IV-14)

$$\frac{n(x,0)}{n(x_o,\infty)} = \frac{\gamma^* d}{4\nu D B_f}\left\{\sin B_f|x-x_o| - \sin B_f(x+x_o) - 2\cot B_f d \sin B_f x_o \sin B_f x\right\},$$

where B_f is a fictitious material buckling ($B_f > B$) chosen so as to make the reactor virtual critical in the presence of the sink. The initial distribution in the critical system is $\sin B_1 x$. The neutron density integrated over time from the moment of instantaneous in-

Fig.4: Thermal neutron distribution in a slab reactor with plane absorber.
curve 1) Harmonics content of the neutron density.
curve 2) Harmonics content of the time integrated density.

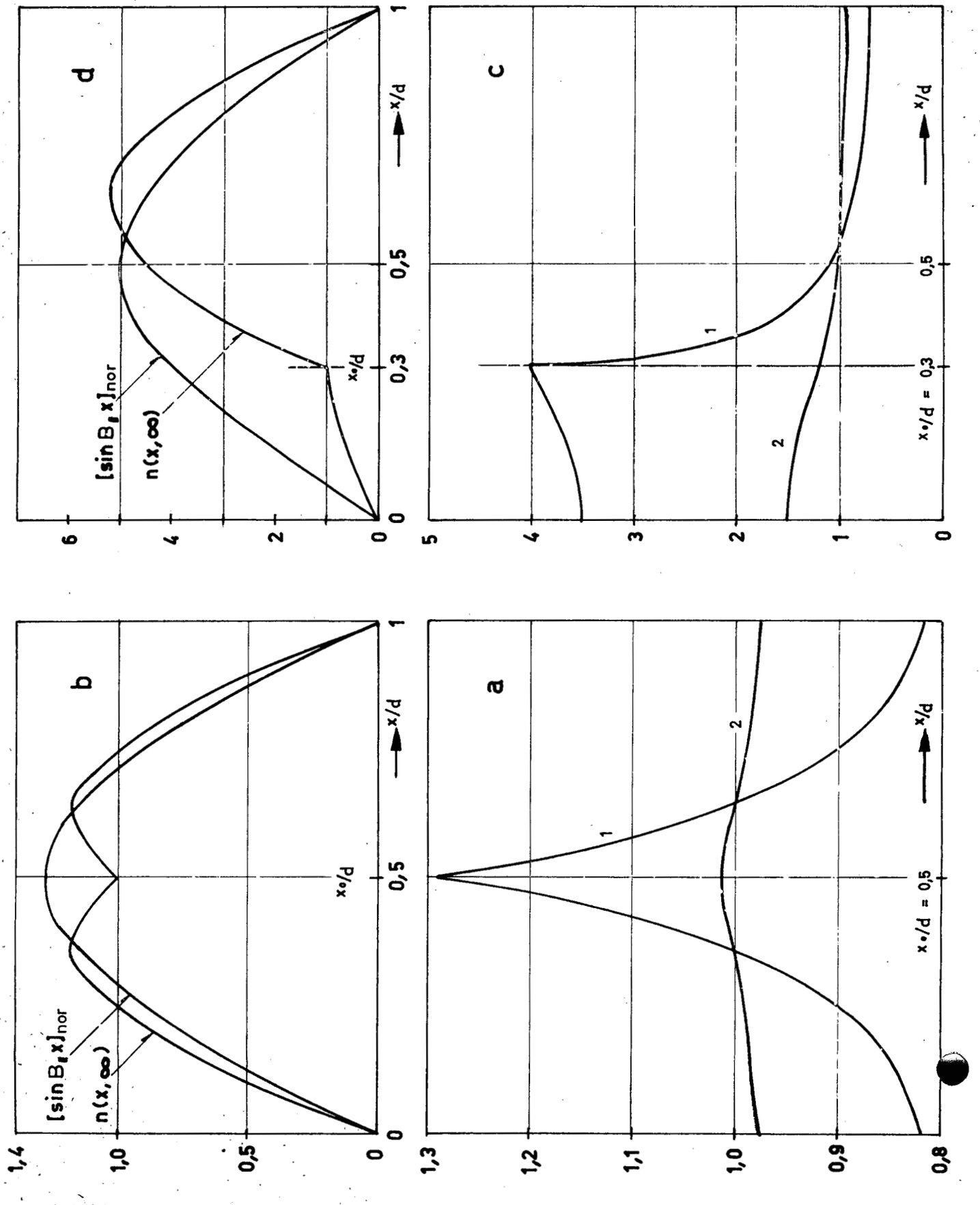

sertion of the sink to infinity is given by (A-IV,10):

$$\int_0^\infty n(x,t)dt = T_0(0)\ [\Lambda^* + \bar{W}(0)]\left\{ \frac{1-\gamma^*\Lambda^* \sum_{p=0}^{\infty} n_p^2(x_0)/\rho_p}{\gamma^*\Lambda^* n_0^2(x_0)}\, n_0(x) + \right.$$

$$\left. + \frac{\sum_{p=1}^{\infty} n_p(x_0)n_p(x)/\rho_p}{n_0(x_0)} \right\} .$$

In slab geometry this expression reduces to Eq. 19 A-IV.

Explicit evaluations of the above expression have been done for a heavy water slab reactor having the modified one-group parameters of the DI-1 configuration (see A-V). Its material buckling is $B^2 = 4{,}101 \cdot 10^{-4}$ cm^2 as before, and its extrapolated thickness is 155,1 cm. The plane sink is dropped at various positions x_0 each time reducing the reactivity to -10 $. Because of this constraint it is clear that the absorption coefficient, γ, of the sink will depend on the location.

The normalized initial density, $[\sin. B_1 x]_{nor.}$, is compared to the persisting mode of the final reactor, $n(x,\infty)$. This is shown in Figs.4 (b),(d) and Fig. 3 (c) for various source locations. A more stringent comparison is achieved by calculating the excess of harmonics

$$r(x,0) = [\sin B_1 x]_{nor.}/n(x,\infty).$$

This ratio is plotted in Figs. 4 (a),(c) and fig. 3 (c), curve (1). The various curves show a considerable abount of harmonics. Since, again, the time integrated excess of harmonics is rather small, the above ratio, $r(x,0)$ gives the error introduced in the reactivity measured by an R.D. experiment with the integral count method. For example, in the case of a central control plane, where the harmonics content is a minimum, there is an overestimate of about 30% when the counter is placed near the sink, and an underestimate of about 15% if the measurement is carried out far from the sink. When the sink is fixed at an off-center position, the amount of harmonics increases considerably. Thus in the case of $x_0/d = 0{,}3$, in the region between the sink and the nearer boundary, an overestimate of 350% to 400% will result, while on the other side the result will be underestimated by about 25% .

To complete the series of comparisons, a two-group calculation for a two-zone cylindrical heavy water reactor, both without and with cen-

tral control rod (configurations DI-3 and DI-4, see A-V), has been carried out. The normalized thermal initial density and the thermal persisting mode of the rodded reactor, $n(r,\infty)$, are shown in Fig. 5, together with a plot of the corresponding harmonics excess. The corresponding fast quantities are plotted in Fig. 6.

In a cylindrical reactor the control-rods are much less effective than the plane sheet absorber in slab geometry. Thus, in order to achieve the same subcriticality, the absorbing properties of the control rod should be stronger than those of the control plane. For this reason the initial flux is less perturbed in the case of a control plane and thus contains less harmonics. Fig. 5 shows the strong volume smearing effect of a two-dimensional configuration. In spite of the extremely high harmonic contamination in the vicinity of the control rod, after two migration distances there is a small, almost constant, amount of harmonics. The fast density, Fig. 6, is evidently much less affected by the control rod. But beyond two migration-distances the fast harmonics have the same magnitude as the thermal ones.

Fig. 5 : Comparison of the thermal density before a rod-drop to the asymptotic density after the drop.

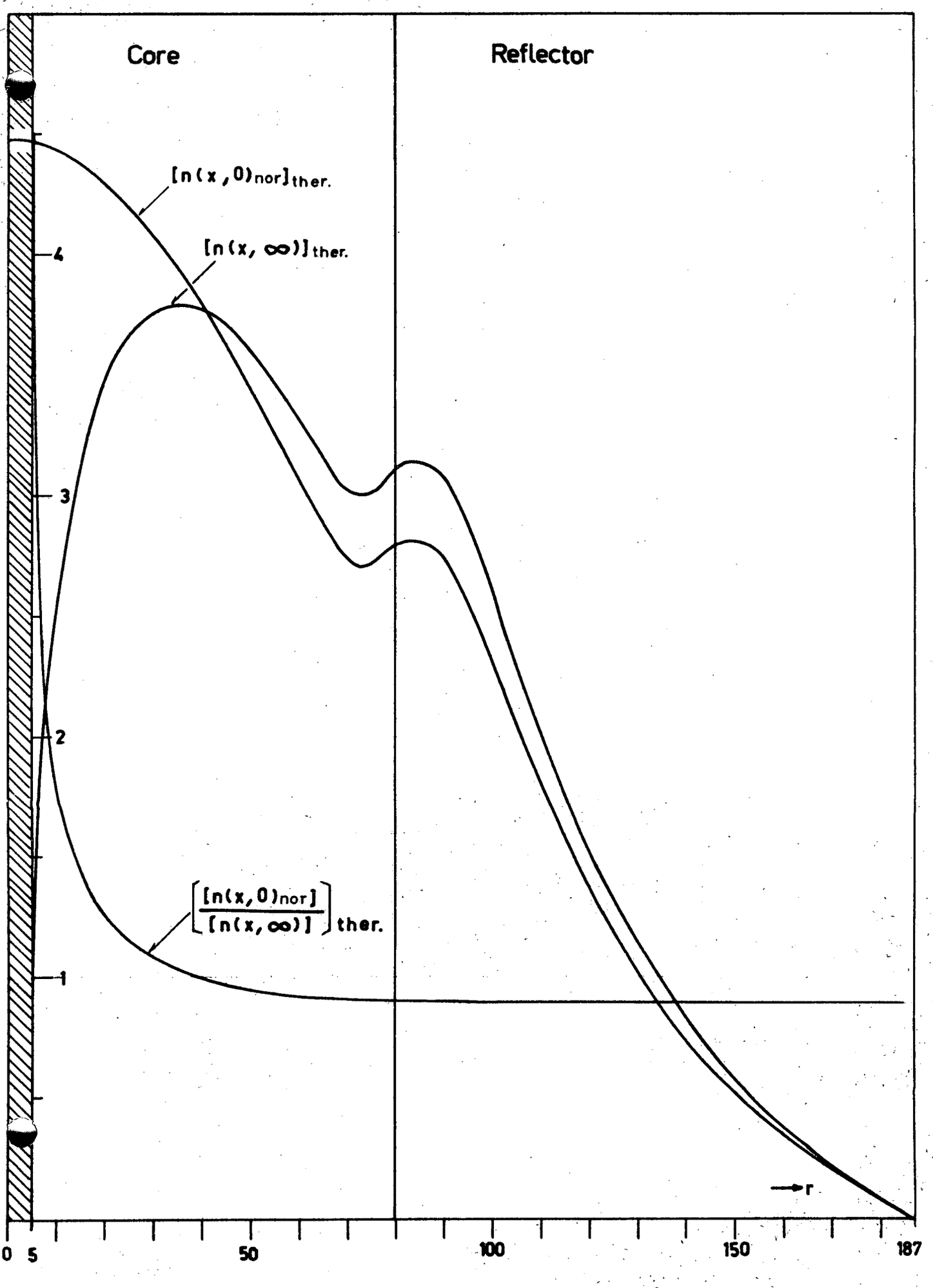

Fig.6: Comparison of the fast density before a rod-drop to the asymptotic density after the drop.

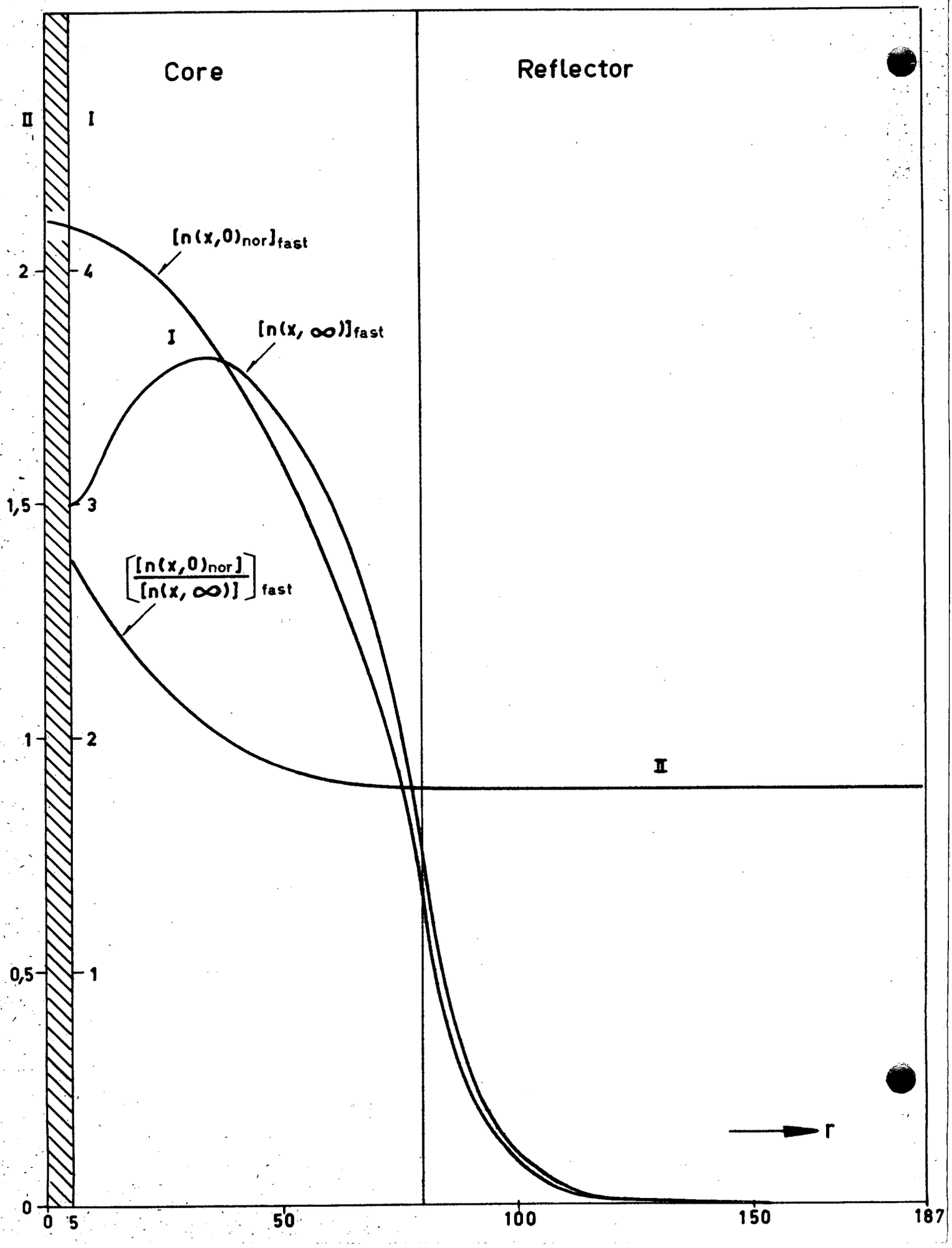

Chapter III

GENERAL REACTOR KINETICS AND THE CONCEPT OF REACTIVITY

1. TIME DEPENDENT TRANSPORT EQUATION

The general time dependent behaviour of a reactor is given by the Boltzmann transport equation. This equation states the detailed balance of neutrons and delayed neutron-precursors in every infinitesimal element of the phase-space. The equation for a fixed fuel reactor may be written in the following form (**refs.45,46**):

$$\frac{\partial}{\partial t} = -\vec{v}\nabla N - v\Sigma(\vec{r},u,t)\,N + Z\cdot N + (1-\beta)\,f(u)\,P\cdot N + \sum_{i=1}^{\ell} \lambda_i C_i f_i(u) + S(\vec{r},u,t), \qquad (1)$$

$$\frac{\partial}{\partial t} = \beta_i P\cdot N - \lambda_i C_i \qquad i = 1,2,..,\ell \quad (\ell \text{ delayed neutron groups}), \qquad (2)$$

where:

$N(\vec{r},\vec{v},t)$ = neutron density in phase space at the point $\vec{r},\vec{v}$; $\vec{v}$ is written sometimes also as $\vec{v} = v\vec{\Omega}$, where $\vec{\Omega}$ is the directional unit vector; the lethargy u will replace v as energy variable wherever possible.

$\Sigma(\vec{r},u,t)$ = the total macroscopic cross-section.

$Z\cdot$ = $\int v(u')\Sigma_s(\vec{r},\vec{v}'\to\vec{v})\cdot \; d\vec{v}'$

$Z\cdot$ is the scattering operator, while Σ is the macroscopic cross section for scattering.

$P\cdot$ = $\int v(u')\nu(u')\Sigma_f(u',\vec{r},t)\cdot \; d\vec{v}'$

$P\cdot$ is the production operator due to fission; Σ_f is the macroscopic cross section for fission and $\nu(u)$ is the prompt neutron yield from the fission process initiated by neutrons of lethargy u.

$f(u)$, $f_i(u)$ = the normalized lethargy distributions of prompt neutrons and of neutrons emitted from the i-th precursor group, respectively.

$\sum_{i=1}^{\ell} \lambda_i C_i(\vec{r},t) f_i(u)$ = delayed neutron source term, where $C_i(\vec{r},t)$ is the precursor density of the i-th group with the decay constant λ_i.

$S(\vec{r},u,t)$ = external source term.

β_i = fractional yield of delayed neutrons of the i-th group.

2. THE HARMONICS AND THE EXISTENCE OF A PERSISTING MODE

The main characteristic of a self sustaining reactor is its tendency to exhibit a very short memory. This is caused essentially by the fact that a neutron, while creating its own chain, diffuses away from its birth place, so that the distribution of its progeny tends to flatten the initial effects. Thus the reactor tends normally to have its own neutron distribution regardless of the initial conditions imposed on it. The effect of the initial conditions is manifested only through the amplitude of the distribution. The distribution which is attained after a relatively short transient time is called the persisting distribution. It will characterize the reactor in the sense that it is independent of the special initial conditions, but depends instead on the inherent characteristics of the reactor.

This behavior is quite general, since it applies as well to most of the nonlinear effects associated with burnup, temperature effects and other feedback processes. The stronger the nonlinear effects, the longer will be the transient period during which the reactor behavior is influenced by the initial conditions. This is true except in unusual cases where no persisting distribution is achieved,and the initial conditions do, in fact, determine the subsequent behavior.

In the treatment to follow the main problems will concern subcritical or zero power states of a reactor. In these situations the limitations mentioned above will not exist, and the persisting distribution will always establish itself. In fact the persisting distribution will not only be independent of the initial conditions, but will also keep its shape, while its amplitude changes.

The fact that the population of neutrons and precursors rises or falls with a common distribution after a certain transient time (the longer the fission-chain the weaker are the transients), means a complete separability of space and time. This suggests the expansion of the neutron and precursor densities in terms of appropriate eigenfunctions.

An expansion in terms of a "natural" complete set of eigenfunctions would mean complete separation of time and space in each mode (a mode is defined by an eigenvalue and its corresponding eigenfunction). The mode which will predominate will have the algebraically largest eigenvalue. This mode, defined as the persis-

ting distribution is a physically realizable quantity, its eigenfunction will be non-negative throughout the reactor and its eigenvalue will be real (a detailed argument for this is found in ref.33 pp 408-410 and a deeper mathematical treatment in refs.47,48).

The remaining eigenfunctions oscillate around zero and hence are not individually realizable. They describe the harmonics content of the instantaneous flux. Since these harmonics possess algebraically smaller eigenvalues than the persisting mode, they will eventually decay and become negligible compared to the prevailing asymptotic eigenfunction.

This decay time is known as the transient period during which the effect of the initial conditions dies off.

The desired expansion describes correctly the reactor under the prescribed conditions, which explicitly demand that the operator on the right side of Eq. 1 is linear and time independent. This is achieved if the physical parameters like cross-sections etc. are time and flux independent. In spite of this limitation, the existence of a persisting distribution in the wider sense makes it useful to have such an expansion as a convenient basis for a solution for the actual power reactor.

There are several choices of appropriate eigenfunctions in terms of which the neutron and precursor densities may be expanded. These will be discussed in the following paragraphs.

3. THE KINETIC EIGENFUNCTIONS

An important set of eigenfunctions are the kinetic eigenfunctions which reveal the simple eigenvalue character of the right hand operator in Eq. 1 and 2 and give a clear separation of time and space in each mode.

The kinetic eigenfunctions $n_q(\vec{r},\vec{v})$ (for neutrons) and $m_{\iota q}(\vec{r})$ (for the ι-th group of precursors) are defined by the following equations:

$$-\vec{v}\vec{\nabla}n_q - v\Sigma(\vec{r},\vec{v})n_q + Z \cdot n_q + (1-\beta)f(u)P\cdot n_q + \sum_{\iota=1}^{\ell} \lambda_\iota f_\iota(u) m_{\iota q} = w_q n_q , \qquad (3)$$

$$\beta_\iota P\cdot n - \lambda_\iota m_{\iota q} = w_q m_{\iota q} \quad \iota = 1,2,..,\ell \quad (\ell \text{ delayed neutron groups}). \qquad (4)$$

The notation used here has already been defined (see Eq. 1 and 2). Written in matrix form Eq. 3 and 4 become:

$$\begin{bmatrix} H\cdot & ; \lambda_1 f_1 & ; \lambda_2 f_2 & ; \dots & ; \lambda_\ell f_\ell \\ \beta_1 P\cdot & ; -\lambda_1 & ; 0 & ; \dots & ; 0 \\ \beta_2 P\cdot & ; 0 & ; -\lambda_2 & ; \dots & ; 0 \\ \dots & & & & \\ \dots & & & & \\ \dots & & & & \\ \beta_\ell P\cdot & ; 0 & ; 0 & ; \dots & ; -\lambda_\ell \end{bmatrix} \begin{bmatrix} n_q \\ m_{1q} \\ m_{2q} \\ \cdot\cdot \\ \cdot\cdot \\ \cdot\cdot \\ m_{\ell q} \end{bmatrix} = w_q \begin{bmatrix} n_q \\ m_{1q} \\ m_{2q} \\ \cdot\cdot \\ \cdot\cdot \\ \cdot\cdot \\ m_{\ell q} \end{bmatrix} \qquad (5)$$

where the operator H is defined by:

$$H = -\vec{v}\nabla\cdot \quad - v\Sigma + Z\cdot \quad + (1-\beta)fP\cdot \quad . \qquad (6)$$

The matrix Eq. 5 elucidates the eigenvalue character of the reactor matrix operator, which will be denoted for the sake of brevity by the symbol [M], while the column matrix of the densities will be denoted by the vector symbol $\vec{n}_q$. Thus w_q is the q-th eigenvalue of the operator [M] with the corresponding eigenvector $\vec{n}_q$. This defines the q-th mode of the density vector, which is seen to be entirely independent of the other modes. Eq. 5 is, of course, not the only possible representation of the set of simultaneous integro-differential equations 3 and 4. These equations may, for instance, be reduced to a simple equation by eliminating the precursor components

$$m_{iq} = \frac{\beta_i}{\lambda_i + w_q} P\cdot n_q , \qquad (7)$$

and substituting into Eq. 3. One then gets a single scalar equation for the q-th mode of the neutron density:

$$(-\vec{v}\nabla\cdot \quad - v\Sigma - w_q)n_q + Z\cdot n_q + \bar{f}(u,w_q)P\cdot n_q = 0, \qquad (8)$$

where $\bar{f}(u,w_q)$ is the average kinetic neutron spectrum of the q-th mode

$$\bar{f}(u,w_q) \equiv \bar{f}_q(u) = (1-\beta)f(u) + \sum_{i=1}^{\ell} \frac{\beta_i \lambda_i f_i(u)}{\lambda_i + w_q} . \qquad (9)$$

Using Eq. 8, the problem looses its clear eigenvalue feature. Nevertheless this equation will sometimes have practical advantages over Eq. 5. Its main use is in actual computation of the densities in multi-group diffusion theory. Then Eq. 8 has a very simi-

lar appearance to the virtual static reactor balance equation, which is easier to treat. (For a definition of the virtual state see Eq. 32). This similarity enables one to find a good initial approximation for the kinetic variables. These points will be elaborated later on.

4. THE FORMAL GENERAL SOLUTION OF THE TIME DEPENDENT EQUATION

Trying to solve the transport equation, Eq. 5, in any of its forms it is necessary to reduce it to a more tractable expression. This can be achieved by first expanding both the directional density vector and the scattering cross-section in spherical harmonics. Following this the diffusion approximation is obtained by neglecting all except the first two terms of the expansion, (refs. 46,49).

One can proceed and make further simplifications for the purpose of solving the energy dependent diffusion equation. One way of doing this is to make some assumptions about the strength of the dependence of the neutron density and the parameters on the energy, (which is usually believed to be weak). This leads either to the continuous slowing down model or to the kernel method.

Another way, which provides a model more amenable for computation, is the reduction to the group diffusion model. This method consists of breaking up the full energy range of the neutrons (from fission energy to average thermal energy) into discrete groups, assuming that in each group the energy is constant and the space and energy variables are separable, (refs. 45,46).

In the multigroup approach, the first row of the operator matrix [M] and the vector $\vec{n}_q$ (eq. 5) will be split into, say N rows, where N is the number of energy groups.

All parameters appearing in the matrix as well as the densities in each group are energy independent.

The above mentioned simplifications, supplemented by space boundary and interface conditions, amount therefore to the replacement of the matrix operator, which operates on $\vec{n}_q$, by an equivalent algebraic matrix. This enables one to write Eq. 5 in the form of a secular equation:

$$\left\{ [M] - w_q [I] \right\} \vec{n}_q = 0 \qquad (10)$$

where [I] is the unit matrix.

A non-trivial solution for $\vec{n}_q(\vec{r},\vec{v})$ demands the vanishing of the secular determinant:

$$\left|[M] - w_q[I]\right| = 0. \tag{11}$$

The last equation is an algebraic equation for w_q, and has infinitely many distinct solutions, depending on the boundary conditions. Each of these solutions describes a mode. Thus w_q describes the eigenvalue of the q-th mode. Knowing the w_q, the corresponding eigenvector may be found with the aid of the normalization condition. Thus, the set of kinetic eigenfunctions based on Eq. 3 and 4 is formally determined. The time dependent transport equations Eqs. 1 and 2 can also be written in the following matrix form:

$$[M]\vec{N} + \vec{S} = \frac{\partial}{\partial t}\vec{N}, \tag{12}$$

where:

$\vec{N} = \left\{N(\vec{r},\vec{v},t),\ C_1(\vec{r},t),\ \ldots,\ C_\ell(\vec{r},t)\right\}$ density vector

$\vec{S} = \left\{S(r,u,t),\ 0,\ \ldots,\ 0\right\}$ source vector.

One is now in a position to expand the density vector $\vec{N}$ in terms of the kinetic eigenvector $\vec{n}_q$:

$$\vec{N}(\vec{r},\vec{v},t) = \sum_{q=0}^{\infty} A_q(t)\vec{n}_q(\vec{r},\vec{v}). \tag{13}$$

In order to isolate the time behaviour $\left(\text{e.g. solve for } A_q(t)\right)$ one needs a set of functions orthonormal to the $\vec{n}_q$. This orthonormal set (or rather the bi-orthonormal set) will be the set of all adjoint vectors $\vec{n}_q^{+}(\vec{r},\vec{v})$, which will be chosen so as to satisfy the following scalar product (bi-orthogonality condition):

$$\begin{aligned}(\vec{n}_q^{+},\vec{n}_p) &= \iint \vec{n}_q^{+}(\vec{r},\vec{v})\vec{n}_p(\vec{r},\vec{v})\vec{dr}\vec{dv} \\ &= \iint\left[n_q^{+}n_p + \sum_{i=1}^{\ell} m_{i\,q}^{+} m_{i\,p}\right]\vec{dr}\vec{dv} = \delta_{qp}.\end{aligned} \tag{14}$$

Thus, $\vec{n}_p^{+}$ is a solution of the eigenvalue equation:

$$[M^{+}]\vec{n}_q^{+} = w_q\vec{n}_q^{+}, \tag{15}$$

where $[M^+]$ is obtained from $[M]$ by the following operations (refs. 50, 51)

a) transposition of lines and rows,

b) replacement of the diagonal terms by their adjoints,

c) changing of integration into its corresponding algebraic operation and vice versa, in the off-diagonal elements.

$$[M^+] = \begin{bmatrix} H^+ & ; & \beta_1 P(\vec{r},u) & ; \ldots ; & \beta_\ell P(\vec{r},u) \\ \lambda_1 \int f_1(u') \cdot d\vec{v}' & ; & -\lambda_1 & ; \ldots ; & 0 \\ \cdots & & \cdots & & \cdots \\ \lambda_\ell \int f_\ell(u') \cdot d\vec{v}' & ; & 0 & ; \ldots ; & -\lambda_\ell \end{bmatrix} \tag{16}$$

where:

$$H^+ = +\vec{v}\nabla \cdot \quad -v\Sigma + v\int \Sigma_s(\vec{r},\vec{v} \rightarrow \vec{v}') \cdot \quad d\vec{v}' + \\ + (1-\beta)v(u)\nu(u)\Sigma_f(\vec{r},u) \int f(u') \cdot \quad d\vec{v}' \tag{16a}$$

$$P(\vec{r},u) = v(u)\nu(u)\Sigma_f(\vec{r},u). \tag{16b}$$

Substituting expansion (13) into the transport equation (12), and multiplying scalarly by $\vec{n}_p^+$, results in an ordinary differential equation for the time dependent amplitude of the p-th mode:

$$\frac{dA_p(t)}{dt} - w_p A_p(t) = \iint S(\vec{r},t)\vec{n}_p^+(\vec{r},\vec{v})d\vec{r}d\vec{v} \equiv S_p^+(t), \tag{17}$$

the general solution of which is (with the help of the convolution symbol):

$$A_p(t) = A_p(0)e^{w_p t} + S_p^+(t) * e^{w_p t}. \tag{18}$$

Therefore the general solution for the neutron density is:

$$N(\vec{r},\vec{v},t) = \sum_{p=0}^{\infty} \left\{ A_p(0)n_p(\vec{r},\vec{v})e^{w_p t} + S_p^+(t) * e^{w_p t} n_p(\vec{r},\vec{v}) \right\}, \tag{19}$$

and for the precursor densities (see Eq. 7):

$$C_i(\vec{r},t) = \sum_{p=0}^{\infty} \left\{ A_p(0)e^{w_p t} + S_p^+(t) * e^{w_p t} \right\} \frac{\beta_i}{\lambda_i + w_p} P \cdot n_p(\vec{r},\vec{v}) \tag{20}$$

$$i = 1,2, \ldots, \ell.$$

In spite of their rather formal appearance, equations (19) and (20) reveal some interesting features of the time dependent reactor. These features are best described when using the multi-group diffusion model and will be discussed later.

5. NEUTRON IMPORTANCE FUNCTION AND THE NEUTRON DETECTING PROCESS

Eq. 17 is actually a reduction of the partial integro-differential equation (12) into an infinite set of non-coupled ordinary differential equations in time. This result was achieved by multiplying the general kinetic equation by the adjoint vector, or, puting it in another way, by averaging the density vector with the adjoint vector.

This procedure of averaging is useful mainly for the purpose of obtaining the general solution in the form of a complete set of separable eigenfunctions. However it is by no means unique.

The general kinetic equation (12) or its eigenvalue counterpart Eq. 5 or Eq. 10 may be reduced either to an ordinary differential equation in time, or to a set of algebraic equations, one for each mode, by multiplying them with some arbitrary weighting function which fulfils the appropriate boundary conditions.

It is true however, that such an averaging process is meaningless for computational (and experimental) purposes, unless the integrals can be evaluated. This, in turn, demands the knowledge of the density vectors.

Using Lewins' interpretation (ref.52) of the importance weight function as the contribution of neutrons to a meter reading, a physical meaning may be attributed to the weighting process which will give some insight into the concept of reactivity.

Actually, the recorded behaviour of the reactor is not determined solely by the neutron density. The detecting devices introduce their own characteristics into the measurement of the density as a result of their spatial distribution and their possible influence on the reactor parameters.

The average neutron population in the reactor which is read from the meter thus reflects not only the neutron density but also the detector characteristics which can be varied at will, at least to

some extent.

The importance function is then defined as the contribution of a neutron at position $\vec{r}$, velocity vector $\vec{v}$ and time t, to the meter reading at a later time t_f (the reading time).

This importance function, which must obey a final condition taking into account the detector characteristics, can be determined by assuming that a law of conservation of importance is valid.

As a matter of fact, it was shown (refs. 50, 54), that under these conditions the time dependent importance function satisfies the time dependent adjoint density equation.

The above arguments lead one to the conclusion that any arbitrary function or vector satisfying the correct boundary conditions, may be used as a weight function for the density vector and is physically realizable as detector distribution in the reactor. This consequently determines the neutron-importance.

6. THE REDUCTION OF THE KINETIC EQUATION

The balance of neutrons in the reactor is characterized by the production and destruction operators. The operator of direct neutron and precursor production is defined by the matrix [P], and the destruction operator, [D], is defined in such a manner that:

$$[M] = [P] - [D] \ . \qquad (21)$$

[M] is seen to describe the net production. Explicitly

$$[P] = \begin{bmatrix} (1-\beta)fP\cdot & ;0;..0 \\ \beta_1 P\cdot & ;0;..0 \\ \cdot\ \cdot\ \cdot\ \cdot\ \cdot\ \cdot\ \cdot\ \cdot\ \cdot & \\ \cdot\ \cdot\ \cdot\ \cdot\ \cdot\ \cdot\ \cdot\ \cdot\ \cdot & \\ \cdot\ \cdot\ \cdot\ \cdot\ \cdot\ \cdot\ \cdot\ \cdot\ \cdot & \\ \beta_\ell P\cdot & ;0;..0 \end{bmatrix} ; \quad [D] = \begin{bmatrix} D & ; & -\lambda_1 f_1 & ;..; & -\lambda_\ell f_\ell \\ 0 & ; & \lambda_1 & ;..; & 0 \\ \cdot\ \cdot\ \cdot\ \cdot\ \cdot\ \cdot\ \cdot\ \cdot\ \cdot & & & & \\ \cdot\ \cdot\ \cdot\ \cdot\ \cdot\ \cdot\ \cdot\ \cdot\ \cdot & & & & \\ \cdot\ \cdot\ \cdot\ \cdot\ \cdot\ \cdot\ \cdot\ \cdot\ \cdot & & & & \\ 0 & ; & 0 & ;..; & \lambda_\ell \end{bmatrix} \qquad (22)$$

where: $D = \vec{v}\nabla + v\Sigma - Z\cdot$ is the neutron destruction operator.

From the eigenvalue equation (Eq.5) and the splitting of the operator [M] one can obtain an algebraic equation involving w_q by scalarly multiplying both sides of the equation by a weighting vector $\vec{W}(\vec{r},\vec{v})$. As already emphasized, this procedure is meaningful as long as the weighting vector $\vec{W}$ describes the actual detector distribution.

The algebraic equation may be presented in two equivalent forms:

$$1 + w_q \frac{(\vec{W},\vec{n}_q)}{(\vec{W},[D]\vec{n}_q)} = \frac{(\vec{W},[P]\vec{n}_q)}{(\vec{W},[D]\vec{n}_q)} \equiv k_q, \tag{23}$$

$$\rho_q \equiv \frac{(\vec{W},\{[P]-[D]\}\vec{n}_q)}{(\vec{W},[P]\vec{n}_q)} = w_q \frac{(\vec{W},\vec{n}_q)}{(\vec{W},[P]\vec{n}_q)}, \tag{24}$$

where the brackets describe a scalar multiplication in the phase space (integration over $\vec{r}$ and $\vec{v}$).

These equations may be considered as the generalized inhour equations for the "inverse period of the q-th mode".

The first equation (Eq. 23) involves only destruction processes, while the second equation involves only production processes. Normally form (24) is to be prefered (see ref. 55). The multiplication constant of the q-th mode, k_q, is here defined as the ratio of weighted overall production to weighted destruction of chain carriers (neutrons plus precursors). On the other hand the reactivity, Eq. 24, of the same mode is the net weighted production of chain carriers per chain carrier produced. It is evident that:

$$\rho_q = \frac{k_q - 1}{k_q}. \tag{25}$$

In analogy with simple kinetics one may define a generalized generation time of carriers in a certain mode:

$$\Theta_q = (\vec{W},\vec{n}_q) \Big/ (\vec{W},[P]\vec{n}_q), \tag{26}$$

i.e. the average time elapsing between production of an average chain carrier and the moment this carrier initiates a new one.

Similarly the generalized life time

$$L_q = (\vec{W},\vec{n}_q) \Big/ (\vec{W},[D]\vec{n}_q), \tag{27}$$

is the average time elapsing between the production of a carrier and its disappearance.

All the expressions defined above refer to general chain carriers. They can, however, easily be reduced to the corresponding expressions for neutrons alone.

As was mentioned above, the density-vectors corresponding to higher harmonics are not individually physically realizable, and the-

refore their corresponding modal quantities like reactivity, generation time etc. cannot possess physical meaning, but rather refer to the perturbing effect of transients.

The reactivity and the generalized generation time, as well as the neutron generation time and the effectiveness of the fractional yield of delayed neutrons (the latter quantity will be defined later on) are arbitrary to the extent that the weight-vector $\vec{W}$ is arbitrary. Nevertheless, some advantages are gained by using the inhour equation and defining reactivity according to Eq. 24. This can be seen if one expresses w_q in Eq. 24 in terms of ρ_q and Θ_q. In most practical cases the main effect of local and global changes in an operating reactor will cause a change in the destruction operator alone, chiefly affecting the net production [P] - [D]. Hence the main result will be a change in the reactivity of the system (see Eq. 24), while Θ, Eq. 26, will hardly suffer any change at all. Even in cases when the reactor production parameters are altered, the influence on the generalized generation time as a result of this change will be much smaller than the corresponding change in reactivity, since the latter is affected by the difference between production and destruction. Hence the usefulness of Eq. 24 lies in the fact that the main dependence of w_q on changes in core-properties is via a global reactor characteristic, the reactivity.

The weighting vector $\vec{W}$ for the q-th mode has not been specified so far. For the sake of generality, oscillating detector-distribution (negative importance) may also be considered as a weight function. Such weight functions would be, for example, the eigenfunctions of the time dependent importance operator. As a matter of fact, the kinetic importance function defined by the adjoint eigenvalue equation (Eq. 15) must have an oscillating behaviour similar to that of the forward eigenvector (normal density vector) in order to fulfil the orthonormalization condition, Eq. 14.

7. THE KINETIC INHOUR EQUATION

A useful set of weight functions would be the adjoint eigenfunctions as defined in Eqs. 14 and 15. Since these functions are orthogonal, one must substitute $\vec{n}^+_q$ for $\vec{W}$ in Eqs. 23 and 24. If normalization is not taken into ac-

count, both numerator and denominator may be separated into neutron and precursor components.

Furthermore, the precursor components may be expressed in terms of the neutron density as follows (see Eqs. 7 and 15):

$$m_{i\,q} = \frac{\beta_i}{\lambda_i + w_q} P \cdot n_q, \qquad \text{(Eq. 7)}$$

$$m_{i\,q}^{+} = \frac{\lambda_i}{\lambda_i + w_q} f_i \cdot n_q^{+}. \qquad (28)$$

Substituting this back into the separated equation, the delayed precursors are completely eliminated, and one is left with the following kinetic inhour equation:

$$\left(1 - \sum_{i=1}^{\ell} \frac{w_q \beta_i}{\lambda_i + w_q}\right) \rho_q = w_q \Lambda_q + w_q \sum_{i=1}^{\ell} \left(\frac{\lambda_i}{\lambda_i + w_q}\right) \frac{\beta_{i\,\mathrm{eff},q}}{\lambda_i + w_q}, \qquad (29)$$

where:

$$\Lambda_q = (n_q^{+}, n_q) \,/\, (n_q^{+}, \bar{f}_q P \cdot n_q) \qquad (30)$$

is the kinetic generation time of the neutrons in the q-th kinetic mode (defined by Eq. 3 and 4),

$$\beta_{i\,\mathrm{eff},q} = \beta_i (n_q^{+}, f_i P \cdot n_q) \,/\, (n_q^{+}, \bar{f}_q P \cdot n_q) \qquad (31)$$

is the kinetic effective delayed neutron fraction of the i-th group of the q-th mode. This definition represents the ratio of the average production of delayed neutrons of the i-th group which are emitted with their normalized spectrum $f_i(u)$ to the average production of all neutrons produced with the average normalized kinetic energy spectrum $\bar{f}_q(u)$, where (see Eq. 9):

$$\bar{f}_q(u) = \frac{\left\{(1-\beta) f(u) + \sum_{i=1}^{\ell} \frac{\lambda_i}{\lambda_i + w_q} \beta_i f_i\right\}}{\left(1 - \sum_{i}^{\ell} \frac{\beta_i w_q}{\lambda_i + w_q}\right)}. \qquad (9a)$$

The kinetic inhour equation (Eq. 29) furnishes for the q-th mode a relation between the kinetic reactivity and the inverse period. This connection is brought about by a consistent definition of the global reactor quantities, namely kinetic neutron generation time, Λ_q, and kinetic effective delayed neutron fraction, $\beta_{i\ eff,q}$.

It is obvious from the discussion above that there exists a great deal of arbitrariness concerning the choice of weight function. Nevertheless, among the various possibilities there are some which merit special attention due to their practical use in reactor theory and experiments.

8. THE STATIC WEIGHT FUNCTION

One of the most useful functions is the static weight function (refs. 58 and 60), which is widely used in perturbation theory (ref. 57). In this approach one weights the neutrons with the importance of a critical reactor. Thus the actual state is considered as a perturbed state of the critical reactor. In principle this picture might be extended to far subcritical reactors (ref. 56), but the real physical significance is lost when the perturbation becomes large, so that there is no longer any similarity between the "unperturbed" and the "perturbed" reactor.

The static weight function helps to establish the relation between stable period (the inverse persisting eigenvalue), which can be conveniently measured, and static reactivity, which may either be calculated or derived from static experiments.

The static eigenvalue ν_p/ν of the static p-th mode is defined as:

$$(\nu_p/\nu)[P]\vec{h}_p = [D]\vec{h}_p, \tag{32}$$

where $\vec{h}_p$ is the corresponding static eigenvector:

$$\vec{h}_p(\vec{r},\vec{v}) = \left\{h_p(\vec{r},\vec{v}),\ g_{1p}(\vec{r}),\ldots,\ g_{lp}(\vec{r})\right\}. \tag{33}$$

The static reactivity is then defined as:

$$\rho_p = \frac{\nu - \nu_p}{\nu}. \tag{34}$$

The reactor is "subcritical, critical, or supercritical in the p-th mode" if $\nu_p > \nu$, $\nu_p = \nu$, or $\nu_p < \nu$ respectively.

The physical nature of this model becomes clear when one compares

the eigenvalue defined in Eq. 32 to the kinetic eigenvalue defined in equation (5) or equation (10). By changing the neutron fission yield ν (which may be considered as averaged over energy) to some fictitious yield ν_p, one brings the actual non critical reactor to "criticality" in the p-th mode (which means that in the new reactor $w_p = 0$). In other words the production is changed homogeneously in the multiplicative zone in order to compensate the destruction until criticality is attained in that mode. The set of equations (32) written in matrix form may be reduced to a single integro-differential equation involving the neutron density, h_p, alone, by eliminating the precursor densities,

$$g_{i\,p} = \frac{\nu_p}{\nu} \frac{\beta_i}{\lambda_i} P \cdot h_p \qquad (i = 1,2,\ldots,\ell). \tag{35}$$

Thus, one obtains the desired reduced equation:

$$D \cdot h_p = (\nu_p/\nu)\bar{f}\, P \cdot h_p, \tag{36}$$

where:

$D \cdot \quad = \vec{v}\nabla + v\Sigma - Z \cdot$, (see Eq.22)

$$\bar{f}(u) = (1-\beta)f(u) + \sum_{i=1}^{\ell} \beta_i f_i(u), \tag{37}$$

is the average static fission spectrum, which corresponds to the average kinetic neutron spectrum of the p-th mode, Eq.9, with $w_p = 0$.

The adjoint static density vector of the p-th mode will naturally satisfy the following relation:

$$(\nu_p/\nu)[P^+]\vec{h}_p^{\,+} = [D^+]\vec{h}_p^{\,+}, \tag{38}$$

where $[P^+]$ and $[D^+]$ can be identified from $[M^+]$ (Eqs.16) to be:

$$[P^+] = \begin{bmatrix} (1-\beta)P(\vec{r},u)\int f(u')\cdot\, d\vec{v}' & ; & \beta_1 P(\vec{r},u) & ; \ldots ; & \beta_\ell P(r,u) \\ 0 & ; & 0 & ; \ldots ; & 0 \\ \cdots & & \cdots & & \cdots \\ \cdots & & \cdots & & \cdots \\ 0 & ; & 0 & ; \ldots ; & 0 \end{bmatrix} \tag{39}$$

$$[D^+] = \begin{bmatrix} D^+ & ; & 0 & ; \ldots ; & 0 \\ \lambda_1\int f_1(u')\cdot\, d\vec{v}' & ; & -\lambda_1 & ; \ldots ; & 0 \\ \cdots & & \cdots & & \cdots \\ \cdots & & \cdots & & \cdots \\ \lambda_\ell\int f_\ell(u')\cdot\, d\vec{v}' & ; & 0 & ; \ldots ; & -\lambda_\ell \end{bmatrix}$$

where: $D^+ \cdot = H^+ \cdot - (1-\beta)P(\vec{r},u)\int f(u') \cdot \quad d\vec{v}'$,

In order to express the static reactivity of the p-th mode, ρ_p, in terms of the kinetic eigenvalue, the kinetic density vector of the q-th mode is weighted with the importance of the carriers in the virtual critical reactor. To this end one substitutes $\vec{h}_p^{\,+}(\vec{r},\vec{v})$ for $\vec{W}(\vec{r},\vec{v})$ in the generalized inhour equation of the first form, Eq. 23, yielding

$$1 + w_q \frac{(\vec{h}_p^{\,+},\vec{n}_q)}{(\vec{h}_p^{\,+},[D]\vec{n}_q)} = \frac{(\vec{h}_p^{\,+},[P]\vec{n}_q)}{(\vec{h}_p^{\,+},[D]\vec{n}_q)}. \tag{40}$$

Making use of the commutation rules for adjoint operators and Eq.38 one has:

$$(\vec{h}_p^{\,+},[D]\vec{n}_q) = (\vec{n}_q,[D^+]\vec{h}_p^{\,+}) = \frac{\nu_p}{\nu}(\vec{n}_q,[P^+]\vec{h}_p^{\,+}) =$$

$$= (1-\rho_p)(\vec{h}_p^{\,+},[P]\vec{n}_q).$$

Substitution into Eq.40 results in the desired relationship:

$$\rho_p = w_q \frac{(\vec{h}_p^{\,+},\vec{n}_q)}{(\vec{h}_p^{\,+},[P]\vec{n}_q)} = w_q \Theta_{pq}, \tag{41}$$

where Θ_{pq} is the generalized generation time of the chain carriers in the q-th kinetic mode, weighted with the p-th static importance function (see Eq. 38).

The last result of Eq. 41 may be obtained directly by substitution of $\vec{h}_p^{\,+}$ for $\vec{W}$ in the second form of the inhour equation (Eq.24). This in turn furnishes an integral definition for ρ_p-static:

$$\rho_p = (\vec{h}_p^{\,+},[M]\vec{n}_q) \;/\; (\vec{h}_p^{\,+},[P]\vec{n}_q). \tag{42}$$

In order to bring Eq. 41 into the form of the conventional inhour equation, it is necessary to separate the generation time of the neutrons alone from the generalized quantity, Θ_{pq}. This is achieved by the following procedure:

$$(\vec{h}_p^{\,+},\vec{n}_q) = (h_p^+,n_q) + \sum_{\iota=1}^{\ell} (g_\iota\, p^+, m_\iota\, q), \tag{43}$$

$$(\vec{h}_p^{\,+},[P]\vec{n}_q) = (1-\beta)(h_p^+, fP \cdot n_q) + \sum_{\iota}^{\ell} \beta_\iota (g_\iota\, p^+, P \cdot n_q). \tag{44}$$

Using Eq. 38 one can express g_{ip}^{+} in terms of the static neutron importance:

$$g_{ip}^{+} = f_i \cdot h_p^{+} = \iint f(u') h_p^{+}(\vec{r},u',\vec{\Omega}') du' d\vec{\Omega}' \qquad (45)$$

Eq. 7 expresses the kinetic precursor densities in terms of the neutron density. From Eqs. 45 and 7 one has:

$$(g_{ip}^{+}, m_{iq}) = \frac{\beta_i}{\lambda_i + w_q} (f_i \cdot h_p^{+}, P \cdot n_q) = \frac{\beta_i}{\lambda_i + w_q} (h_p^{+}, f_i P \cdot n_q). \qquad (46)$$

Substitution of Eq. 45 into Eq. 44 gives:

$$(\vec{h}_p^{+}, [P]\vec{n}_q) = (1-\beta)(h_p^{+}, fP \cdot n_q) + \sum_{i=1}^{\ell} \beta_i (h_p^{+}, f_i P \cdot n_q)$$
$$= (h_p^{+}, \bar{f}P \cdot n_q), \qquad (47)$$

where $\bar{f}(u)$, the average static spectrum is defined by Eq. 37. Substitution of Eqs. 43 and 44, expressed in terms of neutron density only, back into Eq. 41 leads to the conventional form of the static inhour equation, namely

$$\rho_p = \frac{\Lambda_{p,q}}{T_q} + \sum_{i}^{\ell} \frac{\beta_{i\,eff\,p,q}}{1 + \lambda_i T_q}, \qquad (48)$$

where:

$T_q = \frac{1}{w_q}$, is the "period" of the q-th kinetic mode.

$$\Lambda_{p,q} = (h_p^{+}, n_q) \,/\, (h_p^{+}, \bar{f}P \cdot n_q), \qquad (49)$$

is the static-importance weighted, mean neutron generation time.

$$\beta_{i\,eff\,p,q} = \beta_i (h_p^{+}, f_i P \cdot n_q) \,/\, (h_p^{+}, \bar{f}P \cdot n_q), \qquad (50)$$

is the static effective delayed neutron fraction of the i-th group.

The computation of generation time (Eq. 49) and effective delayed neutron fraction (Eq. 50) involves the knowledge of the kinetic and adjoint static densities as well as integration procedures. There is an alternative method involving two static reactivity calculations, which furnishes Λ and $\beta_{i\,eff}$ to a very good degree of approximation. For this method it is convenient to eliminate

the precursor terms from the integral definition of the static reactivity, Eq. 42. The elimination has already been done for the denominator, Eq. 47. In the numerator it can be achieved by carrying out the scalar multiplication and using Eqs. 45 and 7. Finally, one has:

$$\rho_p = \frac{(h_p^+, \bar{f}P\cdot n_q) - \left(h_p^+, (\vec{v}\nabla + v\Sigma - Z)\cdot n_q\right)}{(h_p^+, \bar{f}P\cdot n_q)} = 1 - \frac{(h_p^+, D\cdot n_q)}{(h_p^+, \bar{f}P\cdot n_q)} \quad . \quad (51)$$

Consider now a perturbation of the absorption probability rate, $v\Sigma(\vec{r},u)$, by adding a small amount, 'a' absorptions/sec. This is equivalent to the introduction of a homogeneously distributed a/v absorber, since $v\Sigma + a = v(\Sigma + a/v) = v\Sigma^*$.

As a result, there will be some change in reactivity, and an additional small change in the densities n and h:

$$\rho_p' = 1 - \frac{(h_p'^+, D\cdot n_q')}{(h_p'^+, \bar{f}P\cdot n_q')} - a\,\frac{(h_p'^+, n_q')}{(h_p'^+, \bar{f}P\cdot n'_q)}$$

$$= 1 - \frac{(h_p'^+, D\cdot n_q')}{(h_p'^+, \bar{f}P\cdot n_q')} - a\Lambda'_{p,q} \quad . \quad (52)$$

If a is small enough the change in the densities will be small and, to the first approximation, $\Lambda'_{p,q}$ can be replaced by $\Lambda_{p,q}$. However, $1 - (h_p'^+, D\cdot n_q')/(h_p'^+, \bar{f}Pn_q')$ can not be replaced by ρ_p, Eq. 51. The approximation involved in such substitution is of the order of the quantity to be calculated, namely $a\Lambda_{p,q}$. The above mentioned approximation is valid to the first order, only if the weighting function belongs to the same mode as the neutrons, and both static and kinetic eigenfunctions should be about equal, i.e. $h_p^+ \to h_q^+$ and $n_q \approx h_q$. Then follows

$$\rho_q - \rho_q' \cong a\Lambda'_{p,q} \cong a\Lambda_{p,q} = a\Lambda_{q,q} \equiv a\Lambda_q \quad (53)$$

Thus the reactivity change due to insertion or withdrawal of a 1/v absorber in the whole reactor is proportional to the neutron generation time.

Next assume that the production operator is perturbed by doubling one of the delayed neutron fractions, say the ι-th one. This would naturally affect the reactivity, and to a much smaller extent the

densities:

$$\frac{1}{1-\rho'_p} = \frac{(h'^{+}_p, \bar{f}Pn'_q)}{(h'^{+}_p, Dn'_q)} + \beta_i \frac{(h'^{+}_p, f_i Pn'_q)}{(h'^{+}_p, Dn'_q)}$$

$$= \frac{(h'^{+}_p, \bar{f}Pn'_q)}{(h'^{+}_p, Dn'_q)} \left\{ 1 + \beta'_{i\,\mathrm{eff}\,pq} \right\} . \qquad (54)$$

Since β_i is rather small, replacement of $\beta'_{i\,\mathrm{eff}\,p,q}$ is allowed in the first approximation. However, as in the preceding calculation of Λ, $(h'^{+}_p, \bar{f}\,P\cdot n'_q)/(h'^{+}_p, D\cdot n'_q)$ cannot be replaced by $1/(1-\rho_p)$ unless the conditions involved in Eq. 53 are fulfiled, namely $h^{+}_p \to h^{+}_q$ and $n_q \approx h_q$. Then

$$\frac{1-\rho_q}{1-\rho'_q} - 1 = -\frac{\nu'_q - \nu_q}{\nu_q} \cong \beta_{i\,\mathrm{eff}\,q} . \qquad (55)$$

Thus the effective delayed-neutron fraction of the i-th group is equivalent to the reactivity change, due to the doubling or eliminating of this delayed neutron contribution. This reactivity change refers to the unperturbed fictitious state (with ν_q) as critical.

The appearance of effective delayed neutron fractions in Eq. 50 and in the kinetic case, Eq. 31, is a reflection of the fact that prompt fission neutrons and delayed neutrons have different energy spectra. This difference gives a higher "importance" to the delayed neutrons in contributing to the chain reaction.

A typical consequence of the particular choice of weight-function is the appearance of the average kinetic neutron spectrum, $\bar{f}_q(u)$, in one case, and the average static spectrum, $\bar{f}$, in the other case (see Eqs. 9a and 37). When the reactor is critical in the q-th mode ($w_q = 0$), the kinetic spectrum coincides with the static one. But if the reactor is off critical, the kinetic behavior changes the inherent ratio of delayed neutrons to prompt neutrons:

$$R_{kin} = \sum_{i=1}^{\ell} \frac{\lambda_i \beta_i f_i(u)}{w_q + \lambda_i} \Big/ (1-\beta) f(u); \qquad R_{stat} = \frac{\sum_{i=1}^{\ell} \beta_i f_i(u)}{(1-\beta) f(u)}$$

(56)

For supercritical states ($w_q > 0$): $R_{kin} < R_{static}$, that is the effective yield of delayed neutrons is reduced relative to the yield of prompt neutrons. In subcritical stages ($w_q < 0$) the situation is reversed.

The significance of the static inhour equation (Eq. 48) consists in giving a rigorous relationship between the kinetic eigenvalue, which may be determined by experiment, and the static reactivity, which provides a unique mathematical description of the reactor. The transformation from kinetic eigenvalue to static eigenvalue depends solely on the consistency and precision with which Λ and $\beta_{i\,eff}$ can be calculated.

9. THE DYNAMIC WEIGHT FUNCTION

The third weight function to be discussed, after the kinetic and the static weight functions, is the so called "dynamic" weight function, which was used for the derivation of the elementary time dependent reactor equations (ref. 59). Special consideration to this weight function for a reactor on a stable period was given by Gross and Marable (ref. 58). The basic idea which leads to the "dynamic" weight function in our formalism can be elucidated by installing a system of detectors in the reactor which counts every neutron and precursor everywhere with the same probability. In this case the importance of the chain carriers is constant, and the weight vector $\vec{W}$ just equals the unit vector $\vec{I}$:

$$\vec{W}(\vec{r},\vec{v}) = \vec{I} = (1,\overbrace{1, \ldots ,1}^{\ell}) \qquad (57)$$

Introduction of the unit vector for $\vec{W}$ into Eq. 24 and eliminating the precursor components gives for the numerator and the denominator respectively:

$$(\vec{I},\vec{n}_q) = (1,n_q) + \sum_i (1,m_{i\,q}) = (1,n_q) + (1,P\cdot n_q) \sum_{i=1}^{\ell} \frac{\beta_i}{w_q + \lambda_i} \,, \qquad (58)$$

$$(\vec{I},[P]\vec{n}_q) = (1-\beta)(f,P\cdot n_q) + \beta(1,P\cdot n_q) = (1,P\cdot n_q). \qquad (59)$$

The prompt neutron spectrum f(u) disappears in the final form of Eq. 59, due to its normalization: $\int f(u)du = 1$.

Putting Eqs. 58 and 59 back into the second form of the generalized inhour equation (Eq. 24) leads to the "dynamic" inhour equation:

$$\rho_q = w_q \Lambda_q + w_q \sum_{i=1}^{\ell} \frac{\beta_i}{w_q + \lambda_i} , \qquad (60)$$

where:

$$\Lambda_q = (1,n_q) \,/\, (1,P\cdot n_q) \qquad (61)$$

is the total neutron population of the q-th mode in the reactor divided by the total production of neutrons in the same mode; Λ_q, by definition, is the neutron generation time in the q-th mode.

The main feature expressed in Eq. 60 is the fact that the reactor period $(1/w_q)$ is related to the corresponding dynamic reactivity:

$$\rho_q = (\vec{I},[M]\vec{n}_q) \,/\, (\vec{I},[P]\vec{n}_q) = (\vec{I},[M]\vec{n}_q) \,/\, (1,P\cdot n_q), \qquad (62)$$

through the neutron generation time Λ_q and the purely physical parameter β_i, and does not incorporate any "correction" for the preferential leakage of prompt neutrons relative to delayed neutrons.

10. CONCLUSIONS: THE VARIOUS DEFINITIONS OF REACTIVITY AND ITS DETERMINATION FROM KINETIC EXPERIMENTS

The only characteristic of a reactor which is truly global is the algebraically largest eigenvalue, w_o. It can be determined, at least in principle, by direct measurement without the need for theoretical interpretation. It has already been shown that w_o is the inverse relaxation time (stable period) of the neutron population. It is the time constant with which the neutron population will rise or fall as a whole. After all transients have decayed, the same constant w_o will be found by a detector placed anywhere in the reactor. Until the persisting mode has been established there is no rigorous experimental global parameter which describes the system.

Recognition of this fact will lead to the natural conclusion that for the purpose of direct comparison with stable period measurements, reactor theory should be concerned with Eq. 5 for the largest eigenvalue w_o, rather than with other equations such as the static eigenvalue equations (Eqs. 32 or 36).

In spite of this, in the early days of reactor theory the concept of reactivity was introduced as a matter of convenience. It was mainly due to the fact that the w-eigenvalues are more difficult to compute than the ν_p/ν-eigenvalues. The concept of reactivity was shown to be linked intimately with the balance of reactions in the reactor, which gives a better picture of the state of the reactor than the information furnished by w. In subcritical states the reactivity is much more sensitive to changes in the reactor than the persisting mode eigenvalue. For instance, this eigenvalue changes only slightly when the balance of reactions in changed abruptly from slightly below critical to strongly subcritical.

If one could devise a detector, distributed over the whole volume of the reactor, with some velocity dependent efficiency, then the meter reading would give directly the weighted population of chain carriers.

The average population $\langle N(t)\rangle = [\vec{W},\vec{N}(t)]$, with $\vec{W} = (N^*,C_1^*,\ldots,C_\ell^*)$, will fulfil the well known kinetic equations (ref.59). These time dependent equations are obtained here by scalar multiplication of Eq. 12 with the detector distribution, i.e. the vector weight function $\vec{W}(\vec{r},\vec{v})$ for Eq. 63a and with its C_i^* component for Eq. 63b (see also Sec.III-6 and ref. 60):

$$\frac{d\langle N\rangle}{dt} + \sum_{i=1}^{\ell} \frac{d\langle C_i\rangle}{dt} = \frac{\rho(t)}{\Lambda(t)} \langle N\rangle + \langle S\rangle, \qquad (63a)$$

$$\frac{d\langle C_i\rangle}{dt} = \frac{\beta_i(t)}{\Lambda(t)} \langle N\rangle - \lambda_i \langle C_i\rangle, \qquad (63b)$$

where $\langle N(t)\rangle$ and $\langle C_i(t)\rangle$ are the average neutron and precursor densities, respectively.

Following the time behavior of the meter-reading one can deduce the reactivity:

$$\rho(t) = \left(\vec{W}(\vec{r},\vec{v}),[M]\vec{N}(\vec{r},\vec{v},t)\right) / \left(\vec{W}(\vec{r},\vec{v}),[P]\vec{N}(\vec{r},\vec{v},t)\right), \qquad (64)$$

if the generation time of an average neutron $\Lambda(t)$ and the effective delayed neutron fraction $\beta_i(t)$ are computed according to the consistent definitions,

$$\Lambda(t) = (N^*,N) \;/\; (\vec{W},[P]\vec{N}), \qquad \beta_{i\,eff}(t) = \beta_i\,(C^*,P\cdot N) \;/\; (\vec{W},[P]\vec{N}). \tag{65}$$

The global parameters ρ, Λ and β_i are time dependent, which makes it difficult to compare different systems. They become time independent only if the time behaviour of the average population is measured after the transients have died out, i.e. when $\vec{N}(\vec{r},\vec{v},t) \to \vec{N}(\vec{r},\vec{v})T(t)$, in which case T terms will cancel.

Experimentally the detectors are local and occupy a very small volume of the system. Their response in space and velocity will be described by a vector function $\vec{d}(\vec{r},\vec{v})$, which is non-zero only in a small region around the center point, $(\vec{r}_o,\vec{v}_o)$, of the detector; that is $\vec{d}(\vec{r},\vec{v})$ will be proportional in most cases to $\delta(\vec{r}-\vec{r}_o)\delta(\vec{v}-\vec{v}_o)$. Assuming the importance function $\vec{W}(\vec{r},\vec{v}) = \vec{d}(\vec{r},\vec{v})$, one can calculate the three parameters ρ, Λ, and β_i and compare them with those derived from experiment.

It would, nevertheless, be misleading to call the quantity

$$\rho = \Big(\vec{d}(\vec{r},\vec{v}),[M]\vec{n}_o(\vec{r},\vec{v})\Big) \Big/ \Big(\vec{d}(\vec{r},\vec{v}),[P]\vec{n}_o(\vec{r},\vec{v})\Big), \tag{66}$$

the reactivity of the system, for this reactivity is not a global characteristic of the reactor in the usual sense since it depends strongly on the location and properties of the detectors. Such a situation makes it again difficult to compare different systems. Therefore, from the experimentalist's point of view, a reactivity such as defined in Eq. 66 is unsatisfactory. Alternatively, one can use the local measurement of the detector for determining the largest eigenvalue, which is, of course, independent of position. But now, instead of defining the reactivity with the aid of the actual detector distribution $\vec{d}$, one can relate the stable period to some convenient hypothetical detector distribution such as:

a) The kinetic weight function of the persisting mode, $\vec{n}_o^{+}$ (Eq. 15).
b) The static weight function of the same mode, $\vec{h}_o^{+}$ (Eqs. 32).
c) The "dynamic" weight function, $\vec{I}$ (Eq. 57).

These relationships are given by the inhour equation (e.g. Eqs. 40 or 41), with appropriately defined neutron generation time (Eqs. 30, 49 and 61 for cases (a), (b) and (c) respectively), and effective

fractional yield of delayed neutrons (Eq. 31 in case(a), Eq. 50 in case(b) and the pure fractional yield, β_i, in case(c)).

Although the kinetic inhour equation is the result of a straightforward weighting process, nevertheless a very great difficulty remains, namely the computation of the constants appearing in it. Evaluation of these constants, consisting of β_{eff}, Λ and ρ, involves the complete solution of equations (5) and (15), plus subsequent integration over the reactor.

Of the various inhour equations arising from different weighting functions, the static inhour equation is the one best known. It is more amenable to computation then any other, mainly because of the following reasons:

a) The static reactivity is the eigenvalue of an equation (Eqs.36,38) which is simpler in appearance than the kinetic eigenvalue equation, and its calculation does not necessarily involve integration.
b) The computation of β_{eff} and Λ involves the static adjoint function which is easier to find than the solution of the corresponding adjoint kinetic equation.
c) There is an alternative method for calculation of $\beta_{i\,eff}$ and Λ, which does not involve explicit integration, but the determination of two static eigenvalues (Eqs. 53-55).
d) In most practical cases the persisting distribution is equal, to very good precision, to the static distribution. This occurs mainly in regions of high static importance. Thus, replacement of $\vec{n}_o$ by $\vec{h}_o$ is justified. This facilitates the computation of β_{eff} and Λ.
e) If the production parameters are not drastically changed, β_{eff} and Λ are more or less the same for various states of the same system. This permits the utilization of β_{eff} and Λ, once calculated, for different static reactivities.

The discussion above was confined to the persisting mode. But a direct measurement of the persisting mode eigenvalue, w_o, is rather difficult in far subcritical states of a reactor. In this case another eigenvalue may be found to be more suitable as a characteristic of the reactor and also more convenient for measurement.

The deduction of the static reactivity, say of the zeroth mode ($p = 0$), from any measured eigenvalue w_q, involves the following expressions for Λ and β_{eff},

$$\Lambda_{o,q} = (h_o^+, n_q) / (h_o^+, \bar{f}P \cdot n_q), \tag{67}$$

$$\beta_{i\,eff\;o,q} = \beta_i (h_o^+, f\,P \cdot n_q) / (h_o^+, \bar{f}P \cdot n_q). \tag{68}$$

In this case a replacement of n_q by h_o, which is permissible when dealing with the persisting density, n_o, may be quite erroneous and may invalidate the whole interpretation.

The dynamic inhour equation is an alternative formulation of reactor kinetics. Here again the basic characteristic of both theory and experiment is the kinetic eigenvalue. However, this basic quantity is now related to the dynamic reactivity (Eq. 62) rather than to the static reactivity. The dynamic reactivity, which is simply the ratio of total net production to total production of neutrons, must be calculated by integration of the kinetic flux over the reactor, and no approximation is permissible here.

On the other hand, if the kinetic eigenfunction is known, computation of the generation time consists only of integration over the system and does not involve any spectral terms. An appreciable simplification is achieved with regard to the fractional yield of delayed neutrons. In the dynamic formalism, no effectiveness is necessary, and only the physical constants, β_i, appear. These constants are essentially independent of the reactor configuration (there is a slight dependence through the fast and intermediate fission factors, because of the different delayed neutron yields of different fissionable materials).

The dynamic approach seems to be especially recommended as alternative interpretation of the kinetic behaviour of the reactor, when the approximations used in the static approach are questionable. Under such conditions, the effort involved in exact evaluation of the static parameters may be large. The dynamic approach is then simpler and involves only straightforward kinetic parameters.

Chapter IV

APPROXIMATE SOLUTIONS OF THE GENERAL KINETIC EQUATION

The general kinetic equation is of little use for practical purposes, unless certain simplifying assumptions are made. When this is done, one may learn some more about basic properties of the general solutions discussed in Chap.III. Even when a simplified model is adopted for a given problem (like the multigroup diffusion model), the exact solution for a multi-zone reactor can only be found with the help of a digital computer (Sec.4 of this Chap.). Nevertheless, it may be possible to gain some insight into the problem, or to obtain a good starting point for a computer program, if an approximate analytical solution is known.

1. GENERAL PERTURBATION METHOD

An approximate solution is obtained by direct application of the perturbation concept (ref.33) to the eigenvalue equation of the system,

$$[M]\vec{n} = w\vec{n}. \tag{1}$$

Let the operator $[M_o]$ of the unperturbed reactor satisfy the eigenvalue equation:

$$[M_o]\vec{n}_p = w_p\vec{n}_p, \tag{2}$$

with known eigenvalues w_p and eigenvectors $\vec{n}_p$. The eigenvectors $\vec{n}_p$ are assumed to form a complete bi-orthonormal set, and to satisfy the same boundary conditions as the actual perturbed density. The functions orthogonal to $\vec{n}_p$ are the $\vec{n}_q^+$, which satisfy the adjoint equation to Eq. 2

$$[M_o^+] \quad \vec{n}_q^+ = w_q \vec{n}_q^+. \tag{3}$$

Due to the completeness of the set of $\vec{n}_q$, the perturbed density vector, $\vec{n}$, may be expanded in terms of the unperturbed set:

$$\vec{n} = \sum_{p=o}^{\infty} c_p\vec{n}_p. \tag{4}$$

The matrix operator $[M]$ is composed of the unperturbed operator $[M_o]$ and the perturbation operator $\varepsilon[M']$. Substitution of expansion (4) into Eq. 1 leads to:

$$\sum_p c_p(w-w_p)\vec{n}_p = \varepsilon \sum_p c_p[M']\vec{n}_p, \tag{5}$$

where $\varepsilon(\leqslant 1)$ may be looked upon as parameter characterizing the per-

turbation.

In order to solve for c_p, Eq. (5) is multiplied scalarly by $\vec{n}_q^+$:

$$\sum_{p=o}^{\infty} c_p(w-w_p)\delta_{qp} = \varepsilon \sum_{p=o}^{\infty} c_p M'_{qp}, \qquad q = 0,1,2,.... \tag{6}$$

where:

$$M'_{qp} = (\vec{n}_q^+,[M']\vec{n}_p). \tag{7}$$

Eq. 6 holdsfor each q, so that one has an infinite set of linear homogeneous equations for the coefficients c_p. Such a set of equations will have non-vanishing solution only if the determinant formed by the coefficients of the unknown c_p's vanishes, thus:

$$|(w-w_p)\delta_{qp} - \varepsilon M'_{qp}| = 0, \qquad q,p = 0,1,2,.... \tag{8}$$

Setting the determinant equal to zero results in an infinite order algebraic equation for w. To each w, in turn, corresponds an expantion coefficient c_p.

In practice the infinite series (Eq. 4) must be terminated after a finite number of terms. The c_p's can then be found from the homogeneous equations (Eq. 6) and a normalizing condition.

The actual solution of Eqs. 6 may be achieved by successive approximations, which give a larger radius of convergence than the normal Rayleigh-Schrödinger perturbation process, (ref.61).

For this purpose the equation is written in the form:

$$c_q \{(w-w_q) - \varepsilon M'_{qq}\} = \varepsilon \sum_{p\neq q} c_p M'_{qp} \quad , \tag{9}$$

and successive approximations are carried out as described in Sec.2.

A similar procedure, called the iteration perturbation method, is given by Morse and Feshbach (ref.62), and gives the result in an explicit form.

If the perturbed eigenvalue coincides with the j-th unperturbed eigenvalue when the perturbation is turned off, $\varepsilon=0$, then the eigenvalues and the eigenfunctions to third order will be given by

$$w = w_j + \varepsilon M'_{jj} + \varepsilon^2 \sum_{p\neq j} \frac{M'_{jp} M'_{pj}}{(w-w_p-\varepsilon M'_{pp})} +$$

$$+ \varepsilon^3 \sum_{\substack{p\neq j \\ q\neq j,p}} \frac{M'_{jp} M'_{pq} M'_{qj}}{(w-w_p-\varepsilon M'_{pp})(w-w_q-\varepsilon M'_{qq})} \tag{10}$$

$$\vec{n} = \vec{n}_j + \varepsilon \sum_{p\neq j} \frac{M'_{pj}}{(w-w_p-\varepsilon M'_{pp})} \vec{n}_p + \varepsilon^2 \sum_{\substack{p\neq j \\ q\neq j,p}} \frac{M'_{pq} M'_{qj}}{(w-w_p-\varepsilon M'_{pp})(w-w_q-\varepsilon M'_{qq})} \vec{n}_q +$$

$$+ \varepsilon^3 \sum_{\substack{p\neq j \\ q\neq j,p \\ r\neq j,p,q}} \frac{M'_{pq} M'_{qr} M'_{rj}}{(w-w_p-\varepsilon M'_{pp})(w-w_q-\varepsilon M'_{qq})(w-w_r-\varepsilon M'_{rr})} \vec{n}_r \, . \qquad (11)$$

The straight iteration perturbation method and the modified iteration perturbation method have been compared to the normal Rayleigh-Schrödinger perturbation theory and also to the exact solutions of some simple basic examples in reactor calculations by Blue and Zink (ref.63). The improvement introduced by using these iteration methods is evident from their work.

2. OVERALL EIGENFUNCTIONS METHOD

In the previous section the choice of the unperturbed functions was not specified, but limited to the fulfilment of the appropriate boundary condition. The unperturbed operator should be chosen so as to make calculations simple and still to have a reasonable radius of convergence.

Two other approaches of approximating the kinetic solutions will now be derived by a slight modification and extension to the time dependent case of the method of Holway (ref.64) and the method of Foderaro and Garabedian (ref.65), which was extended to complicated static systems by Auerbach (ref.44).

In these methods the neutron density is expanded in terms of a complete orthonormal set of eigenfunctions over the whole reactor. Therefore, to a certain extent, these methods can be considered as a special case of the general approximation or perturbation approach, where the unperturbed operator is chosen to be the Laplace matrix operator in the multigroup theory.

In spite of their approximate nature, these methods converge relatively fast for many cases and may be used as an alternative method for exact numerical calculation with the aid of a computer. The basic equation to be solved is always Eq. 1. The density vector $\vec{n}$ will be developed in terms of the complete set of eigenfunctions, φ_p, of the Laplace-operator:

$$\nabla^2 \varphi_p + B_p^2 \varphi_p = 0, \qquad (12)$$

so that:

$$\vec{n} = \sum_{p=o}^{\infty} \vec{a}_p \varphi_p, \tag{13}$$

where B_p^2 is the p-th geometrical bucklings.

In the κ-th approximation all $\vec{a}_p = 0$, for $p \geq \kappa$, $\vec{n}$ is replaced by its κ-th approximation equivalent $\vec{m}$, $\vec{a}_p$ by $\vec{b}_p$ and w is replaced by α. Therefore

$$[M]\vec{m} - \alpha\vec{m} = \vec{R}, \tag{14}$$

where:

$$\vec{m} = \sum_{p=o}^{\kappa} \vec{b}_p \varphi_p, \tag{15}$$

and $\vec{R}$ is the remainder.

As $\kappa \to \infty$, $\vec{b}_p \to \vec{a}_p$, $\alpha \to w$ and the remainder $\vec{R}$ tends to zero. If the approximation is so constructed that the remainder $\vec{R}$ will be othogonal to each of the eigenfunctions belonging to the sub-group κ, then $(\kappa+1)$ equations are supplied

$$\vec{0} = (\varphi_q, \vec{R}) = \sum_{p=o}^{\kappa} (\varphi_q, [M]\varphi_p)\vec{b}_p - \alpha \sum_{p=o}^{\kappa} (\varphi_q, \varphi_p)\vec{b}_p, \tag{16}$$

$$q = 0, 1, \ldots, \kappa.$$

$\vec{R}$ is a vector of $N+\ell$ components: N components due to the N energy groups, in the group diffusion model adopted, and additional ℓ components due to the presence of ℓ delayed neutron-groups.

The i-th component of the vector $(\varphi_q, \vec{R})$ is given by:

$$0 = (\varphi_q, R_i) = \sum_{p=o}^{\kappa} \sum_{j=1}^{N+\ell} (\varphi_q, M_{ij}\varphi_p) b_p^j - \alpha \sum_{p=o}^{\kappa} (\varphi_q, \varphi_p) b_p^i. \tag{17}$$

Using Eq. 16 as a starting point for finding a solution characterizes Holway's approach. Solving Eq. 17 for the components of the coefficient vector instead, characterizes the Foderaro method. Eq. 16 supplies us with $(N+\ell)(\kappa+1)$ homogeneous equations for the $(N+\ell)(\kappa+1)$ unknown components of the vector $\vec{b}_p$.

The determinant of this system of equations solves the multigroup problem to the assigned approximation. But direct solution of such a determinant is very difficult, and a perturbation approach will be helpful in getting numerical results. In this approach one

writes,

$$[M] = [M_0] + \varepsilon[M'], \tag{18}$$

where $[M_0]$ is again the unperturbed operator and describes an unperturbed system with constant parameters. Therefore:

$$(\varphi_q, M_{0\,i\,j}\varphi_p) = 0, \qquad q \neq p. \tag{19}$$

Substituting Eq. 18 into Eq. 16 gives:

$$\Big((\varphi_q,[M_0]\varphi_q) - \alpha[I] + \varepsilon(\varphi_q,[M']\varphi_q)\Big)\vec{b}_q = -\varepsilon\sum_{p\neq q}^{K}(\varphi_q,[M']\varphi_p)\vec{b}_p. \tag{20}$$

Eq. 20 is in a convenient form for successive approximations to multigroup vectors $\vec{b}_q$.

The first approximation for $\vec{b}_q$ will be based on the fact that in a homogeneous reactor ($\varepsilon=0$), the density in each group will be proportional to the eigenfunction of the largest eigenvalue (i.e. the persisting mode) after the transients have decayed. Therefore, a suitable starting approximation is to let $\vec{b}_0 = \vec{I}$ and $\vec{b}_q = \vec{0}$ for $q \neq 0$. Thus resulting in

$$\Big((\varphi_0,[M_0]\varphi_0) - \alpha[I] + \varepsilon(\varphi_0,[M']\varphi_0)\Big)\vec{b}_0 = \vec{0}, \tag{21}$$

where $\vec{I}$ and $\vec{0}$ are the unit and the zero vectors.

This provides us with $(N+\ell)(N+\ell)$ homogeneous algebraic equations for the $N+\ell$ unknown components of the vector $\vec{b}_0$. The vanishing of the determinant of the coefficients of Eqs. 21 gives the first order approximation for the α's which will be denoted by $\alpha^{(1)}$.

The next step will be to postulate: $\vec{b}_0$, $\vec{b}_1 \neq \vec{0}$ and $\vec{b}_{p\geq 2} = \vec{0}$, so that one obtains:

$$\Big((\varphi_1,[M_0]\varphi_1) - \alpha^{(1)}[I] + \varepsilon(\varphi_1,[M']\varphi_1)\Big)\vec{b}_1^{(1)} = -\varepsilon(\varphi_1,[M']\varphi_0)\vec{b}_0. \tag{22}$$

With the aid of the determined $\alpha^{(1)}$, the first order approximation to $\vec{b}_1$ (denoted by $\vec{b}_1^{(1)}$) is found. Similarly assuming $\vec{b}_0, \vec{b}_1, \vec{b}_2 \neq 0$ and $\vec{b}_{q\geq 3} = 0$, the following equation for $\vec{b}_2^{(1)}$ is obtained:

$$\Big((\varphi_2,[M_0]\varphi_2) - \alpha[I] + \varepsilon(\varphi_2,[M']\varphi_2)\Big)\vec{b}_2^{(1)} = -\varepsilon\Big((\varphi_2,[M']\varphi_0)\vec{b}_0^{(1)} + (\varphi_2,[M']\varphi_1)\vec{b}_1^{(1)}\Big). \tag{23}$$

By this procedure, the set of vectors $\vec{b}_0^{(1)}$, $\vec{b}_1^{(1)}$, ..., $\vec{b}_K^{(1)}$ and the eigenvalue $\alpha^{(1)}$ are determined to the first approximation.

Substituting the set of vectors $\vec{b}_p^{(1)}$ just found, back into Eq. 20, gives an algebraic equation for the second approximation of α, that is $\alpha^{(2)}$. With this new value one might proceed to get a second order approximation for $\vec{b}_0$, and then for $\vec{b}_1$, $\vec{b}_2$, to $\vec{b}_K$. This is achieved formally by the following procedure:

$$\Big((\varphi_0,[M_0]\varphi_0)-\alpha^{(2)}[I]+\varepsilon(\varphi_0,[M']\varphi_0)\Big)\vec{b}_0^{(2)}=-\varepsilon\sum_{p\neq 0}^{K}(\varphi_0,[M']\varphi_p)\vec{b}_p^{(1)} \qquad (24)$$

$$\Big((\varphi_1,[M_0]\varphi_1)-\alpha^{(2)}[I]+\varepsilon(\varphi_1,[M']\varphi_1)\Big)\vec{b}_1^{(2)}$$
$$=-\varepsilon\Big\{(\varphi_1,[M']\varphi_0)\vec{b}_0^{(2)}+\sum_{p\neq 0,1}^{K}(\varphi_1,[M']\varphi_p)\vec{b}_p^{(1)}\Big\} \qquad (25)$$

$$\Big((\varphi_2,[M_0]\varphi_2)-\alpha^{(2)}[I]+\varepsilon(\varphi_2,[M']\varphi_2)\Big)\vec{b}_2^{(2)}$$
$$=-\varepsilon\Big\{(\varphi_2[M']\varphi_0)\vec{b}_0^{(2)}+(\varphi_2,[M']\varphi_1)\vec{b}_1^{(2)}+\sum_{p\neq 0,1,2}(\varphi_2,[M']\varphi_p)\vec{b}_p^{(1)}\Big\}. \qquad (26)$$

As already mentioned, an alternative method of attacking the problem, would begin with Eq. 17, which treats every energy group and every delayed neutron group separately. Since no particular use is made of the eigenvalue character of Eq. 1, the delayed neutron components may as well be eliminated. Such a procedure simplifies the kinetic multigroup treatment, since the appearance of the reduced operator closely resembles its static counterpart.

The main advantages of this approach are revealed in the simplified, but nevertheless very common and practical, multigroup treatment, where production is due only to the slowest group, (N), fission neutrons appear only in the first group, and energy transfer occurs only between successive groups.

With these restrictions, the operator [M], will look as follows:

$$[M]=\begin{vmatrix} D_1 & 0 & 0 & \cdots & P_N \\ T_1 & D_2 & 0 & \cdots & 0 \\ 0 & T_2 & D_3 & \cdots & 0 \\ 0 & 0 & T_3 & \cdots & 0 \\ \cdot & \cdot & \cdot & \cdot & \cdot \\ \cdot & \cdot & \cdot & \cdot & \cdot \\ 0 & 0 & 0 & T_{N-1} & D_N \end{vmatrix}, \qquad (27)$$

where the D_l's are destruction operators including capture, and

elastic scattering. Inelastic scattering will not be considered in this formalism. The T_i represent transfer operators of neutrons from group i to group $i+1$, and P_N is the thermal fission production operator. A more detailed discussion of the time dependent multigroup treatment will be given later. Substitution of the newly defined [M] into Eq. 17 gives:

$$0 = (\varphi_q, R_i) \begin{cases} = \sum_{p=0}^{\kappa} \left[(\varphi_q, D_i \varphi_p) - \alpha \delta_{qp} \right] b_p^i + \sum_{p=0}^{\kappa} (\varphi_q, T_{i-1} \varphi_p) b_p^{i-1} & (28) \\ \qquad\qquad\qquad\qquad\qquad\qquad i = 2,3,4,\ldots,N \\ = \sum_{p=0}^{\kappa} \left[(\varphi_q, D_1 \varphi_p) - \alpha \delta_{qp} \right] b_p^1 + \sum_{p=0}^{\kappa} (\varphi_q, P_N \varphi_p) b_p^N . & (29) \end{cases}$$

Or, in matrix form:

$$\left\{ [D_i] - \alpha [I] \right\} \vec{B}_i + [T_{i-1}] \vec{B}_{i-1} = \vec{0} \qquad i = 2,3,\ldots,N \qquad (30)$$

$$\left\{ [D_1] - \alpha [I] \right\} \vec{B}_1 + [P_N] \vec{B}_N = \vec{0} \qquad (31)$$

$[D_i]$, $[T_i]$ and $[P_N]$, are square matrices of order $(\kappa+1)$, their elements can be identified easily from Eqs. 28 and 29.

The systematic elimination of all the vectors $\vec{B}_i$ from the matrix Eqs. (30) and (31), with the exception of $\vec{B}_N$, yields an equation for α, and in turn for $\vec{B}_N$ (with an additional normalizing condition):

$$\Big\{ \Big([D_1] - \alpha [I] \Big) [T_1]^{-1} \Big([D_2] - \alpha [I] \Big) [T_2]^{-1} \cdots \\ \cdots \Big([D_{N-1}] - \alpha [I] \Big) [T_{N-1}]^{-1} \Big([D_N] - \alpha [I] \Big) + \\ + [P_N] \Big\} \vec{B}_N = 0. \qquad (32)$$

The vanishing of the determinant of order $(\kappa+1)^2$ of the coefficients provides an equation for the determination of α. An important result of this method is the fact that the determinant for α does not depend on the number of energy groups but on the number of terms kept in the expansion.

So far the boundary conditions at the interface of the different zones were not discussed. It has merely been mentioned that all

eigenfunctions of the expansion should obey the same boundary conditions as the actual density at the external boundaries. Account of the interface conditions is taken either by introducing a special operator (ref.64) which provides for these conditions when the diffusion coefficients are different in two successive zones, or by direct evaluation of terms of the form $\left(\varphi_q(\vec{r}), \nabla D(\vec{r}) \nabla \varphi_p(\vec{r})\right)$, where the integration is extended over the whole reactor. These integrals automatically fulfil the normal boundary conditions of density and current continuity at each interface (ref.65).

3. CONTINUOUS SLOWING-DOWN MODEL AND SPECTRUM EFFECTS

The successive approximations method may also be used to solve the diffusion equations of the system with continuous slowing down. The continuous energy degradation model (e.g. Fermi age theory) is an important tool for estimating the energy spectrum effects on the time behavior of a reactor. Analytically only the bare system can be solved with this model, but the perturbation approximation method demonstrated above, shows its versatility by enabling one to attack the problem in reflected systems as well.

In the Fermi age approximation, the equations which govern both the flux per unit lethargy and the thermal flux are as follows (no production except in the thermal energy group, u_2, is assumed):

$$\nabla D(u,\vec{r}) \nabla \Phi(u,\vec{r},t) - \Sigma(u,\vec{r}) \Phi(u,\vec{r},t) - \frac{\partial}{\partial u} \left[\Sigma_s(u,\vec{r}) \Phi(u,\vec{r},t) \right] +$$

$$+ \nu(1-\beta) \Sigma_f(u_2,\vec{r}) f(u) \Phi_2(\vec{r},t) + \sum_{i=1}^{\ell} \lambda_i f_i(u) C_i(u,\vec{r},t)$$

$$= \frac{1}{v(u)} \frac{\partial \Phi(u,\vec{r},t)}{\partial t} , \qquad (33)$$

$$\nabla D_2(r) \nabla \Phi_2(\vec{r},t) - \Sigma_2(\vec{r}) \Phi_2(\vec{r},t) + \Sigma_s(u_2,\vec{r}) \Phi(u_2,\vec{r},t)$$

$$= \frac{1}{v_2} \frac{\partial \Phi_2(\vec{r},t)}{\partial t} , \qquad (34)$$

$$\beta_i \nu \Sigma_f(\vec{r}) \Phi_2(\vec{r},t) - \lambda_i C_i(\vec{r},t) = \frac{\partial C_i(\vec{r},t)}{\partial t} \cdot \quad i = 1,2,\ldots,\ell \qquad (35)$$

All parameters have already been defined except Σ_s which here des-

cribes the macroscopic scattering cross-section multiplied by ξ, the average logarithmic energy degradation per collision.

Elimination of the delayed neutron precursors by means of the substitution $\frac{\partial}{\partial t} \rightarrow w$ reduces the equations to a set of pseudostatic equations:

$$\left\{\nabla D(u,\vec{r})\nabla\cdot \; - \Sigma^*(u,\vec{r}) - \frac{\partial}{\partial u}\left[\Sigma_s(u,\vec{r})\cdot \;\right]\right\}\Phi(u,\vec{r}) + \\ + \nu F(u,w)\,\Sigma_f(\vec{r})\Phi_2(\vec{r}) = 0, \tag{36}$$

$$\left\{\nabla D_2(r)\nabla\cdot \; - \Sigma_2^*(\vec{r})\right\}\Phi_2(\vec{r}) + \Sigma_s(u_2,\vec{r})\Phi(u_2,\vec{r}) = 0, \tag{37}$$

where:

$$\Sigma^*(u,\vec{r}) = \Sigma(u,\vec{r}) + w/v(u); \quad \Sigma_2^*(\vec{r}) = \Sigma_2(r) + w/v_2. \tag{38}$$

$F(u,w) = (1-\beta)f(u) + \sum_{i=1}^{\ell} \lambda_i \beta_i f_i(u)/(w+\lambda_i)$,
is the kinetic lethargy spectrum (see e.g. Eq.9 Chap.III).

In order to solve the equations, the following expansion is made:

$$\Phi(u,\vec{r}) = \sum_n f_n(u)\varphi_n(\vec{r}), \tag{39}$$

$$\Phi_2(\vec{r}) = \sum_n A_n\,\Phi_n(\vec{r}), \tag{40}$$

where the $\varphi_n(\vec{r})$ satisfy the equation:

$$\nabla^2\varphi_n + B_n^2\varphi_n = 0. \tag{41}$$

To simplify the mathematics in the following example, without loss of essentials, it will be assumed that the reflector is a nonmultiplicative region, but otherwise has the same properties as the core (i.e. $\Sigma^*(u,\vec{r}) = \Sigma^*(u)$, etc.).

After substituting expansions (39) and (40) into Eq. 36, the fraction $f_m(u)$ may be isolated by integration over lethargy,

$$\Sigma_s(u)f_m(u) = \nu\Sigma\gamma_{m,n}\,A_n\int_0^u F(u,w)p^*(u'\rightarrow u)\,\exp\left[-B_m^2\tau(u'\rightarrow u)\right]du', \tag{42}$$

where:

$$p^*(u'\rightarrow u) = \exp\left[-\int_{u'}^{u}\left(\Sigma^*(u'')\,/\,\Sigma_s(u'')\right)du''\right], \tag{43}$$

is the "resonance" escape probability during slowing down from initial lethargy u' to u;

$$\tau(u' \to u) = \int_{u'}^{u} \left(D(u'') \,/\, \Sigma_s(u'') \right) du'' \quad ,$$

is the age of neutrons originating with lethargy u' and being slowed down to u;

$$\gamma_{m,n} = \int_{core} \varphi_m(\vec{r}) \varphi_n(\vec{r}) d\vec{r} \quad . \tag{45}$$

Substitution of expansions (40) and (42) in Eq. 37 yields a relation for the coefficients of the thermal flux, which is amenable to the successive approximation procedure:

$$A_m \left[D_2 B_m^2 + \Sigma_2^* - \nu\Sigma_f \gamma_{m,m} \int_0^{u_2} F(u',w) p^*(u' \to u_2) \exp\left(-B_m^2 \tau(u' \to u_2) \right) du' \right] =$$

$$= \nu\Sigma_f \left\{ \int_0^{u_2} F(u',w) p^*(u' \to u_2) \exp\left[-B_m^2 \tau(u' \to u_2) \right] du' \right\} \sum_{n \neq m} A_n \gamma_{m,n} \,. \tag{46}$$

From the last equation one gets immediately, by assuming $A_{n \neq m} = 0$, a first approximation for the determination of w. A comparison between this equation and a corresponding static approximation ($\nu \to \nu_c$, $w \to o$) yields a static inhour equation, from which the parameter Λ, the neutron generation time can be estimated approximately (e.g. for the case of m = o) to be

$$\Lambda^{-1} = \gamma_{oo} v_2 \nu\Sigma_f \int_0^{u_2} F(u',o) p(u' \to u_2) \exp\left[-B_o^2 \tau(u' \to u_2) \right] du' \quad , \tag{47}$$

and more significantly the effective delayed neutron fraction $\beta_{i\,eff}$ (e.g. for the case of m = o):

$$\frac{\beta_{i\,eff}}{\beta_i} = \gamma_i = \frac{\int_0^{u_2} f_i^2(u') p^*(u' \to u_2) \left[\exp -B_o^2 \tau(u' \to u_2) \right] du'}{\int_0^{u_2} F(u',o) p(u' \to u_2) \exp\left[-B_o^2 \tau(u' \to u_2) \right] du'} \tag{48}$$

$$\cong \frac{\exp\left[-B_o^2 \bar{\tau}_i(u_2) \right]}{\exp\left[-B_o^2 \bar{\tau}(u_2) \right]} = \exp\left[B_o^2 \left(\bar{\tau}(u_2) - \bar{\tau}_i(u_2) \right) \right] . \tag{49}$$

In fact the resonance probabilities may be dropped from Eq. 48, since they are affected only slightly by the different spectra.

4. TIME DEPENDENT MULTIGROUP MODEL

The most useful and common model for reactor calculation, as has been stated before, is probably the multigroup model. The general multigroup operator includes production of prompt fission neutrons and of delayed neutrons in all energy groups. It also includes neutron transfer from each group to all lower groups.

The reactor operator [M], for a fixed fuel will be:

$$[M]=\begin{vmatrix} v_1[\nabla D_1\nabla-\Sigma_{r1}]+ & (1-\beta)f_1P_2 & \dots & (1-\beta)f_1P_N & f_{11}\lambda_1;\dots;f_{\ell 1}\lambda_\ell \\ +(1-\beta)f_1P_1 & & & & \\ v_1\Sigma_{s21}+ & v_2[\nabla D_2\nabla-\Sigma_{r2}]+ & \dots & (1-\beta)f_2P_N & f_{12}\lambda_2;\dots;f_{\ell 2}\lambda_\ell \\ +(1-\beta)f_2P_1 & +(1-\beta)f_2P_2 & & & \\ \dots\dots\dots\dots & \dots\dots\dots\dots & \dots & \dots\dots\dots\dots & \dots\dots;\dots;\dots\dots \\ v_1\Sigma_{sN1}+ & v_2\Sigma_{sN2}+ & \dots & v_N[\nabla D_N\nabla-\Sigma_{rN}]+ & f_{1N}\lambda_1;\ ;f_{\ell N}\lambda_\ell \\ +(1-\beta)f_NP_1 & +(1-\beta)f_NP_2 & & +(1-\beta)f_NP_N & \\ \beta_1P_1 & \beta_1P_2 & \dots & \beta_1P_N & -\lambda_1;\dots;0 \\ \beta_2P_1 & \beta_2P_2 & \dots & \beta_2P_N & 0\ ;-\lambda_2;\ 0 \\ \beta_\ell P_1 & \beta_\ell P_2 & \dots & \beta_\ell P_N & 0\ ;\ 0\ ;-\lambda_\ell \end{vmatrix} \tag{50}$$

where:

$P_j = \nu_j \nu_j \Sigma_{fj}$

$\nu_j, D_j(\vec{r}), \Sigma r_j(\vec{r}), \Sigma_{fj}(\vec{r})$ are respectively, the neutron velocity, the diffusion coefficient, the removal cross section (which includes capture, elastic and inelastic scattering) and the fission cross section in the j-th energy group;

f_j = is the fraction of prompt neutrons born in the energy interval of the j-th group. It is normalized to give $\sum_{j=1}^{N} f_j = 1$;

$f_{\ell j}$ = the fraction of neutrons emitted from the ℓ-th delayed precursor group, with the energy of the j-th group. Also normalized to $\sum_{j=1}^{N} f_{\ell j} = 1$.

$\Sigma_{s\mu j}$ = scattering cross-section of neutrons from group $j(j\leq\mu-1)$ into the μ-th energy group.

The basic equation is again Eq.1, but now with the multigroup operator [M]:

$$[M]\vec{n} = w\vec{n}.$$

The corresponding virtual static equation is given by:

$$(\nu/\nu_0)[P]\vec{h} = [D]\vec{h}, \qquad \text{(Chap.III,Eq.32)} \tag{1}$$

where:

ν/ν_0 is the static eigenvalue, which modifies the balance of production and destruction in order to achieve criticality;

$\vec{h}$ = static density eigenvector;

[P] = production matrix.

$$[P] = \begin{vmatrix} (1-\beta)f_1P_1 & ; & (1-\beta)f_1P_2 & ; & \dots & ; & (1-\beta)f_1P_N & ; & 0 \dots 0 \\ \vdots & & \vdots & & \vdots & & \vdots & & \vdots \\ (1-\beta)f_NP_1 & ; & (1-\beta)f_NP_2 & ; & \dots & ; & (1-\beta)f_NP_N & ; & 0 \dots 0 \\ \beta_1P_1 & ; & \beta_1P_2 & ; & \dots & ; & \beta_1P_N & ; & 0 \dots 0 \\ \vdots & & \vdots & & \vdots & & \vdots & & \vdots \\ \beta_\ell P_1 & ; & \beta_\ell P_2 & ; & \dots & ; & \beta_\ell P_N & ; & 0 \dots 0 \end{vmatrix}, \tag{51}$$

$$[D] = [M] - [P], \text{ the "destruction" matrix.} \tag{52}$$

In order to write down the general expressions for the static reactivity (III, Eq.51) the generation time (III, Eq.49) and the effective delayed neutron fraction (III, Eq.50) one has to transform the total weighted production $(h^+, \bar{f}(u)Pn)$ and the destruction $[h^+(\vec{v}\nabla + v\Sigma - Z\cdot)n]$ into their counterparts in the multigroup model.

The first is transformed easily by noting that:

$$f(u)\cdot h^+ \rightarrow \{f_1h_1^+, f_2h_2^+, \dots, f_Nh_N^+\}; \; f_i(u)\cdot h^+ \rightarrow \{f_{i1}h_1^+, f_{i2}h_2^+, \dots$$

$$\dots, f_{iN}h_N^+\},$$

where h^+ is the neutron component of the adjoint static density vector, which in the multigroup model constitutes an N-component vector.

Finally

$$\left(h^+,\bar{f}(u)Pn\right) \rightarrow \sum_{\kappa,j}^{N} \bar{f}_\kappa \nu_j v_j \Sigma_{f_j}(h_\kappa^+, n_j), \tag{53}$$

with

$$\bar{f}_\kappa = (1-\beta) f_\kappa + \sum_{i=1}^{\ell} \beta_i f_{i\kappa}. \tag{54}$$

For the destruction term, use of the explicit definition of [D] leads to

$$\left(h^+,(\vec{v}\nabla + v\Sigma - Z\cdot\ )n\right) \rightarrow - \sum_{\kappa,j=1}^{N} \left\{ \sum_{\ell=1}^{j-1} v_\ell \Sigma_{sj\ell}(h_\kappa^+, n_\ell) + \right.$$

$$\left. + v_j\left(h_\kappa,(\nabla D_j \nabla - \Sigma_{rj})n_j\right)\right\}. \tag{55}$$

With the aid of the transformation relations (53) and (55), it is possible to write down expressions for the three global parameters, namely static reactivity, static generation time and static weighted effective delayed neutron fraction in the general multigroup model:

$$\rho_s = \frac{\sum_{\kappa,j=1}^{N} \left\{ (h_\kappa^+, n_j)\bar{f}_\kappa \nu_j \Sigma_{f_j} v_j + v_j\left(h_\kappa^+, [\nabla D_j \nabla - \Sigma_{r_j}]n_j\right) + \sum_{\ell=1}^{j-1} v_\ell \Sigma_{sj\ell}(h_\kappa^+, n_\ell) \right.}{\sum_{\kappa,j=1}^{N} (h_\kappa^+, n_j)\bar{f}_\kappa \nu_j \Sigma_{f_j} v_j}, \tag{56}$$

$$\Lambda_s = \frac{\sum_{j=1}^{N} (h_j^+, n_j)}{\sum_{\kappa,j=1}^{N} (h_\kappa^+, n_j)\bar{f}_\kappa \nu_j \Sigma_{f_j} v_j}, \tag{57}$$

$$\frac{\beta_{i\,\mathrm{eff}}}{\beta_i} = \gamma_i = \frac{\sum_{\kappa,j=1}^{N} f_{i\kappa} \nu_j \Sigma_{f_j} v_j (h_\kappa^+, n_j)}{\sum_{\kappa,j=1}^{N} (h_\kappa^+, n_j)\bar{f}_\kappa \nu_j \Sigma_{f_j} v_j}. \tag{58}$$

In the dynamic (Chap.III, Eqs. 61,62) multigroup representation the reactivity and the generation time (in this model all delayed neutrons have the same importance i.e. $\beta_{i\,\mathrm{eff}} = \beta_i$) will be given

by:

$$\rho_d = \frac{\sum_{j=1}^{N}\left\{(1,n_j)\nu_j\Sigma_{fj}\nu_j + \nu_j(1,[\nabla D_j\nabla - \Sigma_{rj}]n_j) + \sum_{\ell=1}^{j-1}\nu_\ell\Sigma_{sj\ell}(1,n_\ell)\right\}}{\sum_{j=1}^{N}(1,n_j)\nu_j\Sigma_{fj}\nu_j}, \quad (56a)$$

$$\Lambda_d = \frac{\sum_{j=1}^{N}(1,n_j)}{\sum_{j=1}^{N}(1,n_j)\nu_j\Sigma_{fj}\nu_j}. \quad (57a)$$

By means of the appropriate boundary conditions, the Laplace operator appearing in [M], Eq.1 may be converted into an algebraic operator (e.g. introduction of zonal bucklings), so that,

$$\left\{[M] - w[I]\right\}\vec{n} = 0.$$

The demand for non vanishing solutions for $\vec{n}$, results in the requirement that the determinant of the coefficients vanishes:

$$\left|[M] - w[I]\right| = 0, \quad (59)$$

which provides an equation for the determination of the w's. The number of solutions for w is infinite. To each w corresponds a density vector $\vec{n}$ (both defining a mode) which can be determined from Eq.1 when an additional normalization condition is provided.

In a single zone system (bare reactor) the bucklings are determined solely by the geometry of the system, for instance, for a bare slab-reactor, having extrapolated thickness 2d, $B_q^2 = \left((q\pi)/(d)\right)^2$ $q=1,2,\ldots$ This in turn fixes the density vector $\vec{n}$, and transforms Eq.59 into a simple algebraic equation of order $N+\ell$ for w_q, where w_q belongs to B_q. All w_q's have the same eigenvectors $\vec{n}_q$. This fact may be looked upon as a type of degeneration phenomenon which should, however, be distinguished from degenerate states in quantum mechanics (ref.61), where several wave-functions belong to the same eigenvalue. This degeneration is removed when a new zone is added to the system. Under these circumstances each eigenvalue has its own distribution vector, but nevertheless ℓ of the $N+\ell$ eigenfunctions, representing the contribution due to delayed neutrons, are usually still very closely spaced. These fine structure functions may be thought of as sub mode of the main mode of the degenerate case.

In computing the eigenvalues of the various modes and sub-modes, use may be made of the similarity of the reduced kinetic-equation (reduction by elimination of the delayed neutron precursors) to the corresponding fictitious static equation.

From Eq.1, the balance equation for the μ-th energy-group is:

$$v_\mu[\nabla D_\mu \nabla - \Sigma_{r\mu}]n_\mu + \sum_{j=1}^{\mu-1} v_j \Sigma_{s\mu_j} n_j + (1-\beta) f_\mu S + \sum_{i=1}^{\ell} f_{i\mu} \lambda_i m_i = w n_\mu, \quad \mu = 1,2,\ldots,N, \tag{60}$$

and for the i-th delayed neutron density m_i:

$$\beta_i S - \lambda_i m_i = w m_i, \quad i = 1,2,\ldots,\ell, \tag{61}$$

where:

$S = \sum_{j=1}^{N} \nu_j \Sigma_{f_j} v_j n_j$, is the fission source.

Elimination of the m_i's by substitution of Eq.61 into Eq.60 leads to the following pseudo-static equation for the densities:

$$v_\mu\left[\nabla D_\mu \nabla - \Sigma_{r\mu} - \frac{w}{v_\mu}\right] n_\mu + \sum_{j=1}^{\mu-1} v_j \Sigma_{s\mu j} n_j + f_\mu(w) S = 0, \quad \mu = 1,2,\ldots,N, \tag{62}$$

where the production is according to the kinetic spectrum:

$$f_\mu(w) = (1-\beta) f_\mu + \sum_{i=1}^{\ell} (\beta_i \lambda_i f_{i\mu})/(w+\lambda_i). \tag{63}$$

A straightforward procedure to determine w and the corresponding eigenfunctions would involve a direct w-iteration of Eq.62. It is, however, feasible only for the w's which are generated by the prompt neutrons, while difficulties will be encorentered in the delayed w-iteration due to the strong varying function $\sum_{i=1}^{\ell} \frac{\beta_i \lambda_i f_{i\mu}}{w+\lambda_i}$ which has poles at $-\lambda_i$. In this case an indirect way may be preferable as described next.

Eq. 62 should be compared to the balance equation of the same reactor which is made fictitiously critical by changing the neutron yield per fission: $S \rightarrow \frac{\nu}{\nu_0} S_s$, and consequently $w \rightarrow 0$,

$$v_\mu[\nabla D_\mu \nabla - \Sigma_{r\mu}]h_\mu + \sum_{j=1}^{\mu-1} v_j \Sigma_{s\mu j} h_j + f_\mu(0)\,\frac{\nu}{\nu_o}\,S_s = 0 \qquad (64)$$

where:

$\frac{\nu}{\nu_o}$ is the static eigenvalue

h_μ is the static neutron density of the μ-th group

$f_\mu(0) = \bar{f}_\mu = (1-\beta)f_\mu + \sum_{i=1}^{\ell} f_{i\mu}\beta_i$ (Eq.54),

the static production spectrum

$S_s = \sum_{j=1}^{N} \nu_j \Sigma_{fj} v_j h_j$, the static fission production term.

If the additional "absorption" term, w/v, appearing in Eq.62 can be neglected, then n_μ and h_μ satisfy essentially the same system of linear differential equations, with source terms differing slightly.

The knowledge of $(\nu/\nu_o)_p$, for the p-th mode, then provides a first approximation for the ℓ w's of the same mode; thus w_p is actually $w_{p,i}$, where $i = 1,2,\ldots,\ell$. The approximation involved is due to the neglection of the term w/v and its influence on the kinetic density. By equating the source terms of Eqs. 62 and 64 one gets:

$$(\rho_s)_p \equiv \frac{\nu_o - \nu_p}{\nu_o} = \frac{1}{\bar{f}_\mu} \sum_{i=1}^{\ell} \frac{w_p \beta_i f_{iu}}{w_p + \lambda_i} \,. \qquad (65)$$

This is an algebraic equation of the ℓ-th order for w_p. For positive $(\rho_s)_p$, there are one positive w, and ℓ-1 negative ones. While for negative ρ all the ℓ solutions are negative. In the last case, when $|\rho|$ is not too near to zero, the w's are very nearly equal to λ's. Thus one may claim that these w's are generated by the corresponding delayed neutron groups. On the other hand these eigenvalue are independent of the energy groups (cf. Eq.1). Therefore one can sum the μ-terms in Eq. 65 after multiplying both sides by $\bar{f}_\mu$. Due to the normalization of f_μ and $f_{i\mu}$ one obtains for $w_p^{(1)}$, in the first approximation, the following algebraic equation:

$$(\rho_s)_p \equiv (\rho_s)_p^{(o)} = \sum_{i=1}^{\ell} \frac{w_p^{(1)} \beta_i}{w_p^{(1)} + \lambda_i} \,. \qquad (66)$$

Adding the new "absorption term" $w_p^{(1)}/v_\mu$ to $\Sigma_{r\mu}$ in Eq. 64, one gets

a new fictitious critical eigenvalue ν'/ν_o. Again with the assumption that $(n_p)_\mu \approx (h_p)_\mu$, the second approximation, $w_p^{(2)}$ is obtained from:

$$(\rho_s)_p^{(1)} = \sum_{i=1}^{\ell} \frac{w_p^{(2)}\beta_i}{w_p^{(2)} + \lambda_i} \,. \qquad (66a)$$

This iteration procedure is repeated, say n times, until the desired convergence is achieved. It should be noted, however that $(\rho_s)_p^{(n-1)}$, from which the correct $w_p^{(n)}$ is derived, does not coincide with the actual static reactivity $(\rho_s)_p \equiv (\rho_s)_p^{(o)}$ of the system. They describe reactivity of two systems differing, by the amount $w_p^{(n)}/v_\mu$, in the removal cross-sections.

As long as w/v can be neglected all the ℓ eigenvalues - $w_1, w_2, \ldots, w_\ell$, have the same eigenfunctions given by $\vec{h}_p$ (Chap.III, Eqs.32,34). This situation can again be looked upon as a type of degeneration (cf.). It is removed if one considers the appearance of the additional "absorption" w/v. But, since w/v is rather small for the delayed neutron-eigenvalues, the splitting caused is still very small and the delayed-neutron sub-modes are usually almost identical with the main-mode. This is an important feature of the kinetic solutions. It means that after the higher harmonics have died away the delayed neutrons have the same spatial distribution as neutrons in the fictitious critical reactor, which is characterized by the static reactivity. In other words, the delayed neutron distributions are very similar to the persisting mode, and the latter almost coincides with the zero mode of the virtually critical reactor (see Sec.7).

The above arguments do not hold for the other N solutions for w, which appear due to the separation into N energy groups, and describe the behavior of the prompt neutrons. These w's are much larger than the eigenvalues of the delayed neutrons, which, for the case of $\rho<0$, lie between the largest $|\lambda_i|$ and 0. It might occur that the prompt w/v, particularly for the thermal group where v is smallest, will be of the same order of magnitude as the removal cross-section or even larger as may happen in a heavy water reflector. Therefore the prompt eigenvalues define "sub-modes", which might deviate quite strongly from the static main mode (see Sec.7).

Computation of the different w and the corresponding eigenfunctions for the zero main mode and its sub-modes, or for higher main modes

and their sub-modes, makes use of the similarity between the reduced kinetic equation and the fictitious critical equation, as described above. The sequence of computation is summarized below (an example of such a calculation in two energy-group model is given in Sec. 7 and in refs. 66,67:

a) The eigenvalue of the main mode: the static eigenvalue of the p-th mode is found first. This corresponds actually to a zero approximation for w_i, since w_i/v is assumed to be zero.
b) The eigenvalues of the delayed-neutron sub-modes: first order approximation for ℓ w's ($w_{i,p}^{(1)}$), is found by solving Eq. 66 for w.
c) The first approximation for the "kinetic absorption" $w_{i,p}^{(1)}/v$, is substituted back into Eq. 62 (or into its matrix equivalent), and a second approximation for ν/ν_0 is sought ($\frac{\nu_p}{\nu_0} f_\mu(0)$ is again substituted for $f_\mu(w)$).
d) Second order approximation for w of the p-th mode, $w_{i,p}^{(2)}$ is found from Eq. 66.
e) This procedure is repeated until the desired convergence is reached. Usually, in the two group model, two iterations will suffice.
f) The eigenfunctions of the delayed neutron sub-modes: Using the final $w_{i,p}^{(f)}$, the corresponding eigenfunction is calculated from Eq. 62 including w/v terms and $f_\mu(w)$. The adjoint density and other quantities can also be found, once the w's are known.
g) The eigenvalue and eigenfunction for the prompt neutron sub-mode: for the prompt w_p of the p-th main mode, one can iterate Eq. 62, or its matrix counterpart, directly, since here divergence of the iterations does not arise. A first approximation may be obtained from the equivalent bare system.

Calculation of β_{eff} and Λ for some realistic reactor-models, with the aid of multigroup theory demands at least a few-group multizone computer programme. Nevertheless, since β_{eff} is much more sensitive to spectral effects and less sensitive to geometrical details, it will be sufficient to use either a few-group single zone, equivalent bare system, or a first approximation in the continuous slowing down model, for its computation. On the other hand, the generation time, Λ, and the reactivity ρ, being insensitive to spectral effects, are calculated with a multizone two-group programme RIFIFI (ref. 66), which neglects any spectral difference between prompt and delayed neutrons.

5. APPROXIMATE CALCULATION OF $\beta_{i\,eff}/\beta_i = \gamma_i$.

A minimum of three energy groups is necessary in the multigroup model to adequately describe the spectral effects on the effectiveness of delayed neutrons:

a) The first group describes the average prompt neutrons.
b) All delayed neutrons are born in the second group; thus the same effectiveness is assigned to all delayed neutrons.
c) The third group describes thermal neutrons.

If two fuels are considered, e.g. U^{238}, yielding only fast fissions, and U^{235}, yielding only thermal fissions, then in the multigroup notation, the fission cross-section in each group will be:

$$\Sigma_{f1} = \Sigma_f(238) = \Sigma_f^8 \; ; \quad \Sigma_{f2} = 0 \; ; \quad \Sigma_{f3} = \Sigma_f(235) = \Sigma_f^5 \; .$$

There are, in addition, β_i^5 and β_i^8 for the delayed neutron fraction of the i-th group in U^{235} and U^{238}, Following the separation into three groups, as defined above, it is clear that the spectrum-coefficient f will be:

$$f_{i1} = 0; \quad f_{i2} = 1; \quad f_{i3} = 0; \quad f_1 = 1 \quad f_2 = f_3 = 0.$$

Substituting all parameters into Eq.58 one gets (e.g. in the persisting mode)

$$\beta_{i\,eff} = \frac{\left[\beta_i^8 R^8 + \beta_i^5\right]\left(h_2, n_3\right)\Big/\left(h_1, n_3\right)}{\left[(1-\beta^8)R^8 + (1-\beta^5)\right] + \left[\beta^8 R^8 + \beta^5\right]\left(h_2, n_3\right)\Big/\left(h_1, n_3\right)} \; , \quad (67)$$

where:

$$R^8 = (\nu^8 \Sigma_f^8 / \nu^5 \Sigma_f^5) \cdot (h_2, n_1) \; / \; (h_2, n_3) \quad (68)$$

is the ratio of total weighted fast fissions to the total weighted thermal fissions.

For natural uranium, it is approximately

$$R^8 \cong 1{,}74(\varepsilon - 1) \qquad \text{(ref.68)},$$

where ε is the fast fission factor of the reactor;

n_j - the kinetic persisting mode neutron density of the j-th energy group;

h_j - the adjoint zero static mode density of neutrons from the j-th energy group;

$$(h_\mu, n_j) = \int_R h_\mu(\vec{r}) n_j(\vec{r}) d\vec{r}.$$

Eq.67 shows that the effect of the fast fissions is not necessarily a spectrum effect. It can be taken into account by modifying β_i^5 with the aid of the fast fission factor. A simple result is obtained for the ratio $(h_2, n_3) / (h_1, n_3)$ if the bare system assumption is made. In the bare system all densities have the same spatial distribution, but with different amplitudes. Under the additional assumption of no absorption during slowing down, and no direct contribution of neutrons from the first group to the thermal group, one gets:

$$\beta_{i\,eff} = \frac{\left[\beta_i^8 R^8 + \beta_i^5\right]\left[1 + B^2(\tau_1 - \tau_2)\right]}{\left[(1-\beta^8)R^8 + (1-\beta^5)\right] + \left[\beta^8 R^8 + \beta^5\right]\left[1 + B^2(\tau_1 - \tau_2)\right]}, \quad (69)$$

$$\cong \left[\beta_i^8 R^8 + \beta_i^5\right]\left[1 + B^2(\tau_1 - \tau_2)\right]\left[1 - \left(R^8(1+\beta^8) + \beta^5\right)B^2(\tau_1 - \tau_2)\right]. \quad (69a)$$

where τ_1 and τ_2 are the slowing down areas of fission neutrons and delayed neutrons to thermal energy, respectively.

In most practical cases $B^2\tau \ll 1$ and the result of the first approximation in the continuous slowing down model, Eq.49, reduces to Eq.69a for a single fuel, where β is neglected compared with unity.

Fig.1 demonstrates the dependence of β_{eff}/β on the square of the backling B^2 for different $\tau_2 - \tau_1$.

The large bucklings characterizing highly enriched light water reactors, amplify the spectral difference between the prompt fission neutrons and the delayed neutrons, through the fast leakage probability $B^2\tau/(1+B^2\tau) \cong B^2\tau$. The fast non-leakage probability thus favours the delayed neutrons, since they are born with lower energy, ~0,5 Mev, than the prompt fission neutrons, born with an average energy of ~2 Mev.

For a more accurate calculation by direct integration (Chap.III, Eq.50), or by production-perturbation (III, Eq.55) one has to apply the multizone multigroup diffusion codes (e.g. refs. 69-71). The calculations described in ref. 69, e.g. compare fairly well with the results of a careful substitution experiment, which is also described there.

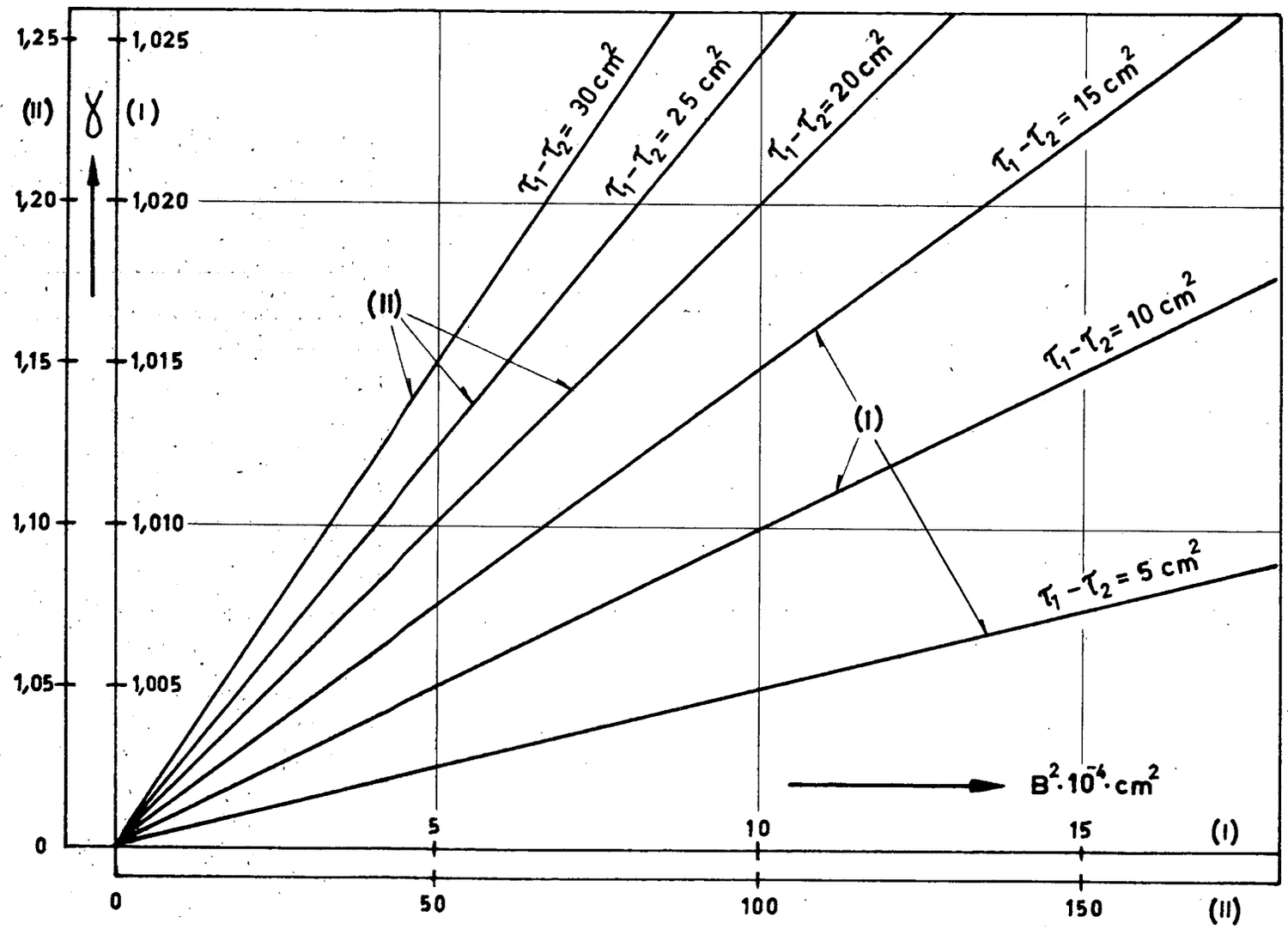

Fig. 1: Delayed neutron effectiveness as a function of buckling.

6. CALCULATION OF THE STATIC GENERATION TIME, Λ.

The static generation time (and the neutron lifetime, as well) depends only weakly on the neutron spectrum. This is evident from the general definition of Λ (III, Eq.49). The contribution of the delayed neutron spectrum $f_i(u)$ to the average static spectrum $\bar{f}(u)$, is only of the order of β_i. Therefore one may expect to get good results by computing Λ, using a normal two group calculation, which does not take into account the difference in the spectra of prompt and delayed neutrons. The most important factor affecting the generation time is the reactor configuration, especially the presence or absence of non-multiplying zones (e.g. reflectors).

The direct computation of the zero mode static generation time for a critical reactor does not involve any approximations, except those inherent in the two group model and its adaptation to multi-zone heterogeneous reactors. By direct computation is meant the application of Eq.57 to the case of two energy groups. With this model, if fast and thermal fissions are included, the generation time will be:

$$\Lambda_{critical} = \frac{(h_1^+, h_1) + (h_2^+, h_2)}{\nu_1^* \Sigma_{f_1} v_1 (h_1^+, h_1) + \nu_2^* \Sigma_{f_2} v_2 (h_1^+, h_2)} , \qquad (70)$$

where:

ν_1^*, ν_2^* = fast and thermal fission yields respectively, in the critical reactor. If the reactor is off-critical, ν_1^* and ν_2^* are not the physical fission yields but fictitious values needed to make the reactor virtually critical.

The calculation of Λ for the actual off-critical reactor by direct application of Eq.56 demands a knowledge of the kinetic flux. In the case under consideration this is the persisting mode. However, as argued in section 4 and demonstrated in Sec.7, this distribution is, to a very high precision, equal to the zeroth mode of the neutron density in the fictitious critical reactor: $\vec{n}(\vec{r}) = \vec{h}(\vec{r})$, and consequently ($\Lambda_a$ = Λ of the actual reactor):

$$\Lambda_a \cong \frac{(h_1^+, h_1) + (h_2^+, h_2)}{\nu_1 \Sigma_{f_1} v_1 (h_1^+, h_1) + \nu_2 \Sigma_{f_2} (h_1^+, h_2)} . \qquad (70a)$$

An alternative method for computing Λ_a or $\Lambda_{critical}$ has been described in Chap.III,Eq.52. This method, which may be used for calculational as well as for experimental purposes, is based on the effect on reactivity of slightly perturbing the entire reactor with a 1/v absorber. The approximations pertinent to this method are:

a) The assumption normally made in perturbation theory that the neutron density in the actual and the perturbed system remains unchanged.
b) The adjoint densities in the virtual critical states before and after perturbation are equal.

If the basic assumption concerning the very close resemblance of the persisting distribution, $\vec{n}$ and its adjoint, to the fictitious critical distribution, $\vec{h}$, and its adjoint is fulfilled, the approximations listed above reduce to the normal assumptions of perturbation theory.

It has been mentioned earlier that occasionally the prompt sub-mode of the essential mode corresponds to an eigenvalue which is particularly convenient to measure (e.g. in a pulsed neutron experiment). To interpret such a measurement in terms of a static reactivity would require using the generation time of this sub-mode instead of that of the persisting mode or that of a critical reactor. The kinetic flux of the prompt sub-mode, as mentioned in section 4, may differ appreciably from $\vec{h}$. This occurs mainly in strongly reflected heavy water reactors. Neglection of the difference between these fluxes may introduce a non-negligible error in the reactivity.

7. EXAMINATION OF THE BASIC KINETIC PARAMETERS IN THE MULTI-GROUP APPROACH

In the preceding chapters some basic features of the kinetic parameters have been discussed on the basis of general reactor theory. In this section the various kinetic parameters will be discussed in more detail, mainly with the aid of the two-group model.

The main points to be elucidated here may be summarized as follows:

a) The very weak sensitivity of the effective fractional yield of delayed neutrons, β_{eff}, to geometrical details of the system.

b) The very strong resemblance between the delayed sub-mode and the main virtual critical mode.

c) The possible deviation of the prompt sub-mode from the main virtual critical mode.

d) The dependence of generation time on reactor configuration and the difference between persisting generation time and prompt sub-mode generation time.

a) The static effective delayed neutron fraction of the i-th delayed group is defined by the multigroup model in Eq.58. The only difference between numerator and denominator of this ratio is due to the difference between the fraction of delayed and prompt neutrons appearing in the various energy groups.

The γ_i of a reactor, which is perturbed by an absorber, will hardly change, because the only changes that result after insertion of an absorber (e.g. control rod) occur in the fluxes. However, these changes usually are much effective in the thermal range, where the difference between the spectra of delayed and prompt neutrons is negligible.

Using Eq.69a, one may write down the approximate ratio of γ_1 to γ_2; i.e. the ratio of effectiveness of delayed neutrons in the perturbed and unperturbed (e.g. critical) systems. Using the definition of static reactivity in the modified one group theory (ref.68)one gets:

$$\frac{\gamma_1}{\gamma_0} \simeq 1 - k_\infty \frac{\tau - \tau_d}{M^2} \rho_1 \quad , \tag{71}$$

where:

τ, τ_d - ages to thermal of prompt and delayed neutrons respectively.

M^2 - migration area.

ρ_1 - static reactivity of the perturbed state.

Eq.71 shows that the perturbation has negligible effect on γ_0. The effect is of the order of ρ_1 which is at most a few percent.

A stringent check on the constancy of γ is its behaviour in a small (high buckling) thermal reactor. For instance in a homogeneous light water moderated U^{235} spherical reactor, having a diameter of 19.90cm (ref.72), the changes in β_{eff} as a function of the volume concentra-

tion of the fuel, U^{235}, is as follows:

TABLE 1

Vol.fraction U^{235}	10^{-4}	$2 \cdot 10^{-4}$	$4 \cdot 10^{-4}$	$6 \cdot 10^{-4}$	10^{-3}
$\beta_{eff} \cdot 10^{-3}$	6,82	7,00	7,45	7,82	8,40

Information on the change of β_{eff} in fast reactors is provided in ref.71. Values of β_{eff} are given for spherical reactors having a Pu^{239}-U^{238} core and a U^{238} blanket.

Tables 2 and 3 show that β_{eff} stays almost constant over a wide range of changes in volume (Table 2) and changes slightly as the energy distribution is changing (Table 3).

TABLE 2

Core-vol. liter	800	1500	2500
$\beta_{eff} \cdot 10^{-3}$	3,902	3,908	3,907

TABLE 3

type	Pu(c)-metal	Pu(c)-oxide	Pu(c)-carbide
$10^{-3} \beta_{eff}$	4,865	4,474	4,644

The arguments and examples above clearly show the global nature of β_{eff} as a kinetic parameter. Therefore, β_{eff} once calculated for a reference system, can be used without further computation in other systems having properties similar to those of the reference system. This is of importance in kinetic measurements of reactivity, where different configurations (e.g. control-rods fully inserted, partially inserted or completly withdrawn) are compared.

b) Since the eigenvalues of the delayed sub-modes are rather small, of the order of the precursor decay constants, the delayed sub-mode eigenfunctions may be considered as those of the perturbed fictitious critical state. The perturbation is an additional absorption of magnitude w/v, (see e.g. Eq.62).

Under almost all circumstances $\Sigma >> w/v$. Even in a heavy-water reactor of the DIORIT type this condition is always fulfilled:

$$(\Sigma \text{ core})_{\text{thermal}} = 7{,}37 \cdot 10^{-3}\ \text{cm}^{-1}$$

$$(\Sigma \text{ reflector})_{\text{thermal}} = 1{,}85 \cdot 10^{-4}\ \text{cm}^{-1}$$

$$(w/v_{th}) \text{ for fastest delayed group} \cong 1{,}4 \cdot 10^{-5}\ \text{cm}^{-1}$$

$$\langle\lambda\rangle/v_{th} \cong 0{,}45 \cdot 10^{-6}\ \text{cm}^{-1},$$

where: $\langle\lambda\rangle$ is the average decay constant of delayed neutrons.

It is evident, therefore, that the delayed eigenfunctions will be very similar to the corresponding virtual critical eigenfunction of the same main mode.

In order to check this point for a real system, a configuration was chosen which will emphasize this fine structure. The configuration studied by means of the two group time dependent model (refs.66,67) is based on the small core, K-132 (A-V, config. DI-4) of the reactor DIORIT, in which a central control rod was inserted. The parameters of the system are given in Appendix V, together with some iterated values of w. The configuration chosen thus gives a relatively high importance to the reflector, in which the assumption of $\Sigma >> w/v$ may not be applied with full rigour.

The most sensitive test to check the difference between the delayed densities and the virtual critical density is a comparison of these densities in the thermal group.

In Fig. 2 , curve (1) shows the persisting thermal density (the sub-mode of the slowest delayed group), $n_{o,oth}$, which is identical with the thermal density of the zero main mode for the virtual critical state. The plotted points show the largest deviation of the thermal sub-mode of the fastest delayed group (see A-V).

The difference between the delayed densities and the virtual critical density, belonging to the fast group, is even less pronounced

(since $v_f >> v_{th}$). These fast densities are plotted in Fig. 3 , curve (1).

The adjoint density , curve (1) Fig. 4 , the current , curve (1), Fig. 5 , and the densities of higher modes curves (1),(3), Fig. 6,7 of the delayed sub-modes are also rather close to the corresponding quantities of the main mode in the virtual critical reactor.

The fact that the delayed neutron distributions in the fast and thermal groups are practically identical with the corresponding distributions in the virtual critical reactor, is rather important. The former distributions, which are measurable, may be used experimentally as a means for determining the static reactivity which characterizes the virtual critical distributions.

c) The eigenvalues of the prompt sub-mode, w_p, may also be considered as some perturbation on the destruction operator of the virtual critical reactor. But since w_p/v might be relatively large, mainly in heavy water reactors, the resulting perturbation is also large. Thus the prompt sub-mode may deviate considerably from the virtual critical main eigenfunction or, which is the same, from the persisting eigenfunction of the same main mode.

This difference is shown in Figs. 2, 6 and 7 for D_2O reactor, configuration DI-4.

The largest deviation occurs naturally in the thermal group, the cross-section of which is strongly modified by the prompt eigenvalue. This is shown in Fig. 2 curve (2), where the prompt thermal density of the zeroth main mode, $n_{o,pth}$, is plotted. In Fig.3 curve (2) $n_{o,pf}$, the prompt fast density of the zeroth main mode is plotted. It shows a much smaller deviation. Fig. 4 shows the deviation between the persisting $n^+_{o,th}$ (curve (1)) from the prompt $n_{o,pth}$ (curve (2)) thermal adjoint density. Fig. 5 shows the corresponding thermal current.

For higher modes the deviation between the prompt sub-mode and the virtual critical main mode are much larger due to the magnitude of the prompt eigenvalues. For example (see also A-V) $w_{op} \simeq -44$, $w_{1p} \simeq -278$ and $w_{2p} = -462$ sec^{-1}. Fig. 6 shows the fast, thermal, delayed, and prompt densities for the first main mode, while Fig. 7 shows the same quantities for the second main mode.

In a light water reactor the deviations mentioned above in each main mode are smaller, as the removal and absorption cross-sections

Fig. 2: (1) Virtual critical main mode density of thermal neutrons, h_{oth} ≡ persisting mode of thermal neutrons in the actual reactor, $n_{o,oth}$.
(2) Prompt sub-mode of the main mode of thermal neutrons, $n_{o,pth}$ (in the actual reactor).

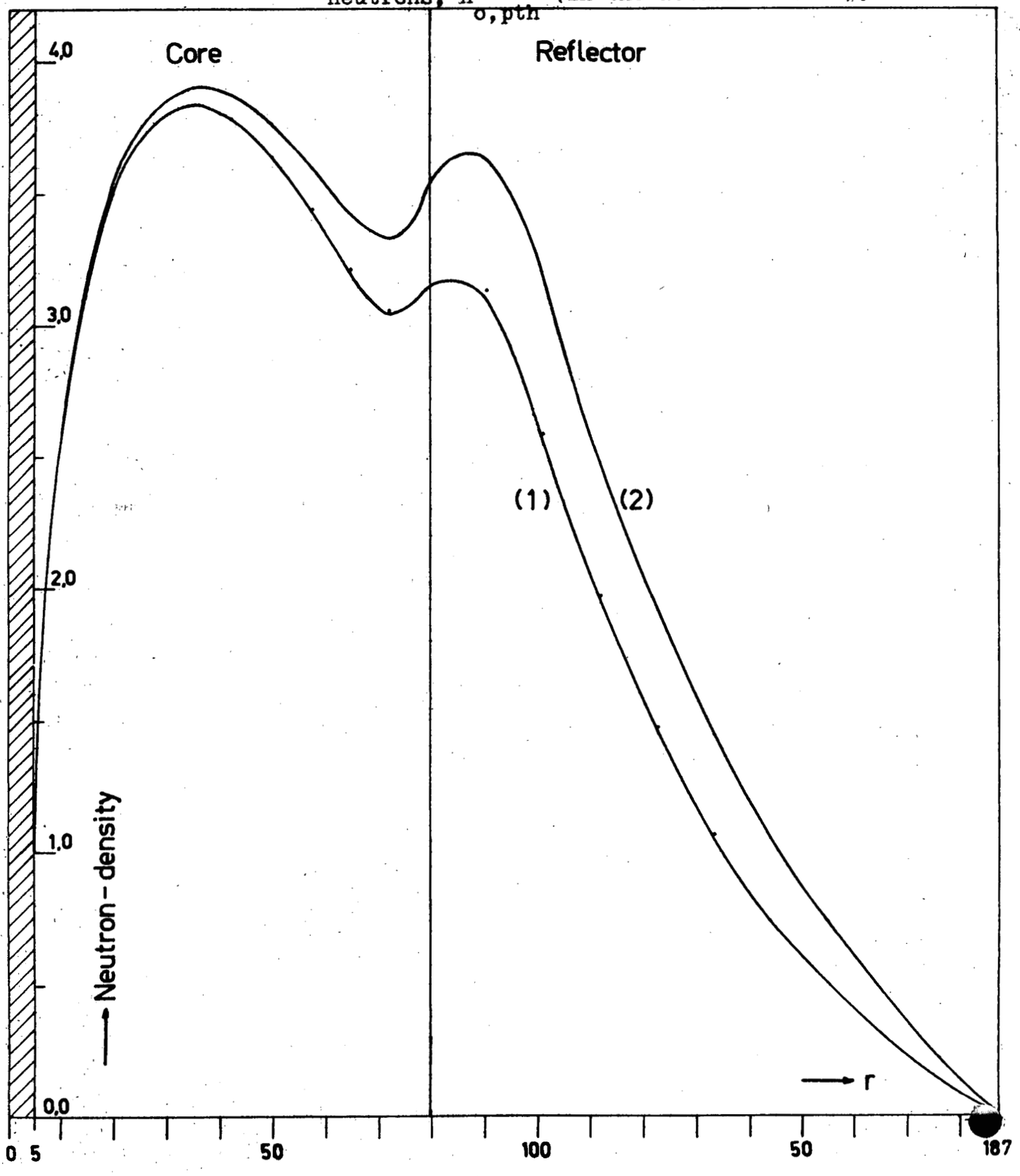

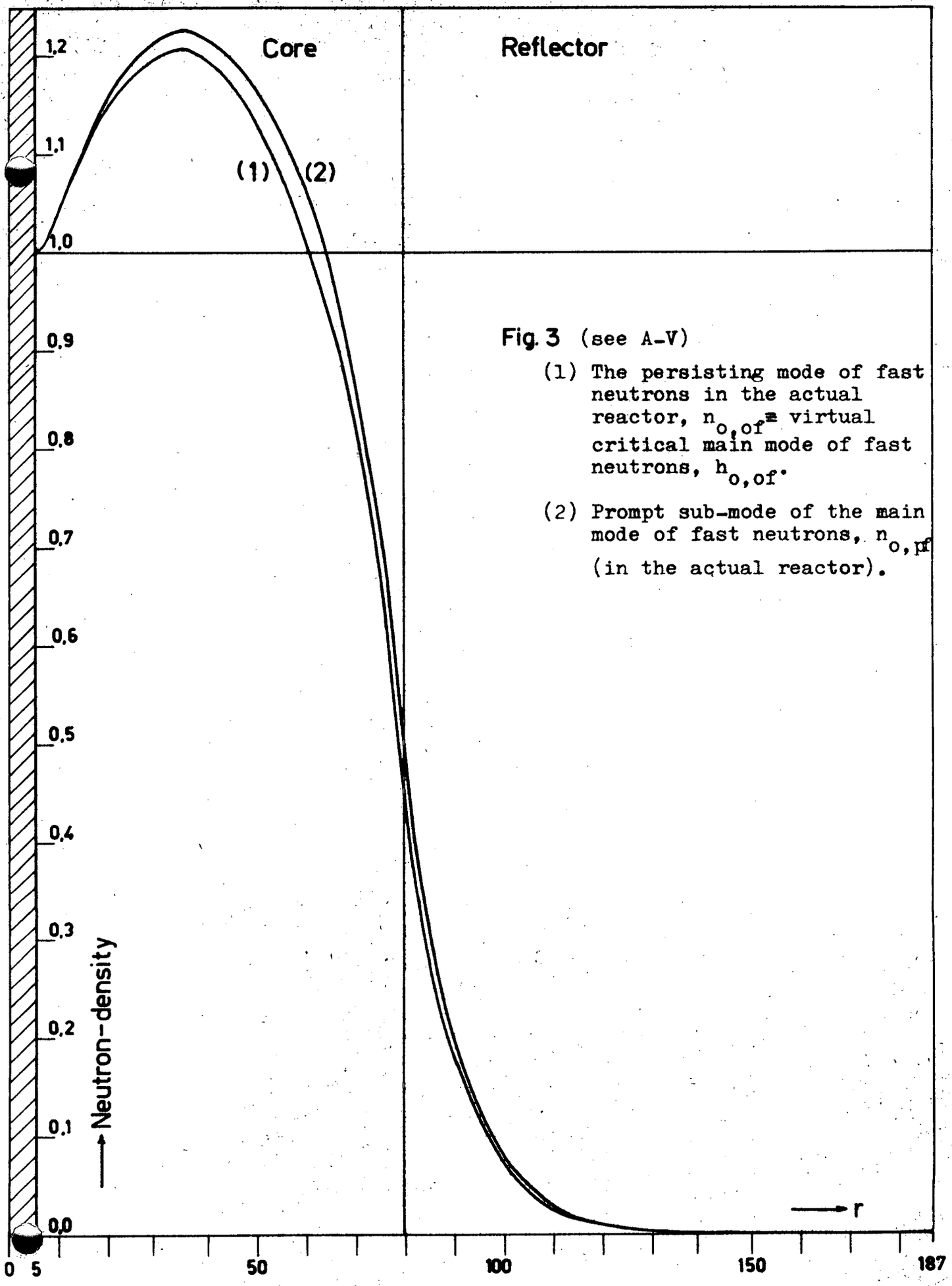

Fig. 3 (see A-V)

(1) The persisting mode of fast neutrons in the actual reactor, $n_{o,of}$ ≡ virtual critical main mode of fast neutrons, $h_{o,of}$.

(2) Prompt sub-mode of the main mode of fast neutrons, $n_{o,pf}$ (in the actual reactor).

Fig. 4 (see A-V)
Adjoint densities
(1) $n^{+}_{o,oth} = h^{+}_{o\ th}$
(2) $n^{+}_{o,pth}$

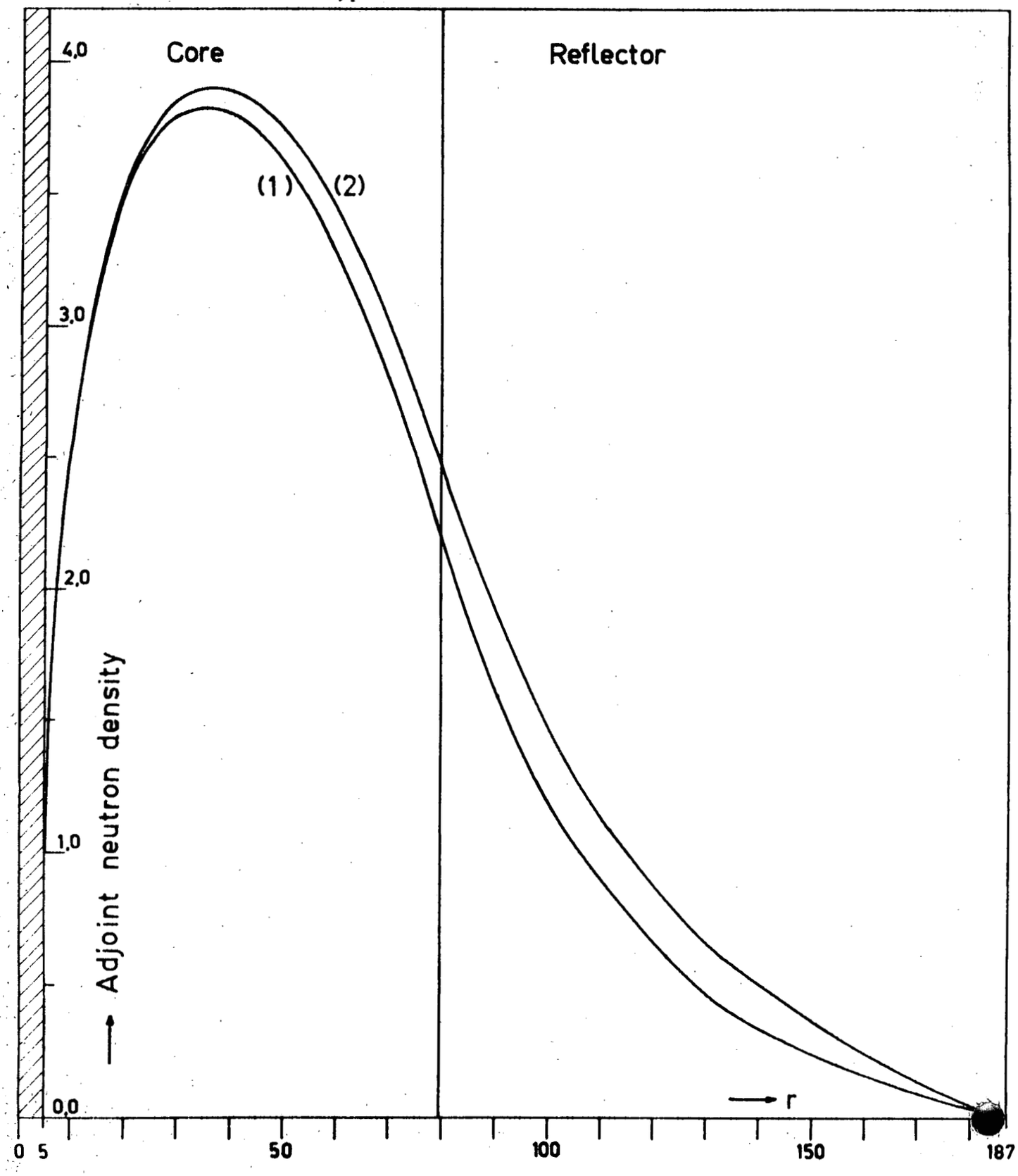

Fig. 5 (see A-V)

Neutron currents: (1) $v_{th}\nabla Dn_{o,oth} = v_{th}\nabla Dh_{oth}$ (2) $v_{th}\nabla Dn_{o,pth}$.

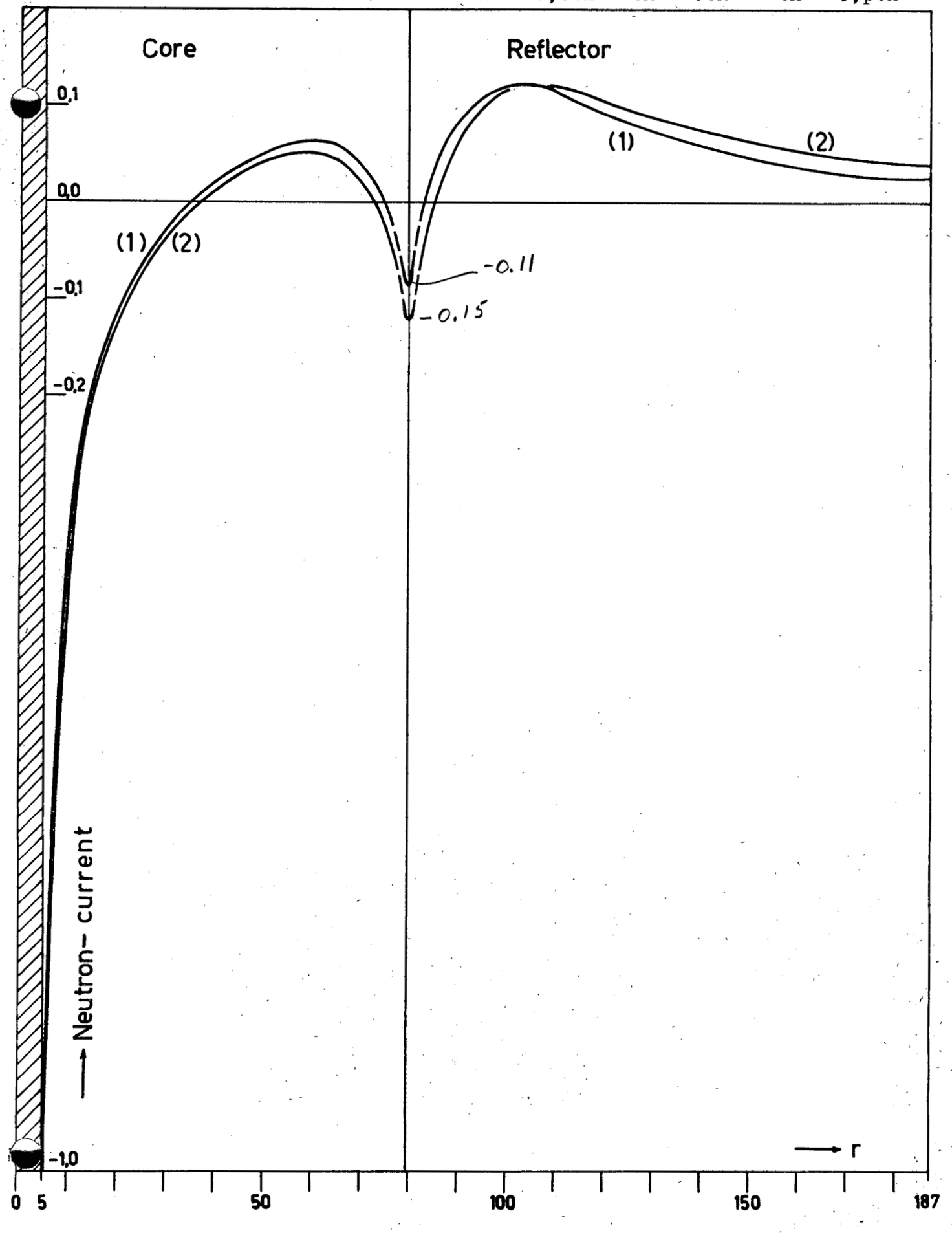

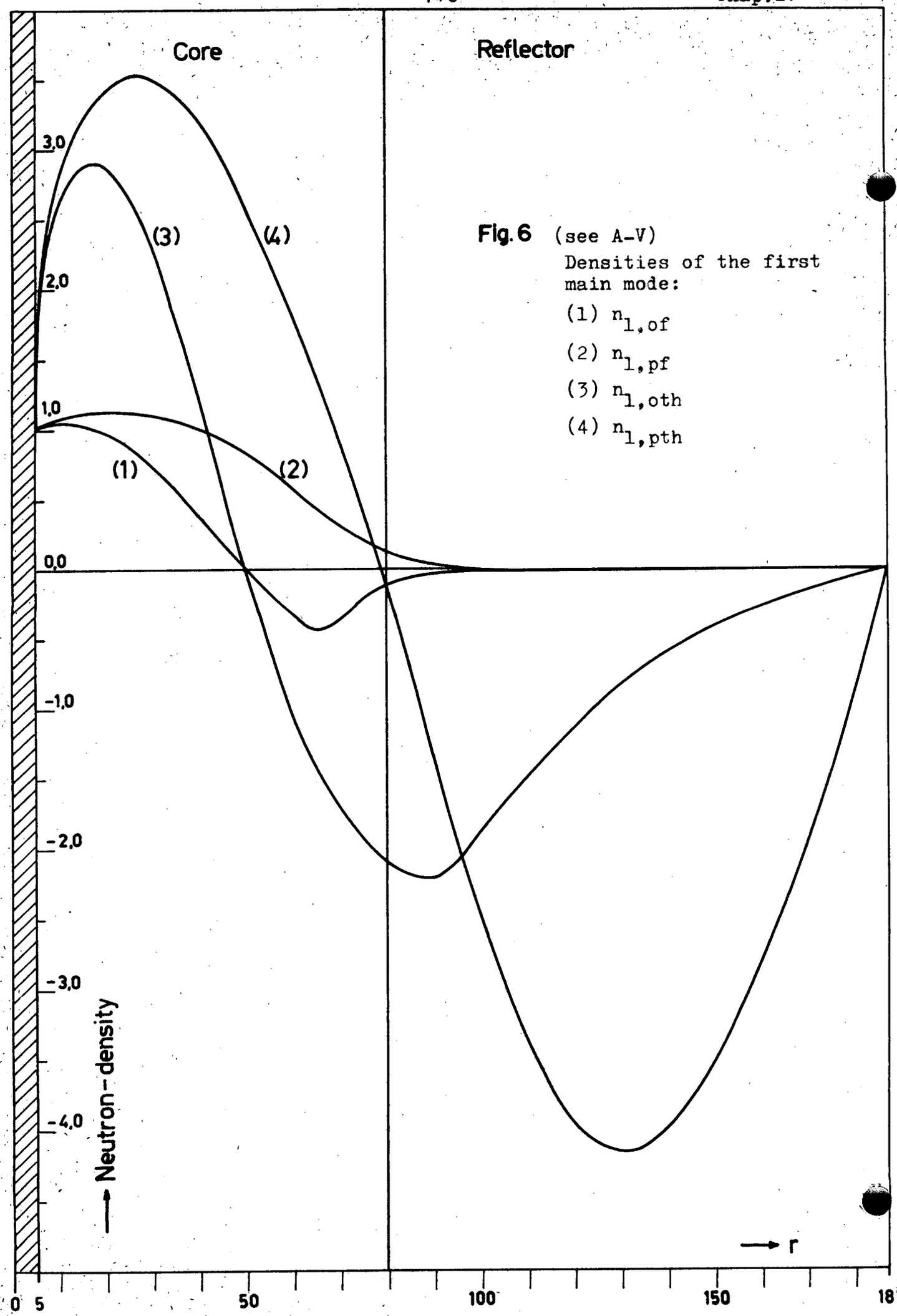

Fig. 6 (see A-V)
Densities of the first main mode:
(1) $n_{1,of}$
(2) $n_{1,pf}$
(3) $n_{1,oth}$
(4) $n_{1,pth}$

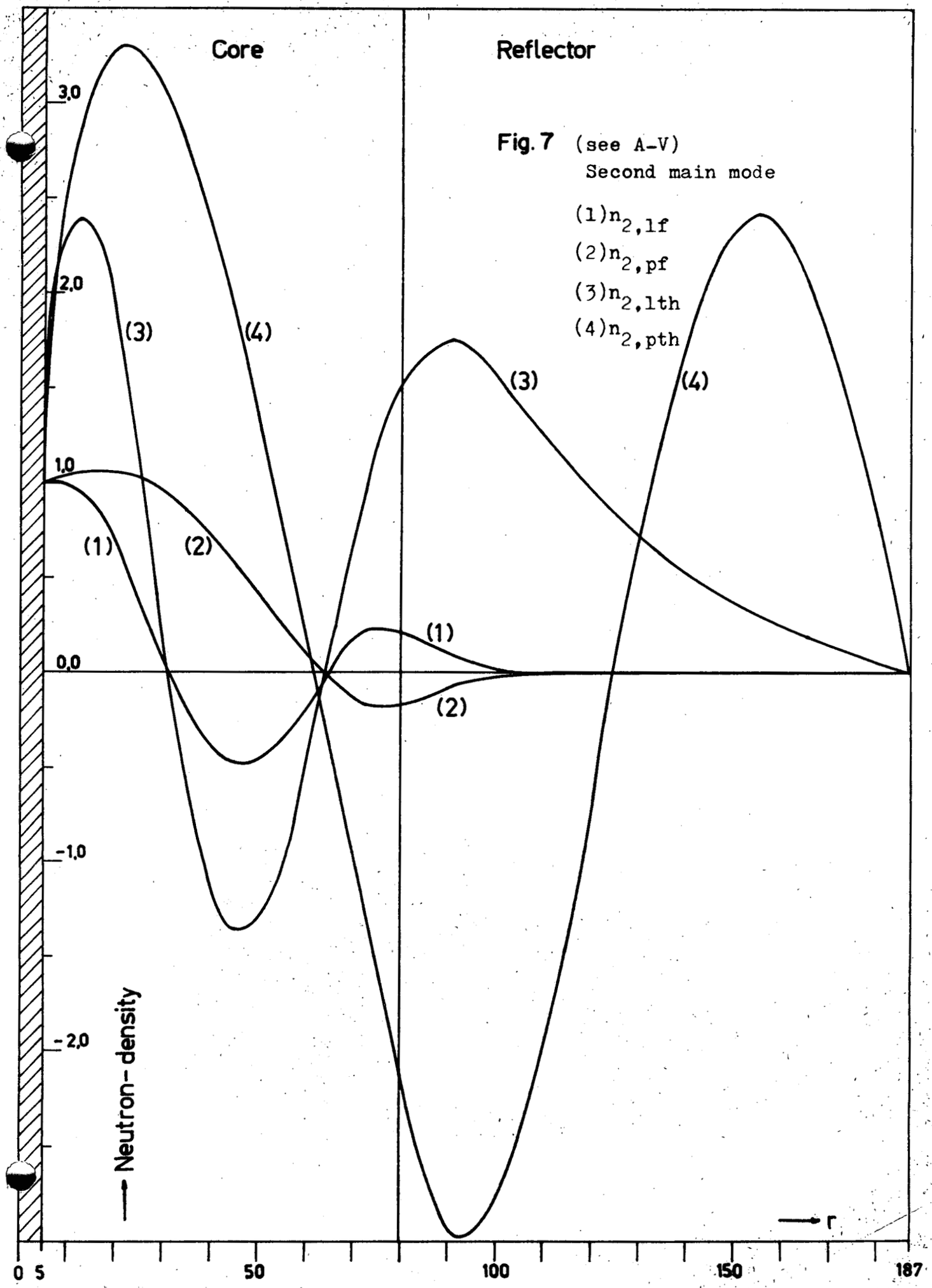

Fig. 7 (see A-V)
Second main mode

(1) $n_{2,1f}$
(2) $n_{2,pf}$
(3) $n_{2,1th}$
(4) $n_{2,pth}$

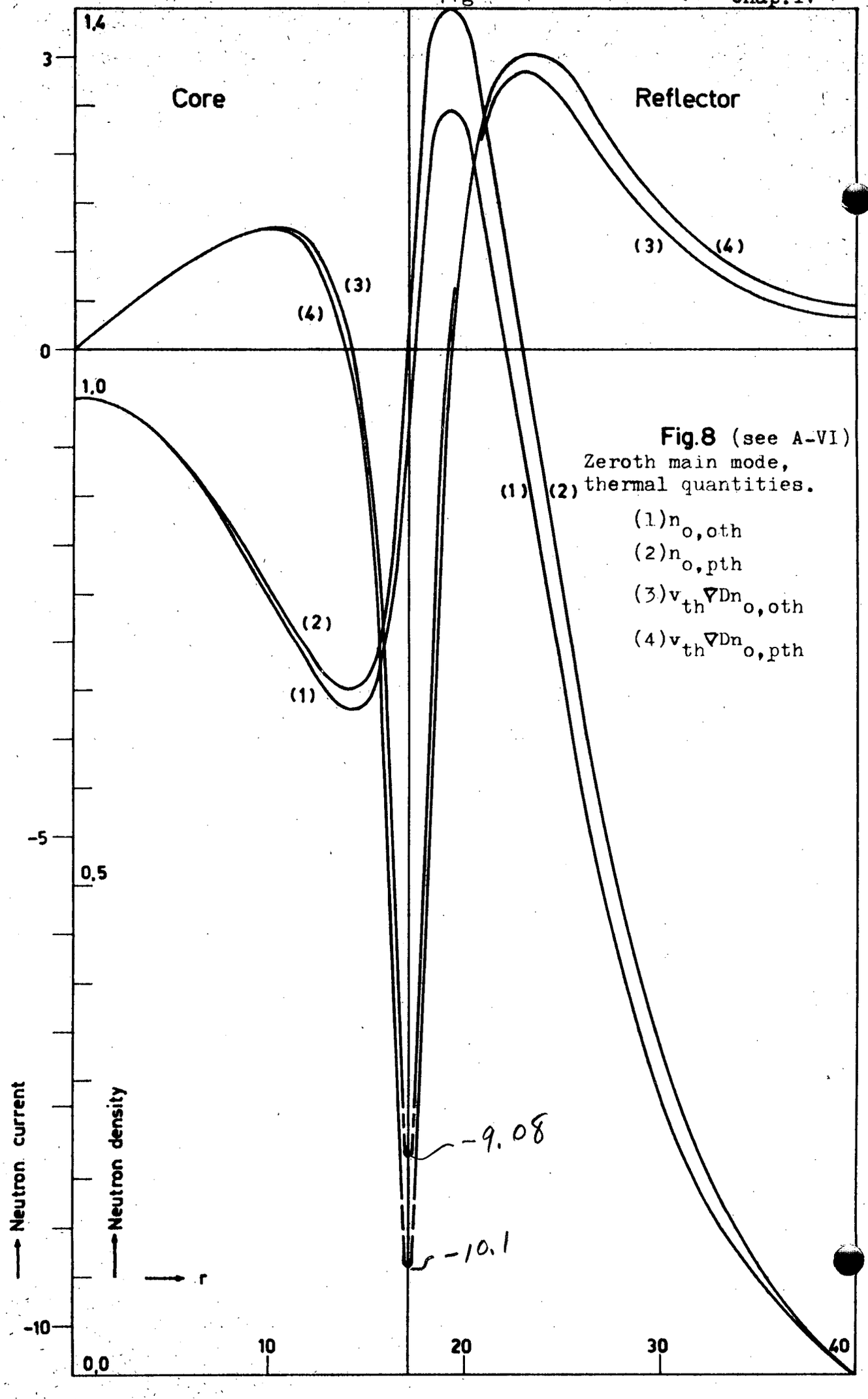

Fig.8 (see A-VI)
Zeroth main mode, thermal quantities.

(1) $n_{o,oth}$
(2) $n_{o,pth}$
(3) $v_{th}\nabla Dn_{o,oth}$
(4) $v_{th}\nabla Dn_{o,pth}$

are much larger than those in heavy water reactors. In Fig. 8 the most sensitive quantities, namely the thermal neutron densities and currents are plotted. These quantities have been calculated in a light water reactor based on the normal loading of the swimming pool reactor SAPHIR (see Appendix VI, configuration SR-1*).

The fact that the prompt sub-mode eigenfunction may deviate appreciably from the persisting eigenfunction or from the fictitious critical eigenfunction which is characterized by the static reactivity has to be taken into account if the prompt eigenvalue is used for the determination of static reactivity, (see also Sec.10, Chap.III).

d) The last two points to be verified are: (1) the difference between the generation time of neutrons distributed in the persisting mode and the generation time of neutrons distributed in the prompt sub-mode of the zeroth main mode, and (2) the dependence of the generation time on the reactor configuration.

The generation time, in any of its definitions, describes the average time taken by a neutron to produce a new fission-neutron. The difference between the various definitions lies in the different weighting functions used for averaging, namely: the kinetic, the static and the dynamic weight-functions (Sec.10, Chap.III).

The main reason for introducing the generation time and the effective delayed neutron fractions as the means to relate the measurable kinetic quantity w, to the global entity ρ, i.e. the reactivity of the system, is their inherent insensitivity to details of the system. It has been shown above that, in fact, β_{eff} is rather insensitive. This result is essential to all methods of reactivity measurements, since β_{eff} establishes the transformation from the relative units, the dollar, to the absolute units of reactivity e.g. mk or percent.

Knowledge of the dependence of the generation time, and in particular of the prompt sub-mode, on reactor configuration is essential to the methods of reactivity measurement, which are based on details of the prompt burst, mainly the pulsed neutron technique.

One is usually able both to calculate and to measure in a reliable manner the generation time in the critical or near critical state of relatively clean configurations. In order to determine the reactivity in a perturbed state (e.g. when a control rod is partially or fully inserted) one should know the generation time in the new state. Therefore the information on the possible changes in genera-

tion time as the result of the perturbation is essential to the precision of reactivity measurements.

As mentioned earlier, the concept of generation time is preferable for a reactor, the control of which is achieved by changing the absorption operator, while the production operator remains unchanged. Thus any change in generation time from one reactor state to another is induced only by a density redistribution. For a reactor which is controlled by changing the production, the life time concept is to be preferred.

It is clear, therefore, that the smaller the change in the neutron distribution as a result of perturbing the reactor by absorbers, the smaller will be the change in the generation time.

In fact it was found experimentally (ref.27) that under constraint of criticality with no fuel or moderator changes, considerable rearrangement of lumped poisons did not cause any change in the generation time, within an experimental accuracy of 1%. These measurements were carried out in hydrogen moderated critical assemblies, with bucklings of the order of $30 \cdot 10^{-4} cm^{-2}$.

A maximum variation of less than 2% in generation time has been observed as bucklings were changed by insertion of safety rods (ref.73). It is evident, however, that extreme rearrangements of absorber could cause larger changes in generation time.

Simultaneous addition of fuel and poison, again under constraint of criticality, will cause an appreciable change in Λ (refs. 73,74).

In the calculations quoted above, the possible difference between the persisting generation time $\Lambda_{o,o}$ and the generation time $\Lambda_{o,p}$ in the prompt sub-mode of the zeroth main mode has been neglected. This is likely to be correct in hydrogeneous reactors. In what follows, this point and other related points will be checked on the basis of two group theory for a typical light water reactor of the SAPHIR type, which will be denoted in the following by SR, and heavy water reactor, of the DIORIT type, which will be denoted by DI. The generation time of the persisting mode in the two group model is given in Eq.70a. In the usual two group notation and with production due to thermal fissions confined to the fast group it becomes:

$$\Lambda_{o,o} = \left[\frac{(h_2^+, \Phi_2) + (h_1^+, \Phi_1)(v_2/v_1)}{(h_1^+, \Phi_2)_c} \right] P_c \, \Lambda_{\infty_2}, \qquad (72)$$

where:

$\Lambda_{\infty 2} = 1/v_2 k_\infty \Sigma_{2c}$ - generation time of thermal neutrons in the infinite core;

p_c - resonance escape probability in the core.

In the numerator the integration is extended over the whole reactor, while in the denominator it extends over the core alone.

$\Lambda_{0,o}$, as mentioned above, may be calculated by applying the 1/v homogeneous poison method (Chap.III,Eq.52):

$$\Lambda_{0,o} = \left(\rho_o - \rho_o'(a)\right) \Big/ a = \left(\nu_o(a) - \nu_o\right) \Big/ \nu a \,, \qquad (73)$$

where:

ρ_o, ν_o - static reactivity of the zeroth main mode, and fictitious fission yield which maintains criticality in the same mode of the off-critical reactor, respectively;

$\nu_o(a)$ - fictitious fission yield at criticality after insertion of the a/v absorber;

ν - energy averaged fission yield of prompt neutrons.

$\Lambda_{0,o}$ calculated from Eq.72 (such calculations will be denoted in the following by a = 0) and Eq.73 coincides in light water and heavy water reactors over a fairly wide range of poison concentrations -a. The fairly weak dependence of $\Lambda_{0,o}$ on a is demonstrated in Table 4 (for the first column, see A-V and A-VI):

TABLE 4

Config. No	-ρ%	a sec^{-1}	$\Lambda_{0,o} \times 10^{-4}$ sec
DI-1	3,23	-0,273	8,6510
"	3,23	-0,5	8,6570
"	3,23	-3,138	8,6766
SR-1	0	-1,0	0,7469
"	0	-10,0	0,7470
SR-1*	4,0	-3,856	0,7829
"	4,0	+3,856	0,7830

In order to study the variation of the persisting and prompt sub-mode static generation times a variety of configurations of DI and SR have been chosen. The details of these configurations are given in Appendices V and VI.

The prompt sub-mode generation-time is calculated from the static inhour equation (Chap.III, Eq.48):

$$\Lambda_{o,p} \simeq \frac{|\rho_c|}{|w_{o,p}|} + \sum_{i=1}^{\ell} \frac{\beta_{i\,o,p}}{|w_{o,p}| - \lambda_i} \qquad \rho_o < 0 \qquad (74)$$

where: ρ_o - static reactivity of the zeroth main mode.

The persisting $\beta_{i\,o,p}$ is used in Eq.74 instead of $\beta_{i\,o,p}$ since the main difference between the prompt sub-mode and the persisting sub-mode is in the thermal range, where the spectral differences are negligible.

Results of the computation are given in Tables 5 and 6.

TABLE 5

Config. No.	D_2O-level mm	k_∞	$-\rho\%$	$-a$ sec^{-1}	$-w_p$	$\Lambda_{o,o}$ 10^{-4} sec	$\Lambda_{o,p}$
DI-1	2346	1,100567	0	0,1		7,140	
"	2346	1,100567	0		10,67		7,156
"	2346	1,100567	core alone	0,1		6,440	
"	2200	1,100567	0,45	0,5		7,141	
"	2200	1,100567	0,45		16,75		7,166
"	2000	1,100567	1,22	1,0		7,146	
"	2000	1,100567	1,22		27,28		7,172
DI-2	1411	1,159399	0	0,5		6,819	
"	1411	1,159399	0		11,15		6,823
"	1253	1,159399	1,80	0		6,850	
"	1253	1,159399	1,80		36,89		6,883
"	1140	1,159399	3,60	0		6,879	
"	1140	1,159399	3,60		62,57		6,932
DI-3	1345	1,201600	0	1		8,088	
"	1345	1,201600	0		9,45		8,139
"	1345	1,201600	core alone	0		6,177	
DI-4	1345	1,201600	3,23	0,273		8,651	
"	1345	1,201600	3,23		43,86		9,043
"	1345	1,201600	core alone	0		6,281	

TABLE 6

Configuration No.	core radius	k_∞	-ρ %	-a sec^{-1}	$-w_p$	$\Lambda_{o,o}$ 10^{-4} sec	$\Lambda_{o,p}$
SR-1	18,7	1,607080	0	-1		0,7438	
"	18,7	1,607080	0		108,53		0,7401
"	18,0	1,607080	1,6	-1		0,7599	
"	18,0	1,607080	1,6		316,30		0,7593
"	17,5	1,607080	2,91	-1		0,7730	
"	17,5	1,607080	2,91		478,85		0,7739
"	17,11	1,607080	4,0	-1		0,7838	
"	17,11	1,607080	4,0		609,00		0,7861
"	16,5	1,607080	5,77	-1		0,8023	
"	16,5	1,607080	5,77		815,29		0,8068
SR-2		1,607090	0	-1		0,7810	
"		1,607090	0		102,89		0,7809
SR-3		1,607150	0	-1		1,0062	
"		1,607150	0		79,79		1,0083

Table 6 shows that in a light water reactor the difference between the generation time of neutrons distributed in the prompt sub-mode and the generation time of neutrons in the persisting mode is negligible. Variation of the generation times within one configuration e.g. SR-1, which is made sub-critical by reducing the core-radius, is noticeable: it is about 7% when ρ is changed from zero to -5,8 %. The presence of a medium of a much longer diffusion length than that of the core, e.g. a graphite reflector (SR-3), considerably increases the generation time.

As expected, the difference between the two generation-times for a typical heavy water reactor is larger. This difference in a given configuration increases as the reactor deviates more and more from criticality. Between the critical configuration of DI-1 and DI-2 there is a homogeneous change in the production (k_∞), which is the main cause for the difference in the Λ's. In DI-3 the comparatively high importance of the reflector is the reason for the increase in generation time, and for the difference between $\Lambda_{o,o}$ and $\Lambda_{o,p}$. The transformation from the critical state, DI-3 to a

sub-critical state, DI-4, is achieved by insertion of a central control rod which causes a strong deformation in the density pattern (see Fig.5,II). This increases the relative importance of the heavy water reflector and thus increases the generation time by ~7 % in $\Lambda_{o,o}$ and ~11 % in $\Lambda_{o,p}$. This fact explains also the fairly large difference, ~4,5 %, between $\Lambda_{o,o}$ and $\Lambda_{o,p}$ in the subcritical state.

The effect of neglecting this difference between $\Lambda_{o,o}$ and $\Lambda_{o,p}$ can be demonstrated by the error introduced in the value of reactivity as deduced from $w_{o,p}$ and the inhour equation, Eq.74.

Suppose that the increase in $\Lambda_{o,o}$ from the critical state to the sub-critical state DI-4 can be calculated exactly: $\Lambda_{o,o} = 8{,}651 \cdot 10^{-4}$ sec. Then the static reactivity with this generation time and $w_{o,p} = 43{,}86\ \text{sec}^{-1}$ is $\rho = 3{,}058\ \%$, instead of 3,23 %. Neglecting the increase in generation time from critical to -3,23 %, would result in $\rho = -2{,}81\ \%$!

In the two group treatment, only one prompt eigenvalue was considered. But, as shown previously, splitting the density into energy groups introduces eigenvalues (and in turn corresponding eigenfunctions) for each group. In most, if not in all experiments for determining reactivity, one is interested in, and is able to measure relatively easily the thermal density. In fact, the prompt sub-mode decays very rapidly and describes the time behaviour during slowing down. In heavy water reactors (e.g. config. DI-1) the fast prompt eigenvalue is about (see A-II) $2 \cdot 10^4\ \text{sec}^{-1}$ with negligible dependence on reactivity, while the thermal prompt eigenvalue is $\sim 0{,}113 \cdot 10^2\ \text{sec}^{-1}$ (for $\rho = 0$) and $1{,}24 \cdot 10^2\ \text{sec}^{-1}$ (for $\rho = -10\ \$$). Thus the thermal prompt neutron density does not even change while the fast prompt density practically vanishes. It is clear, however, that the fast neutron distribution in the various modes deviates considerably from the persisting mode distribution, since the cross sections are drastically perturbed, e.g. $(w_{o,p})_1 / v_2 \cong -0{,}091\ \text{cm}^{-1}$ while $(\Sigma_{\text{core}})_{\text{ther.}} \cong 7{,}4 \cdot 10^{-3}$! for DI-1 and even for SR, $(w_{o,p})_1 / v_2 = -0{,}407\ \text{cm}^{-1}$ for SR-1 while $(\Sigma_{\text{core}})_{\text{ther.}} \cong 0{,}092\ \text{cm}^{-1}$.

Chapter V

MODIFICATION OF THE SOURCE-JERK (S.J.) AND ROD-DROP (R.D.) TECHNIQUES: SHAPE-METHOD AND CORRECTED AMPLITUDE-METHOD

1. INTRODUCTION

In the preceding chapters, particularly in Chap.II, it was demonstrated that the initial density, which plays the basic rôle in the normal S.J. and R.D. techniques, is the main contributor to systematic errors induced by harmonics in the measured reactivity. Any attempt to eliminate these errors may follow two obvious avenues of attack: theoretical correction for harmonics in the initial density, or modification of the experimental procedure and the way of evaluating it.

Numerical corrections, or theoretical arguments for finding measuring points which are essentially free of harmonics, can be found only for simple reactor configurations (refs.75,76,78).In a real multizone complex reactor, theoretical analysis, which can be done on a greatly simplified version of the reactor, may give some hints and helpful suggestions, but by no means the correct solution.

However, a considerable reduction of systematic error due to the harmonics may be achieved by some modification of the experimental technique described previously.

The time dependent density established after a step-change in the source or in the reactivity obviously contains much less harmonics or traces of the initial condition than the initial density itself (Chap.III, Sec.2; Chap. II). In Chap. II the time-integrated density was chosen as the representative for this kinetic behavior for reasons of convenience and because of its use in the integral count method. But, naturally, this choice is not unique. Any measurement based on the kinetic density, with no reference whatsoever to the initial density, will considerably reduce the content of harmonics. It is clear that the correct reactivity (kinetic, static or dynamic) will be obtained if the kinetic flux used for its measurement is the persisting mode. But this distribution is insensitive to reactivity from about $\rho<-0,3\$$ on downwards. Therefore one can not afford to wait for the establishment of the persisting mode, and one is obliged to use the kinetic density, which will inevitably include some amount of harmonics. Fortunately, however, this harmonics content is rather small (Chap.II, Sec.4). The neutron population a few generation-times after the step is practically due to the delayed neutrons alone. As proven in Chap.IV, apart from delayed neutron harmonics, their distribution is practically identical with that of the persisting mode, thus yielding the correct reactivity if consistently

defined generation-time and $\beta_{i\,eff}$ are used.

Another approach is to find experimentally, if possible, the correction factor for the harmonics of the initial density.

2. THE SHAPE METHOD

2.1 Description of the method

Considering the reactivity as the only unknown parameter in the kinetic density, then the form of the decay curve, or its shape, is determined solely by the reactivity of the system.

Generally the delayed neutron distribution is a very weak function of reactivity. If the multiplication constant of the system is small, the neutron production, following the withdrawal of the source or the insertion of a strong absorber, will be essentially due to the radioactive decay of the precursors. An increase in the multiplication constant will slow down the decay of the neutron population. Since these decay constants are limited to the range lying between zero (for critical systems) and the corresponding decay constants λ_i (for $\rho = -\infty$), the whole dependence is clearly weak, the faster groups being more affected. The first part of the decay curve is, therefore somewhat more sensitive to the reactivity than the remainder. Thus, any measurement which uses the delayed neutron density is destined to be insensitive towards reactivity. This is evidently the biggest disadvantage of the "shape" method.

Among the many ways of measuring the shape, those giving higher weight to the first few seconds after the step are to be preferred. A straight-forward utilization of the ratio of the zeroth moment to the first moment with respect to time (ref.39, pp 9,11) is not to be recommended. Such a choice gives higher importance to later times and thus results in poor sensitivity; for instance, a 1 % error in the ratio of the moments results in a 30 % error in a reactivity of -10 $.

It was found convenient to determine the reactivity from a measured "shape-index". This index is just the ratio of suitable time integrals of the decaying densitiy, n(x,t):

$$f_{sh}(\rho,x) = \int_{t_1}^{t_2} n(x,t)dt \Big/ \int_{t_3}^{t_4} n(x,t)dt, \qquad t_1<t_2<t_3<t_4. \qquad (1)$$

If the measurement would be carried out on the persisting mode, then one would have,

$$f_{sh}(\rho,x) \rightarrow f_{sh}(\rho) = \int_{t_1}^{t_2} n_0(x)T_0(t)dt \Big/ \int_{t_3}^{t_4} n_0(x)T_0(t)dt =$$

$$= \int_{t_1}^{t_2} T_0(t)dt \Big/ \int_{t_3}^{t_4} T_0(t)dt, \qquad (2)$$

where $T_0(t)$ is the time dependent part of the density, and is the same everywhere throughout the reactor. When dealing with the persisting mode, the index zero will be dropped out and T(t) will describe the count-rate at the point of measurement.

If the harmonics contribution is indeed negligible, as has been argued, the experimental $f_{sh}(\rho,x)$ can be compared with the theoretically calculated $f_{sh}(\rho)$ to determine the reactivity. $f_{sh}(\rho)$ may be calculated either with the aid of the space independent model (ref. 41) or from the space integrated model (Chap.II, Sec.10).

The choice of times t_1, t_2, t_3 and t_4 is not dictated by the sensitivity of $f_{sh}(\rho)$ to reactivity alone, but also by the problem of statistical accuracy in the presence of background. For example, a larger t_3 and t_4 may be desirable at first sight, since the later portion of the decay curve contains almost no information on reactivity. However, such a choice would add little of the desired signal and a great deal of the background, thus seriously reducing the statistical precision. A relatively large interval t_1-t_2 would be desirable from the statistical point of view, but undesirable from the point of view of sensitivity.

Using the above mentioned arguments and comparing the normalized time dependent parts, $T(t)/\int_0^\infty T(t)dt$, (ref. 39, p.7a) for different reactivities, the following times have been chosen:

t_1 = 0 or 1 sec; t_2 = 5 sec; t_3 = 8 sec; t_4 = 30 sec.

$f_{sh}(\rho)$ for these time intervals has been calculated for the following two cases with the computer programmes AGAMA and GFUNK (ref. 78):

Light water reactor, Λ^*=0,01 sec (SR-case)						
i	1	2	3	4	5	6
λ_i sec^{-1}	3,87	1,40	0,311	0,1155	0,0317	0,0127
β_i/β	0,026	0,128	0,407	0,188	0,213	0,038

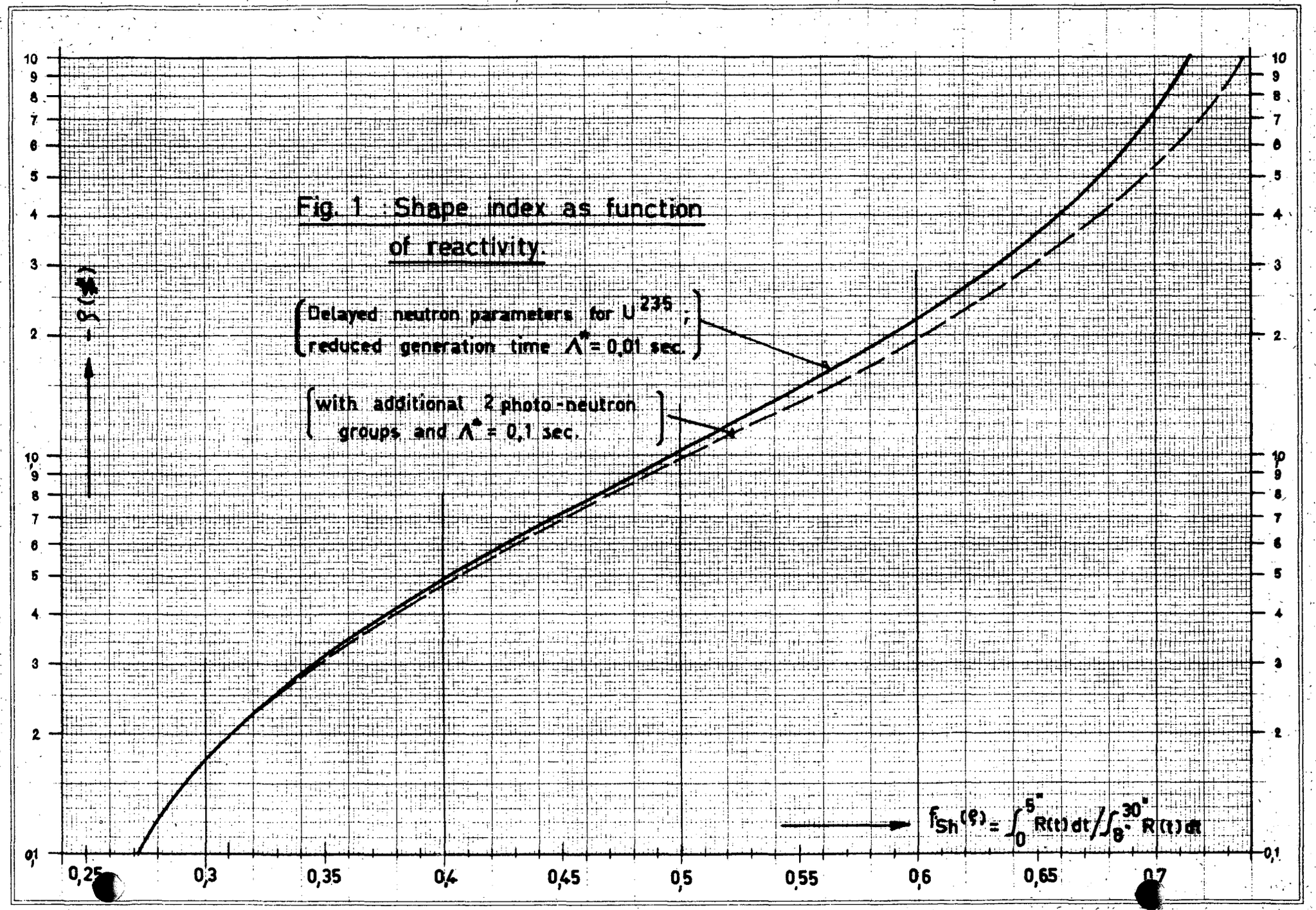

Logar. Teilung / Division 1 - 100, Einheit / Unité 83,33 mm

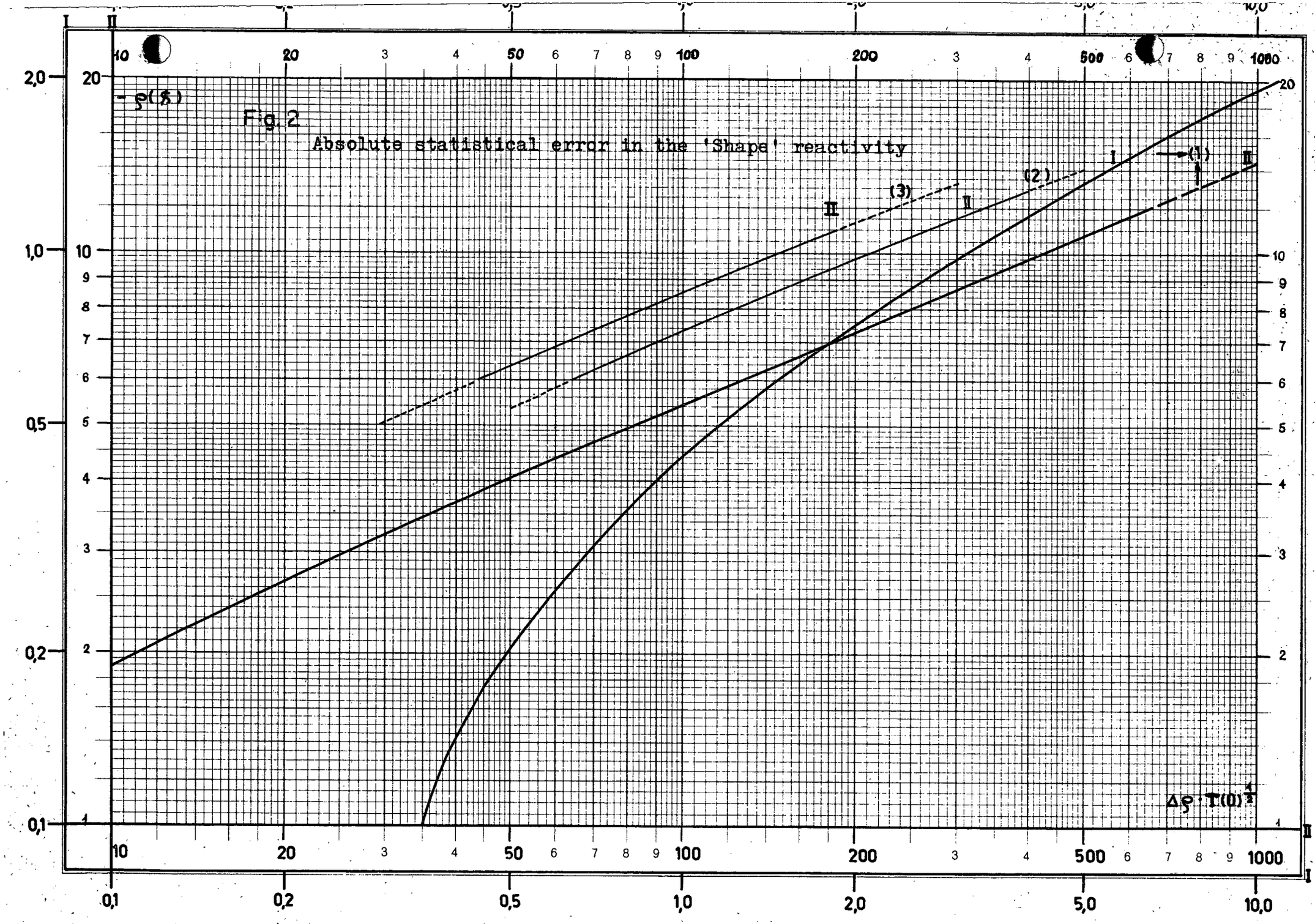
Fig. 2
Absolute statistical error in the 'Shape' reactivity
- ρ(%)
Δρ · T(0)^½
(1)
(2)
(3)
I
II

Heavy water reactor, Λ^*=0,1 sec (DI-case)								
i	1	2	3	4	5	6	7	8
λ_i sec^{-1}	3,87	1,40	0,311	0,277	0,1155	0,0317	0,0169	0,0127
β_i/β	0,025	0,122	0,390	0,033	0,180	0,204	0,010	0,036

$f_{sh}(\rho) = \int_0^5 T(t)dt \int_8^{30} T(t)dt$, for both cases is given in Fig.1.

2.2 Sensitivity and statistical precision

The low sensitivity of the shape index is reflected in the error induced by the statistical fluctuations of $f_{sh}(\rho)$ in the reactivity. The symmetrized error ε in the measured reactivity as a function of reactivity is obtained from

$$\varepsilon(\rho) = \frac{\text{relative statistical error}}{\text{relative sensitivity}} = \left(\frac{\Delta f_{sh}}{f_{sh}}\right)_{statis.} \Big/ \frac{1}{f_{sh}} \frac{\partial f_{sh}(\rho)}{\partial \rho} = \frac{\Delta\rho}{T(0)^{1/2}} \quad . \qquad (3)$$

$\varepsilon(\rho)$ for $T(0)$ equal one is plotted in Fig.2. It shows that high statistical precision in $f_{sh}(\rho)$ is needed for a reasonably accurate value of reactivity in far subcritical states.

A possible improvement in the sensitivity may be achieved by the use of a weight function for the experimental signal. Since most of the information concerning the reactivity is concentrated in the first portion of the decay curve, it would be reasonable to amplify this portion with the aid of a theoretical weight function, $W(t)$, which does not fluctuate statistically. Otherwise the gain in sensitivity would be overridden by the increase in statistical error.

If the statistical error of the total count in the interval $t_j - t_i$ is:

$$\Delta\left\{\int_{t_i}^{t_j} T(\rho,t)dt\right\}_{statis.} = T(0)^{1/2} \sqrt{\int_{t_i}^{t_j} R(\rho,t)dt} \quad , \qquad (4)$$

where:

$T(0)$ = initial count-rate

$R(\rho,t) = T(\rho,t) / T(0)$ = relative count-rate.

then it can be shown that the statistical error of the weighted total count in the same time interval will be:

$$\Delta\left\{\int_{t_i}^{t_j} T^*(\rho,t)dt\right\}_{statis.} = T(0)^{1/2} \sqrt{\int_{t_i}^{t_j} W^2(t)R(\rho,t)dt}, \qquad (5)$$

where:

$T^*(\rho,t) = W(t)T(\rho,t)$ = weighted count-rate.

A weight function which is appropriate for this purpose will be the theoretical $R(\rho,t)$ to an arbitrary power: $W(t) = R^{\nu}(\rho_1,t)$.

The best amplification is achieved if the weight function is calculated for the measured reactivity. The statistical accuracy of the reactivity derived from the weighted shape indices for $\nu = 1$ and $\nu = 2$ has been calculated (for the SR-case) and plotted in Fig.2, curves (2) and (3). Comparison of these courves with curve (1), in which the weighting function is unity, reveals a considerable reduction in the error. Such a weighting procedure need not necessarily be done by electronic means. It can be done as well by step-wise weighting and integration, if the experimental $R(\rho,t)$ is known in these integration steps. The result does not depend strongly on the integration steps, Δt, when $\Delta t \leq 1,5$ sec.

Some disadvantage still exists because the reactivity must be known a priori. However if the first value is reasonably well estimated from the experimental results of the normal method, a better approximation will result from the above mentioned weighting procedure.

2.3 Counting losses

The poor sensitivity of the shape method may be partially overcome by having, if possible, high initial count-rates, thus measuring the shape index $f_{sh}(\rho)$ with very high precision, which in turn yields the reactivity with fair precision. The use of a very high count rate introduces counting losses due to dead-time of the counter and of the whole electronic system.

However, it is to be expected that the shape index will be rather insensitive to counting losses, primarily due to the lack of any reference to the initial count-rate, and secondly due to the fact that f is a ratio of two quantities whose physical nature is essentially the same.

The effect of counting losses on the shape index can be calculated

Fig. 3

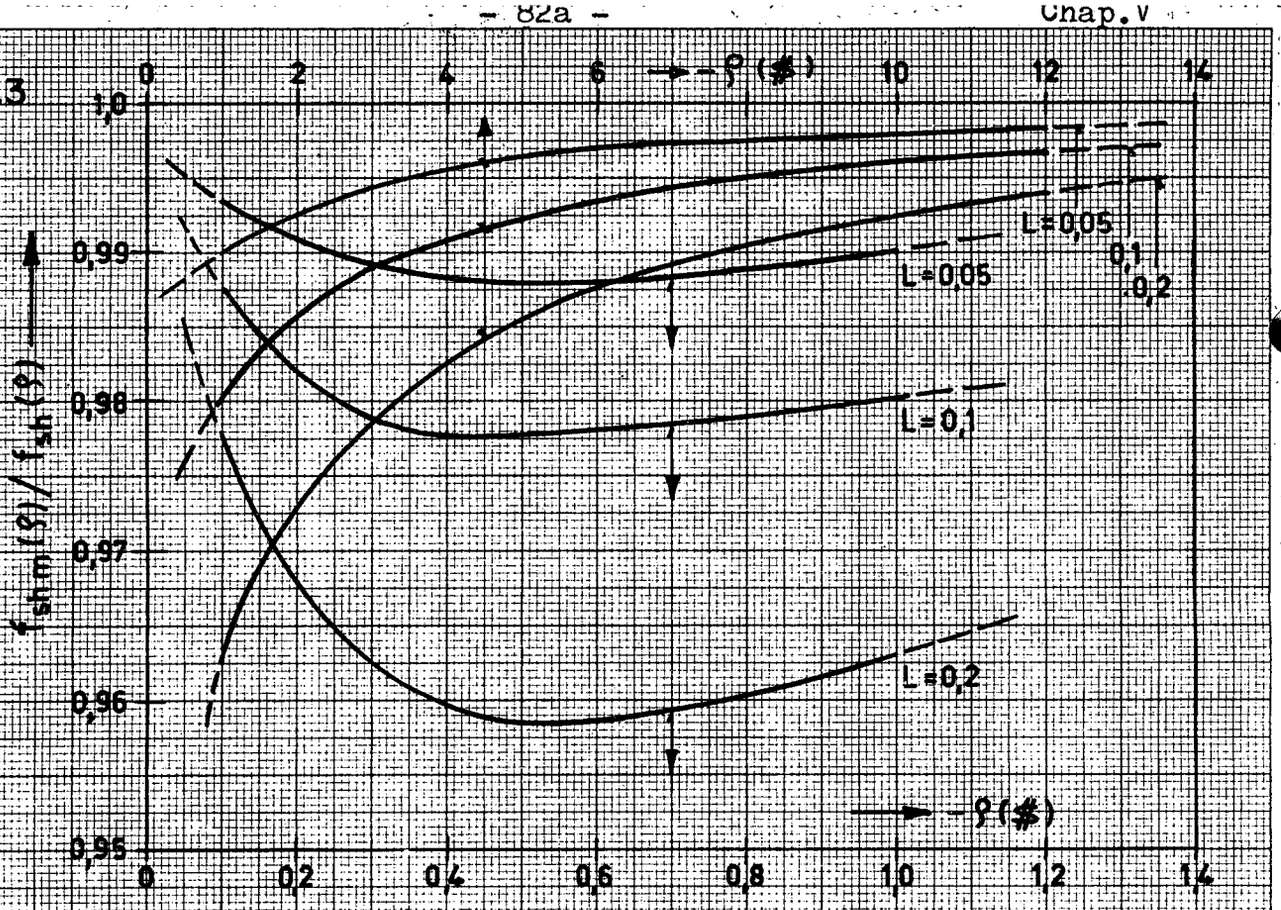

a) Counting-loss effect on the shape index.

Reverse addresses

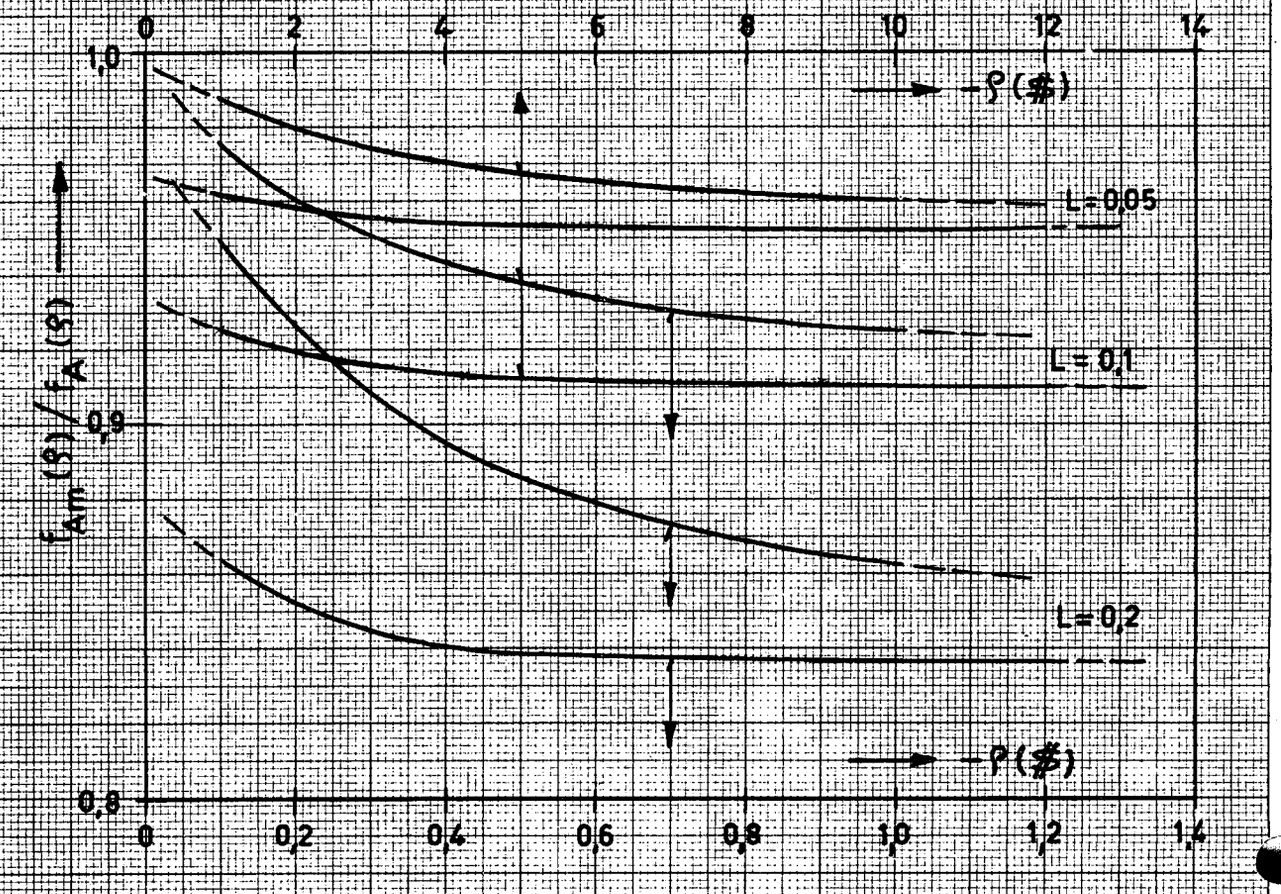

b) Counting loss effect on the amplitude index.

from the following expression:

$$\frac{\left[f_{sh}(\rho)\right]_m}{f_{sh}(\rho)} \cong \frac{1 - L\int_{t_1}^{t_2} R^2(t)dt \Big/ \int_{t_1}^{t_2} R(t)dt + L^2 \int_{t_1}^{t_2} R^3(t)dt \Big/ \int_{t_1}^{t_2} R(t)dt \ \ldots}{1 - L\int_{t_3}^{t_4} R^2(t)dt \Big/ \int_{t_3}^{t_4} R(t)dt + L^2 \int_{t_3}^{t_4} R^3(t)dt \Big/ \int_{t_3}^{t_4} R(t)dt \ \ldots} . \qquad (6)$$

This expression is based on the assumption that the losses are in the linear region. Thus one can write (m = measured):

$$Tm(t) = T(t) \ / \ [1 + \tau T(t)] \cong T(t)\ [1 - \tau T(t) + \tau^2 T^2(t) \cdot \ldots], \qquad (7)$$

where:

$Tm(t)$ - measured count-rate (which includes counting losses)

τ - dead time (in seconds)

$L = \tau T(0)$ - initial counting losses.

Eq.6 is plotted in Fig.3(a) for L = 0,2; 0,1 and 0,05.

2.4 Systematic errors due to harmonics

The order of magnitude of the systematic errors involved in the shape index can be found by using the one-group harmonics calculation presented in Chap.II and Appendix I. The final results thus strictly apply to the case of an S.J. experiment in a subcritical homogeneous bare system.

With use of Eqs. A-I,6 and Chap.II,13 one can write for the integral:

$$\int_{t_i}^{t_j} n(x,t)dt = \Lambda^* Q_0(0) n_0(x) \sum_{\mu=0}^{\ell} [A_{0\mu}/\gamma_{0\mu}^2][\exp(\gamma_{0\mu} t_j) - \exp(\gamma_{0\mu} t_i)] +$$

$$+ \Lambda^* \sum_{p=1}^{\infty} Q_p(0) n_p(x) \sum_{\mu=0}^{\ell} [A_{p\mu}/\gamma_{p\mu}^2][\exp(\gamma_{p\mu} t_j) - \exp(\gamma_{p\mu} t_i)]. \qquad (8)$$

Some simplification may be achieved if one recalls that the modal reactivities, even of the first modes, have a large absolute value (see e.g. A-5). This means that the solutions for delayed neutrons of the inhour equation practically coincide with the decay constants λ_i. The dependence on the modal index is weak. In view of this one may

make the following substitution:

$$\sum_{\mu=0}^{\ell} [A_{p\mu}/\gamma_{p\mu}^2][\exp(\gamma_{p\mu} t_j) - \exp(\gamma_{p\mu} t_i)] = E_{i,j}/\rho_p^2, \qquad (9)$$

where:

$$E_{i,j} = \lim_{\rho_p \to -\infty} \left\{ \rho_{p\mu=0}^2 \sum_{\mu=0}^{\ell} [A_{p\mu}/\gamma_{p\mu}^2][\exp(\gamma_{p\mu} t_j) - \exp(\gamma_{o\mu} t_i)] \right. ,$$

$$= \sum_{\mu=0}^{\ell} [b_\mu/\lambda_\mu][\exp(-\lambda_\mu t_j) - \exp(-\lambda_\mu t_i)]. \qquad (9a)$$

Substitution of Eq.9 into Eq.8 and of the latter into the definition of $f_{sh}(\rho,x)$, leads to:

$$f_{sh}(\rho,x) = f_{sh}(\rho) \left\{ 1 + \frac{r(x) - 1}{\int_{t_1}^{t_2} R(t)dt} \frac{E_{1,2} - E_{3,4}\, f_{sh}(\rho)}{\rho} \right\}, \qquad (10)$$

where:

$$r(x) = \sum_{p=0}^{\infty} Q_p n_p(x) / \rho_p^2 \Big/ Q_o n_o(x_o) n_o(x) / \rho_o^2 \qquad (11)$$

$$= \left[\int_o^{\infty} n(x,t)dt \right]_{nor} \Big/ n_o(x), \quad \text{(see Eq.A-I-14a)} \qquad (11a)$$

For the chosen t_i, t_j, namely: $t_1 = 0"$, $t_2 = 5"$, $t_3 = 8"$ and $t_4 = 30"$ one gets: $E_{0,5} = 3{,}012$ $E_{8,30} = 3{,}982$. For $\rho = -10$ ~~%~~ and with a rather large fraction of harmonics in the time-integrated density: $r(x) = 1{,}1$, it is found that $f_{sh}(\rho,x) / f_{sh}(\rho) - 1 = 0{,}577$ % .

Taking into account the approximations made, the error due to harmonics in a typical experiment is even smaller.

3. THE AMPLITUDE METHOD

3.1 Description of the method and its systematic errors

In this modification one is looking for an approximate corrected initial density. It applies essentially to the S.J. technique combined, for example, with the integral count method (Chap.II, Sec.2)

The normal amplitude index is defined as:

$$f_A(\rho,x) = n(x,0) \Big/ \int_{t_i}^{t_j} n(x,t)dt \,/\, (t_j - t_i). \qquad (12)$$

If the measurement could be carried out in the persisting mode then:

$$f_A(\rho,x) \to f_A(\rho) = T(0) \Big/ \int_{t_i}^{t_j} T(t)dt \,/\, (t_j - t_i) = (t_j - t_i) \Big/ \int_{t_i}^{t_j} R(t)dt. \qquad (13)$$

For reasons of statistical precision the following times were chosen: t_i = 0" or 1" and t_j = 30". $f_A(\rho)$ for the interval 0-30 for SR and DI is plotted in Fig.4.

Since the denominator, i.e. the time integrated density, contains a negligible amount of harmonics, compared to the initial density, the harmonics content of $f_A(\rho,x)$ is given essentially by that of the initial flux $n(x,0)$. The ratio $r(x,0) = [n(x,0]_{nor.} / n_0(x)$ is plotted in Figs.2,3,4, Chap.II, for a slab reactor. Since $f_A(\rho)$ varies almost linearly with reactivity, the systematic error of $f_A(\rho)$ introduces about the same error in the reactivity. As seen in the last figures, this error is rather large.

In order to avoid such a large error, one is obliged to conduct the measurement at a point where the harmonics as a whole, or their main part, vanish (ref.39,p.13). Such a point can only be found in simple configurations, whereas in real configurations its existence is of little practical importance. However, far from the perturbed region, there is a region where the actual density deviates by a small negative, almost constant, amount from the persisting mode (see Figs.II-2, 3,4 and in particular Fig.II-5). This is due to the fact that virgin neutrons as well as those belonging to the first few generations have very low probability of arriving in this region. The neutrons which do arrive there "forget" their history and their initial distribution and assume a distribution close to the persisting mode. This fact is seen very clearly in Fig.II-5, which illustrates the cylindrical case. It is seen that the local flux depression resulting from control-rod insertion is very strong, but that a few migration lengths from the center, there is nevertheless only a small negative deviation of the actual density from the persisting one. Thus a measurement at point x_o in this region, if accessible, would introduce a comparatively small error, or $f_A(\rho,x_o) \approx f_A(\rho)$.

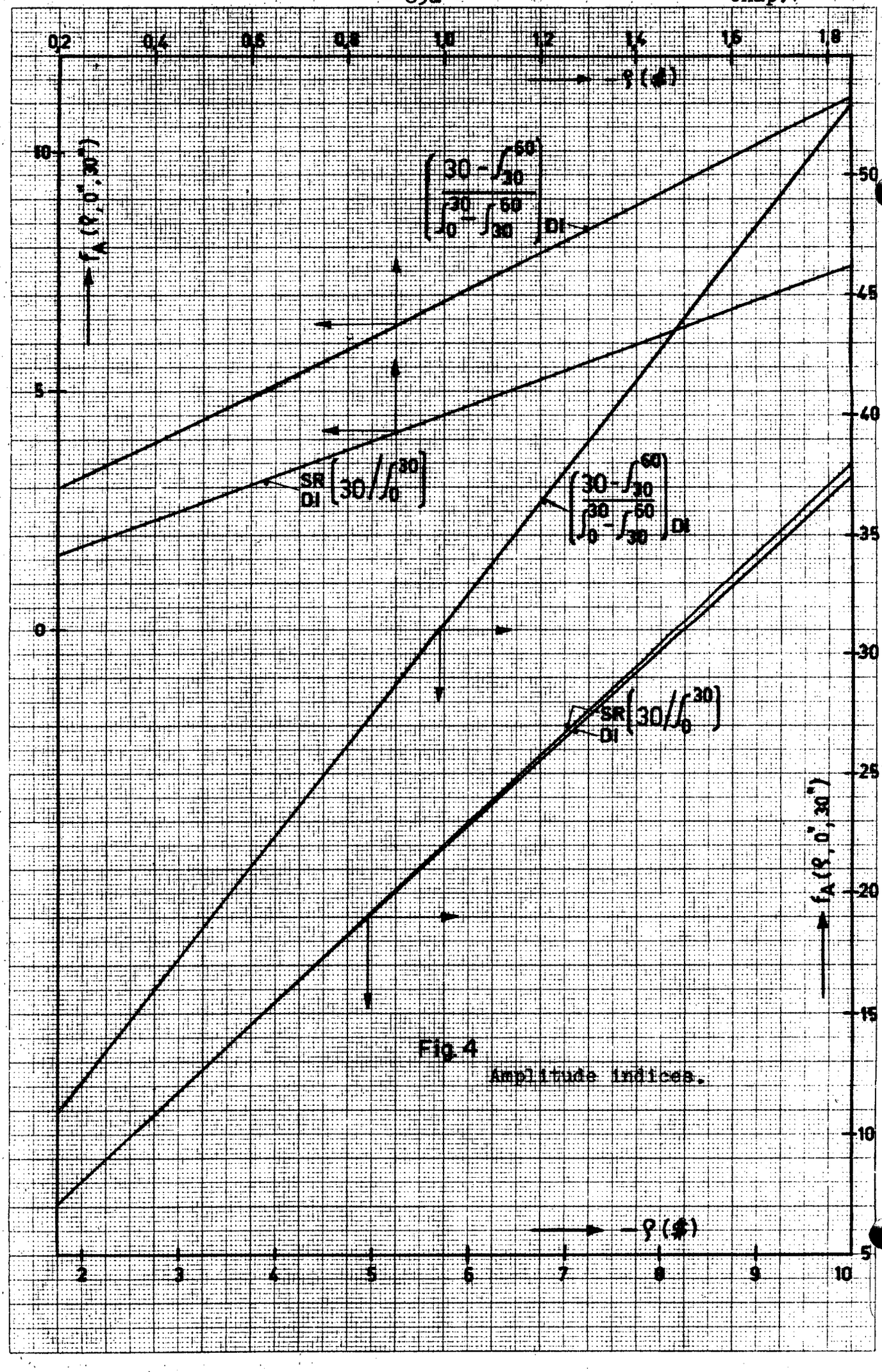

Fig.4

Amplitude indices.

In order to apply such a technique one has to show experimentally that the region chosen has the desired property. Measurement of the persisting mode can be carried out with fairly good precision by measuring any time integral of the density. The similarity of neutron distributions, normalized at the same point, under various conditions (e.g. configurations with control rods inserted to different heights, with distributed source etc.) leads to the conclusion that in the region of ccincidence the persisting modes of different configurations are more or less alike. Hence, this region is free of harmonics within the prescribed experimental accuracy. Actually a region which is free from harmonics may be found without using the time integrated density. It is sufficient to compare the normalized density at a given point for a variety of reactor configurations. If the densities coincide this may be used as an indication of the fact that one is in the region of the persisting mode.

3.2 Background normalization

It might occur that the region which is free of harmonics is inaccessible, or does not exist at all. In such a case one is obliged to conduct the S.J. experiment in the presence of harmonics induced by the initial density. Some improvement may be gained by referring to the distributed background source density instead of the initial flux. In a reactor with hot fuel the background sources consist mainly of photoneutrons (in heavy and light water reactors) and of the residual point source of the S.J. equipment. The photoneutron sources are essentially distributed along the latest critical distribution (it is somewhat smeared out due to the longer mean free path of photons compared with the migration area of neutrons). If the measured subcritical configuration is considered as a perturbed state of the critical reactor (e.g. if subcriticality is attained by control rod insertion) then the persisting density far from the perturbation will still be very similar to the critical persisting mode. The latter distribution may be described to a good approximation by the photoneutron density. Therefore, referring to the background density at the measuring point may lessen the error due to harmonics.

Assuming that the background density $b(x,0)$ resembles the persisting mode, one has,

$$b(x,0) = \Lambda^* B_0 n_0(x) / \rho_0 , \qquad (14)$$

where:

$$B_0 = \int B(x)n_0(x)dx \Big/ \int n_0^2(x)dx$$

with B(x) representing the background source distribution.

The persisting component of the initial flux is:

$$n_0(x,0) = \Lambda^* Q_0(0)n_0(x) \;/\; \rho_0 \qquad (15)$$

where:

$$Q_0 = \int Q(x,0)n_0(x)dx \Big/ \int n_0^2(x)dx,$$

with Q(x,0) representing the intensity of the external point source before the step.

Thus,

$$n_0(x,0) \,/\, b(x,0) = Q_0(0) \,/\, B_0 = S \sim \text{const.} \qquad (16)$$

The constant S may be measured, while keeping the source in the same position, as the ratio of two densities: one with loaded source and one with unloaded source in a near critical state, provided that attainment of criticality will not introduce new sources. Under these circumstances the harmonics content throughout the reactor will be small and the ratio S, being independent of position, can, in principle, be measured everywhere.

Knowing S, and determining the background density (with source unloaded) at the position of measurement, permits replacing the actual initial density by an approximate equivalent persisting mode density:

$$f_A(x,\rho) \rightarrow f_A(bg.,\rho) = Sb(x,0) \Big/ \int_{t_i}^{t_j} n(x,t)dt \,/\, (t_j - t_i). \qquad (17)$$

It might well happen that the background at the point of measurement will still include a considerable amount of harmonics. This will happen in rather far subcritical states and in the proximity of the residual point source. In such a case one may try to search a region where harmonics of the background are negligible and there conduct the background normalization procedure. Such a search should, in principle, be successful, since the background distribution is anyway closer to the persisting distribution than the actual source-density.

3.3 Sensitivity and counting losses

The main advantage of the amplitude method, in any of its forms, lies in its high sensitivity to reactivity. The amplitude index is linear with reactivity almost throughout the whole range of reactivities. There is a slight deviation from this linearity in near critical states, where the increased sensitivity to reactivity of the time integrated density cancels part of the sensitivity in the numerator. Thus, from the statistical point of view, this method is rather accurate.

On the other hand, the amplitude index $f_A(\rho)$ is sensitive to counting losses due to the dead-time effect on the initial count rate. Close to criticality this effect is weakened by non-negligible counting losses which appear also in the time integrated density (denominator Eq.12). But in far subcritical states the counting losses of the initial count-rate predominate (see Fig.3(b)).

4. ELIMINATION OF SLOWLY VARYING BACKGROUND

Some ambiguity due to the presence of photoneutrons exists in kinetic measurements done in heavy water reactors or to an even greater extent, in beryllium moderated reactors. This ambiguity, which particularly effects stable period measurements (ref. 79,14), makes itself felt also in the S.J. technique (ref.15). It derives from the fact that the stable state in the presence of sources is not really established until all long lived photoneutrons have come to an equilibrium, which will take a few days. It is, of course, impossible in practice to wait that long, and since one has to conduct experiments in shorter intervals, the long lived groups have to be treated as background. This background, being dependent on the history of the reactor, may change during an experiment, and must be remeasured after each measurement. This is again time consuming, and the slow time variation due to the long-lived groups is still not entirely eliminated.

To avoid this ambiguity one may slightly change the definition of both the shape and the amplitude indices. Since the change in photoneutron "background" (groups 11 to 14, ref.80, say) is slow compared to the measuring time, one can safely assume that the background is constant during the period of one minute. Thus,

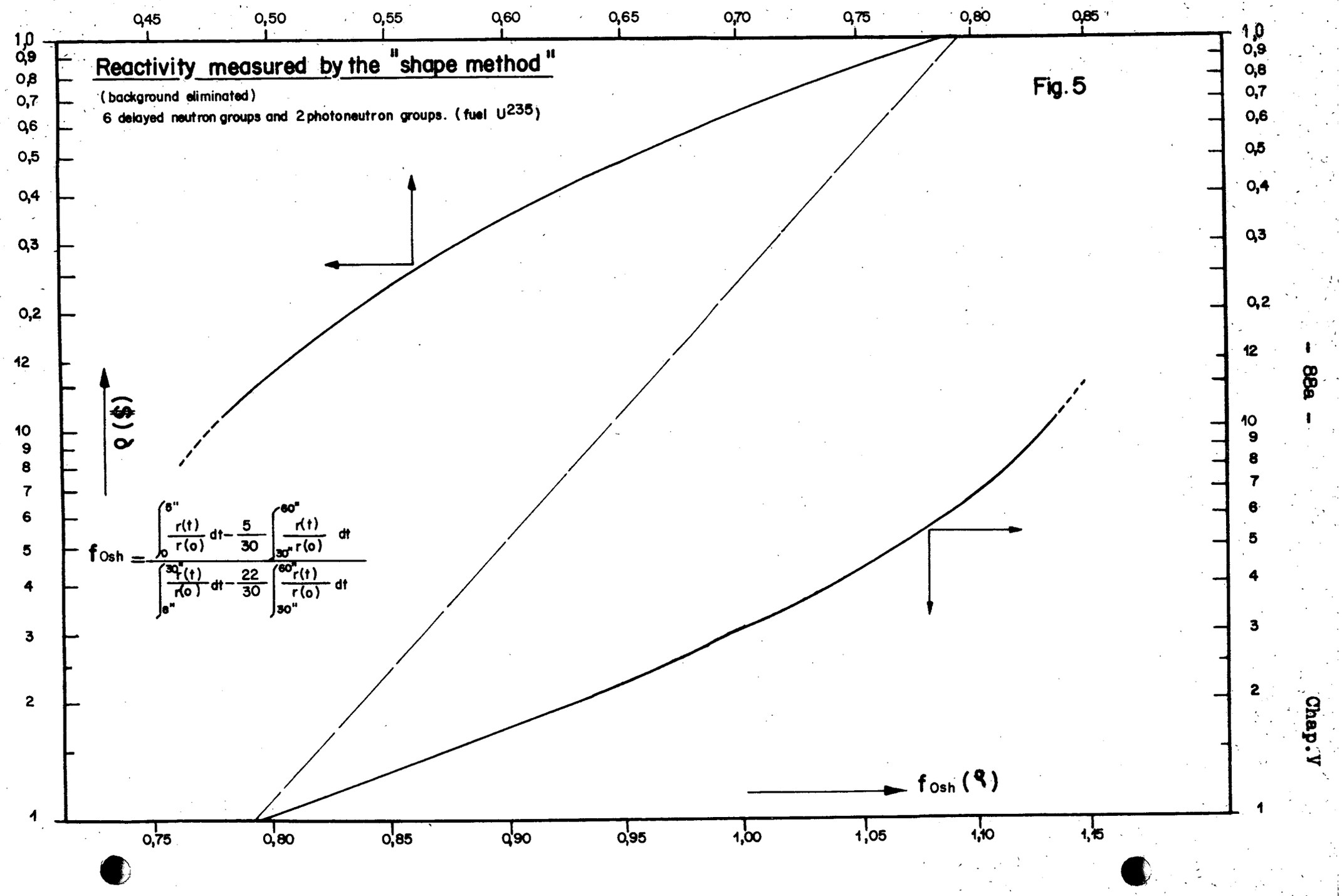
Reactivity measured by the "shape method"
(background eliminated)
6 delayed neutron groups and 2 photoneutron groups. (fuel U235)
Fig. 5
Q ($)
$f_{Osh} = \frac{\int_0^{5''} \frac{r(t)}{r(o)}\,dt - \frac{5}{30}\int_{30''}^{60''} \frac{r(t)}{r(o)}\,dt}{\int_{8''}^{30''} \frac{r(t)}{r(o)}\,dt - \frac{22}{30}\int_{30''}^{60''} \frac{r(t)}{r(o)}\,dt}$
f_{Osh} (ρ)
0,45 0,50 0,55 0,60 0,65 0,70 0,75 0,80 0,85
0,75 0,80 0,85 0,90 0,95 1,00 1,05 1,10 1,15
1,0 0,9 0,8 0,7 0,6 0,5 0,4 0,3 0,2 12 10 9 8 7 6 5 4 3 2 1

$$\int_{t_i}^{t_j}\Big[n(x,t)+b(x,0)\Big]dt-\frac{t_j-t_i}{t_\ell-t_\kappa}\int_{t_\kappa}^{t_\ell}\Big[n(x,t)+b(x,0)\Big]dt=$$

$$\int_{t_i}^{t_j}n(x,t)dt-\frac{t_j-t_i}{t_\ell-t_\kappa}\int_{t_\kappa}^{t_\ell}n(x,t)dt\;\alpha\int_{t_i}^{t_j}R(t)dt-\frac{t_j-t_i}{t_\ell-t_\kappa}\int_{t_\kappa}^{t_\ell}R(t)dt. \qquad (18)$$

In this way one entirely eliminates the background. Expression 18 can be calculated theoretically as usual, giving shape and amplitude indices from which the background is automatically eliminated:

$$f_{sh}(\rho)=\left(\int_{0''}^{5''}\cdot\;-\frac{5}{30}\int_{30''}^{60''}\cdot\;\right)R(t)dt\Big/\left(\int_{8''}^{30''}\cdot\;-\frac{22}{30}\int_{30''}^{60''}\cdot\;\right)R(t)dt$$

(see Fig.5) (19

$$f_A(\rho)=\left(30''-\int_{30''}^{60''}R(t)dt\right)\Big/\left(\int_{0''}^{30''}\cdot\;-\int_{30''}^{60''}\cdot\;\right)R(t)dt$$

(see Fig. 4) (20)

These indices have been calculated for DI, with ten delayed neutron groups:

i	1	2	3	4	5	6	7	8	9	10
λ_i (sec^{-1})	3,014	1,136	0,301	0,277	0,111	0,0305	0,0169	0,0124	0,00481	0,0015
β_i/β	0,0437	0,1215	0,3753	0,0328	0,1827	0,1995	0,0103	0,0291	0,0035	0,0017

It should be noted that there is no loss in sensitivity to reactivity, since the integral $\int_{30}^{60}$ includes almost no signal. In any case, the choice of this interval is dictated mainly by statistical reasons. Another advantage emerges from the elimination of background, namely the fact that it is not necessary to know all parameters of the photoneutrons. The groups whose parameters should be known exactly are those which change appreciably from the time of shooting the source to the time of loading it again. The time of shooting, measuring the partial time integral and loading again, is about 2 minutes. One may thus assume that groups having half lives greater than 7,7 minutes (group 10) do not change at all, and need not be included in the theoretical computation of the indices in Eqs.19,20, while the parameters of groups 9 and 10 (2,4 min. and 7,7 min.) which

change only slightly during the interval of measurement need not be known exactly. This may be advantageous, for example, in Be moderated reactors, where some photoneutron parameters are unknown.

5. EXPERIMENTAL VERIFICATION OF THE MODIFIED S.J. METHODS

5.1 Equipment

The source used in these experiments was nearly always a so-called "slow" step-source (30 msec equivalent step, for details see refs.38,39) except at the beginning, where a "fast" step-source (7 msec equivalent step, ref.81) was used.

The electronics drawn schematically in Fig. 6 represents, in principle, a simple counting channel. However a slow time analyzer was used instead of a simple scaler. It contains five scalers: the first gives the integral count, while the others operate in succession according to pre-determined variable time-intervals and give the partial time-integral of the decaying neutron population. The pulse from shooting the source or from stopping it at a predetermined position (which determines in part the intensity of the residual source) resets the scaler and opens the gates of the first and second scalers.

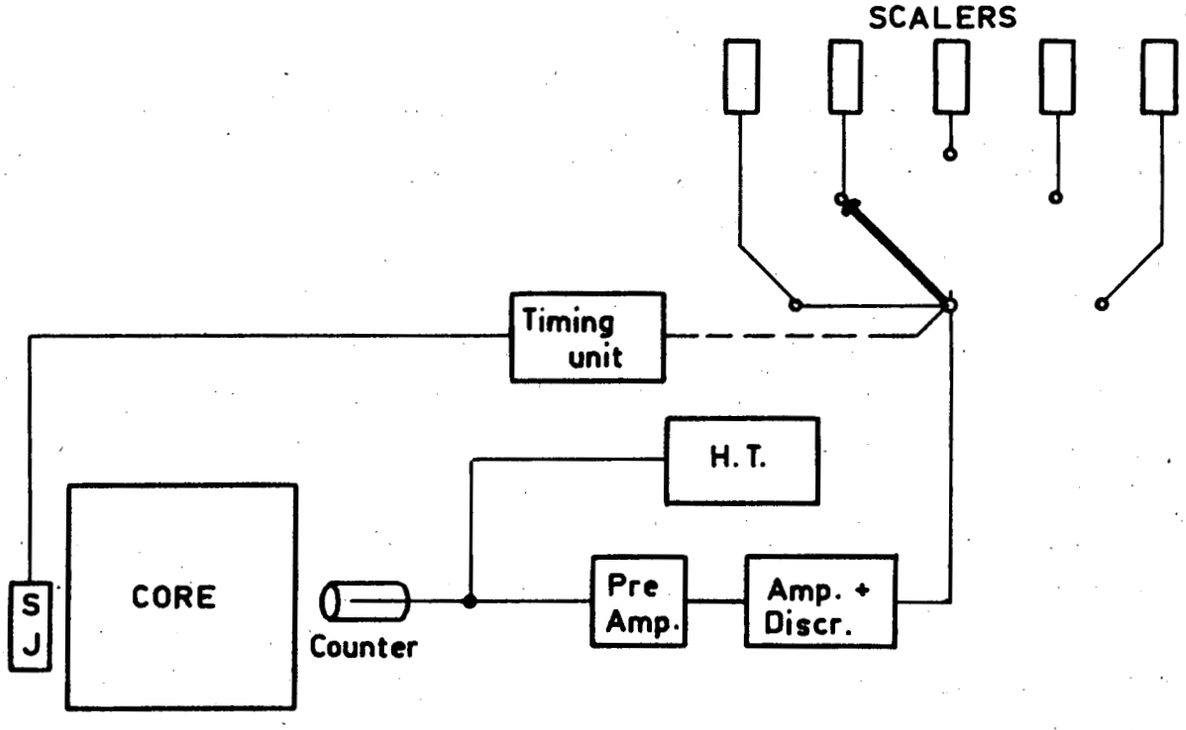

Fig. 6 Schematic diagram of the experimental arrangement

The experiments aimed at establishing the methods were conducted in the Swiss Swimming Pool Reactor SAPHIR. Two permanent fission counters in power channels, FC-1 and FC-2, were used. In addition, a movable fission chamber, FC-3, was used to measure distributions and reactivities as a function of position. Because of technical reasons the distributions and the reactivities in different SAPHIR laodings were measured only around the core at the interface of core and reflector. Some measurements which will be quoted here were carried out in the heavy water reactor DIORIT.

Due to the sensitivity of the amplitude method to counting losses, the dead time of the channel in the actual experimental arrangements was measured before experiments were begun. The dead time was measured with different methods: the method of two sources, measurement of the deviation from the exponential power increase after reaching the stable period, and comparison of different count-rates (e.g. with loaded and unloaded source) in the channel under consideration to a reference channel, which was known to be free from counting losses. A variety of conditions yielded about the same dead time of $\tau = 2{,}0 \pm 0{,}4$ µsec for all three counters, valid up to about 10^5 c/sec.

5.2 Near critical measurements

In the region near critical, source harmonics are practically absent, except in close proximity to the source. In this region one may compare the S.J. technique with the conventional method such as the stable period method. Such a comparison has been done during calibration of the fine control rod in loading No.82 of SAPHIR. The reactor was kept critical by poison with all safety rods, S_1, S_2 and S_3 completely withdrawn. The result of the calibration is shown in Fig.7. Measurements in the supercritical domain down to - 0,0425 $ have been done by period measurements, and below - 0,0425 $ by the S.J. technique using the amplitude and the shape methods. The results were completely independent of the place of measurement. The curve plotted in Fig.7 has been verified over long periods of time, using different loadings and methods.

The points fit extremely well, which shows that shape and amplitude methods are consistent with other well-established methods. Similar measurements have been done in the heavy water reactor DIORIT. There the calibration of one of the fine control rods (F_2) was also done by means of the stable period. Criticality was attained by compensa-

Fig. 7 Calibration of the fine control rod S_4 (in Sephir)

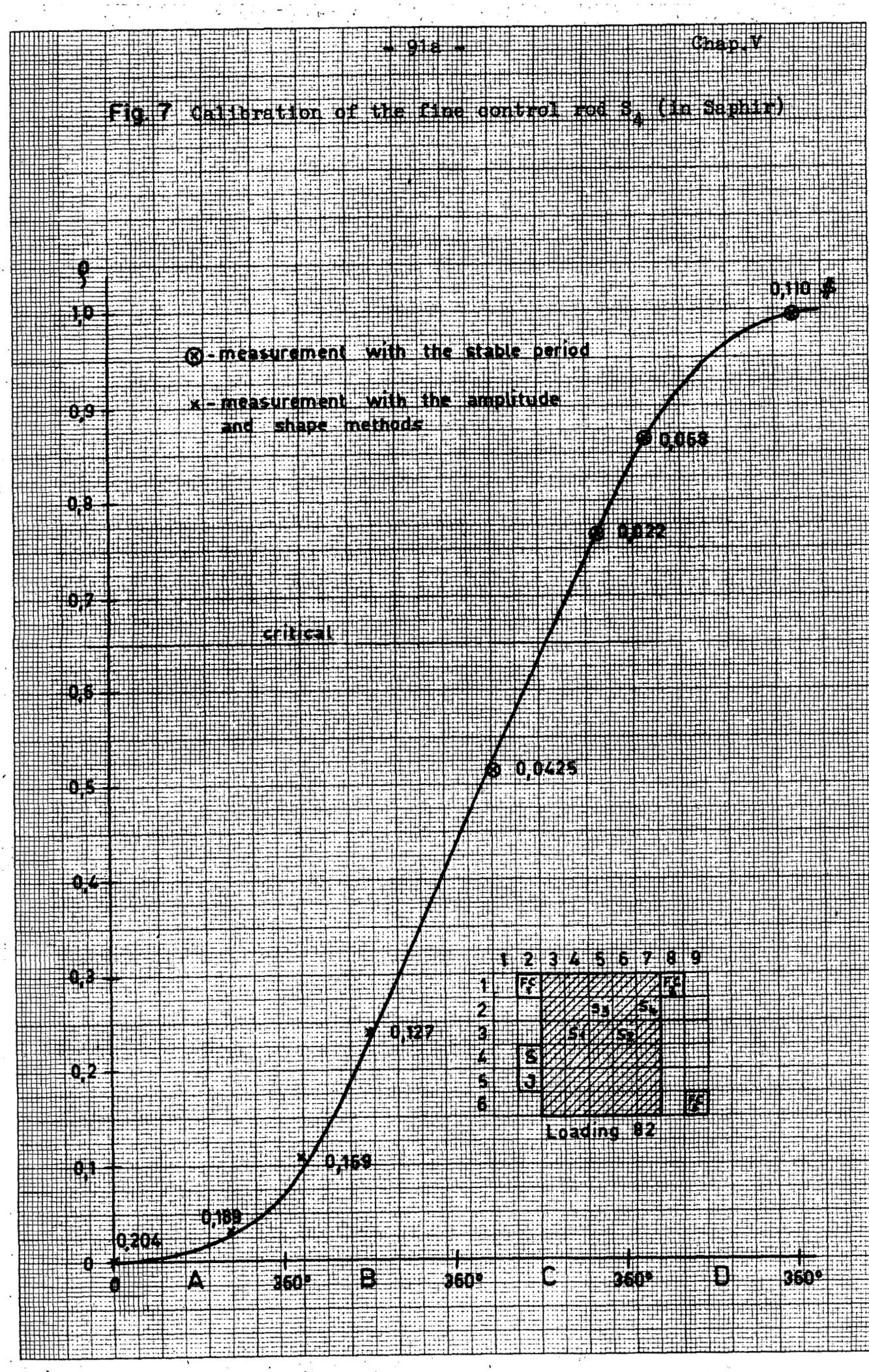

tion with the other fine control rod (F_1), which is sufficiently far away to render any interaction effects negligible. The results of the S.J. measurements are given in Tables 1 and 2. In Table 1 amplitude and shape indices are given with background eliminated. f_{0sh} and f_{0A} are defined in Eqs. 19 and 20. f_{1sh} and f_{1A} are the corresponding indices with integration starting one second later, in order to check the influence of the prompt decay. The measurements listed in Table 1 (ref. 82) were done in the small core of DIORIT (K-132), using the channel X-32 with the help of a BF_3-counter. C.R. F-1 was always completely inserted. The dead time of the system is about 2 μ sec. The source was approximately in the center, and the counter was 90 cm away from the source and about one meter below it. Occasionally measurements were done with the counter lifted. The change of the counter position has practically no effect on the indices, which indicates a negligible amount of harmonics. In Table 2 the results of the period measurements (ref. 83) are compared with those of the S.J. technique.

TABLE 1: Calibration of F-2 (K-132)

F_2-pos.	$f_{0A} \pm$ %	$f_{1A} \pm$ %	$f_{0sh} \pm$ %	$f_{1sh} \pm$ %
F_2- UL	3,894 ± 0,34	4,209 ± 0,35	0,6223 ± 0,70	0,4691 ± 0,77
F_2- UL	3,858 ± 0,34	4,195 ± 0,35	0,6203 ± 0,70	0,4680 ± 0,77
F_2- UL	3,724 ± 0,7	4,029 ± 0,8	0,6233 ± 1,12	0,4773 ± 1,5
F_2- 800	5,463 ± 0,47	6,029 ± 0,5	0,7280 ± 0,90	0,5377 ± 1,30
F_2- LL	6,764 ± 0,60	7,555 ± 0,98	0,8089 ± 1,08	0,5845 ± 1,12
F_2- LL Counter-100cm	6,623 ± 0,70	7,370 ± 0,70	0,8038 ± 0,85	0,5859 ± 1,5

TABLE 2: Calibration of F-2 (K-132)

F_2-pos.	$\frac{mk}{S.J.} \pm$ %	$\frac{mk}{period} \pm$ %
F_2-UL	0	0
F_2- 800	2,47 ± 1	2,49 ± 1,5
F_2- LL	4,44 ± 1,1	4,49 ± 1,5

UL = C.R. completely withdrawn = Upper Limit
LL = C.R. completely inserted = Lower Limit.

5.3 Measurement of the shape and amplitude indices

Another series of experiments may be used to show the independence of the shape index of counter position. In Loading No.57 of the SAPHIR reactor accurate shape measurements have been done. Due to the low sensitivity of the shape index, the source had to be fired many times. Results of the uncorrected "amplitude reactivity" (normal integral count method) and "shape reactivity" are given in Table 3 for a position close to the source (pos. 63) and far from the source (pos. 22). The improvement introduced by the shape method is evident. The results furthermore show that pos. 22 is in the zone which is free from harmonics.

Loading 57

	1	2	3	4	5	6	7	8	9
1			X	X	X	X	X		
2		C	X	X	S_3	X	S_4	X	
3			X	S_1	X	S_2	X	X	
4			X	X	X	X	X		
5			X	X	S	X	X		
6			C	X	J	X			

S_1, S_2, S_4 - UL, S_3 - LL

TABLE 3: Independence of shape index of position (SR).

Meas.pos.	Uncorrected Amplitude meth. $	Shape index	Shape ρ $
22	-3,75 ± 0,04	0,553 ± 0,002	3,70 ± 0,12
63	-5,00 ± 0,05	0,554 ± 0,003	3,70 ± 0,15

Similar measurements have been conducted in the DIORIT. In this case, the small core (K-132) was made subcritical by full insertion of the three safety-rods (about ~ -7 $). One series of measurements (ref.82) was done along channel X-32, thus indicating the axial harmonics along its

length (see Table 4). Another measurement was done in the center of the reactor, in the immediate vicinity of the source (30 cm from it) (Table 4).

TABLE 4: Independence of shape index of position (DI).

Counter pos. along X-32	$f_{0A} \pm 5\ \%$	$f_{1A} \pm 5{,}5\ \%$	$f_{0sh} \pm 5\ \%$	$f_{1sh} \pm 6\ \%$
0,19 $\tilde{H}$ *)	35,485	40,798	1,0906	0,7666
0,19 "	37,590	43,005	1,0913	0,7798
0,40 "	37,434	43,251	1,1126	0,7798
0,60 "	36,736	42,753	1,0936	0,7480
0,80 "	count-rate too low			
average	36,811	42,518	1,0970	0,7630
in reactor center	$97{,}56 \pm 0{,}1\%$	$116{,}15 \pm 0{,}1\%$	$1{,}1024 \pm 2{,}5\ \%$	$0{,}7653 \pm 1{,}5\%$

*) $\tilde{H}$ - extrapolated reactor height.

TABLE 5: "Shape" and "Amplitude" reactivities (DI).

Counter pos.	$-\rho_{0A}$ ¢	$-\rho_{1A}$ ¢	$-\rho_{0sh}$ ¢	$-\rho_{1sh}$ ¢
<X-32>	6,90	6,85	6,55	6,70
Reactor center	18,60	18,80	6,85	7,00

The resultant reactivities are tabulated in Table 5. The evident superiority of the shape method with regard to systematic errors due to harmonics is evident.

The results above show as a by-product the existence of a zone which is almost free of harmonics. The existence of such a zone, regardless of circumstances (e.g. different amounts of C.R. insertion) may be very helpful for a rapid determination of reactivity by means of the amplitude method. Experimentally the existence of such a region was checked with different loadings of the SAPHIR. In each loading the flux

was measured around the core for different reactivities (achieved by changing the C.R. height) while the source was loaded, unloaded or completely removed (to eliminate the effect of beryllium). The resulting flux distribution, normalized at position 32 for Loading No.54, 43 (which is very similar to Loading 57) and at position 48 for Loading No.82, are given in Figs. 8,9,10 respectively. In spite of the fact that these flux distributions describe different conditions, the existence of a region low in harmonics is evident. In Loading No.54 with source located in pos. 38-48 this region extends approximately from pos. 61 to pos. 12. In Loading No.57 it extends approximately from pos. 68 to pos. 18, and in Loading No.82 it extends throughout approximately the same region. This means that amplitude measurements conducted in these regions will involve only a small systematic error.

After establishing the validity of the shape method, the two types of amplitude method discussed earlier were examined. These consist of regular amplitude measurements (particularly in the zone free from harmonics) and background normalization. The results reported below were found in Loading No.54, the flux distribution of which is given in Fig. 8. The measurements were done in three locations: far from the source, pos. 22, intermediate, pos. 64, and in close proximity to the source, pos. 58. The amplitude method demands only a few source-jerks (in fact quite often one is sufficient) in order to obtain good precision in the reactivity. Thus, the reactivity measured at the same time by means of the shape method has rather low precision and serves only as a check. The results of measurements without correction (normal integral count method) and with correction, together with control-rod positions, are given in Table 6, below.

TABLE 6 : "Amplitude" reactivities (SR)

C.R. pos.	pos. of counter	f_{oA} uncorrected	$-\rho$ $	$-\rho$ $ corrected background norm.	f_{osh}	$\rightarrow -\rho$ $
all S LL	22	34.693	9.1 ±0.03	10.10±0.39	0.6047±0.0300	9.0
	64	43.168	11.45 ±0.04	10.80±0.48		
	58	176.310	41.33 ±5.4	22.49±2.30		
S_1, S_2, S_4-UL	22	13.989	3.55 ±0.04	3.50±0.05	0.5538±0.0083	3.8
	64	15.065	3.85 ±0.04	3.60±0.05	0.5669±0.0397	4.4
S_3-LL	58	35.330	9.35 ±0.7	5.70±0.46	0.5830±0.0466	5.7
S_1, S_2, S_3-UL	22	2.610	0.47 ±0.001	---	0.3255±0.0010	0.475
	64	2.498	0.445±0.001	---	0.3192±0.0010	0.445
S_4-LL	58	2.965	0.565±0.002	---	0.3185±0.0020	0.4[illegible]

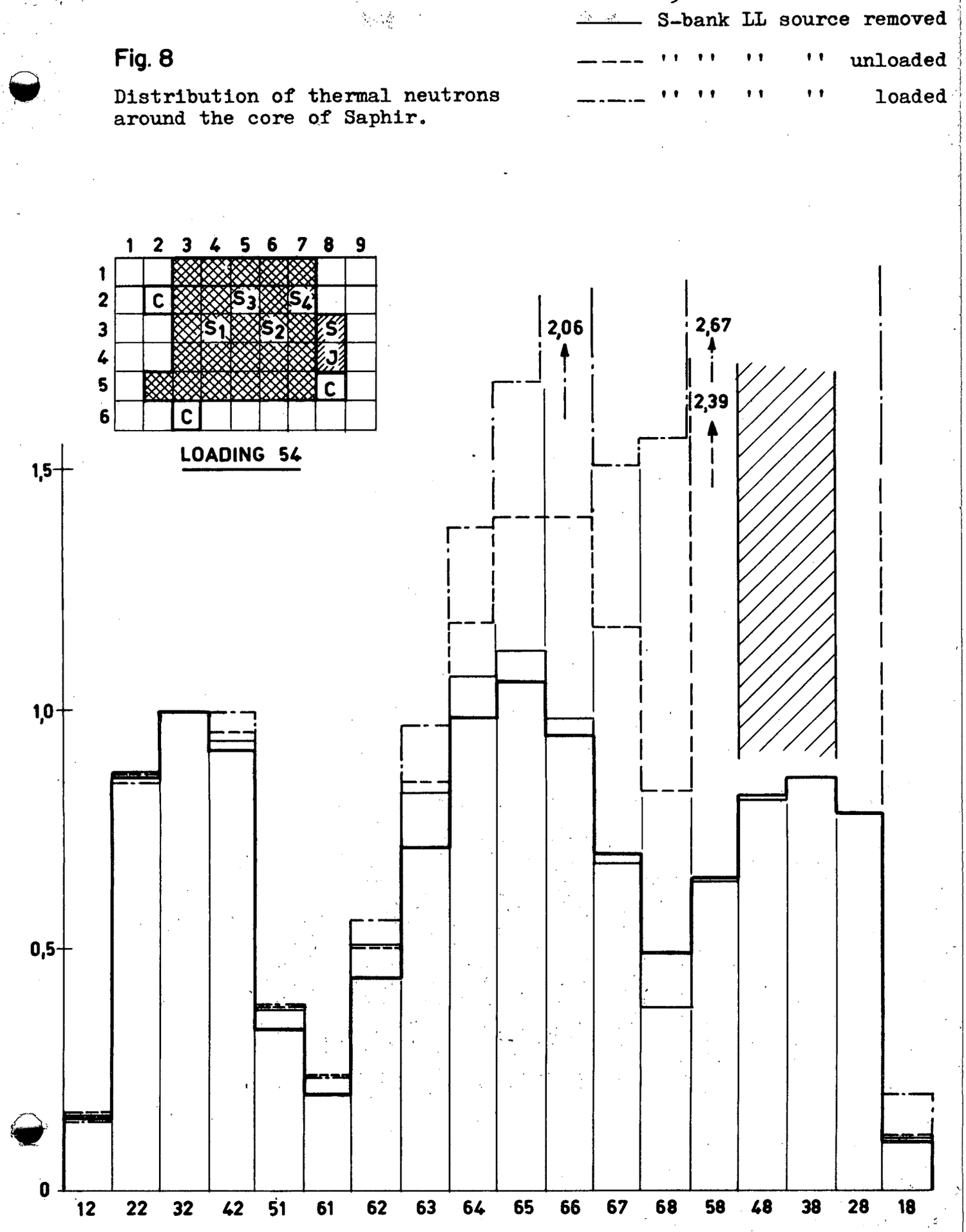

Fig. 8

Distribution of thermal neutrons around the core of Saphir.

Fig. 9

Distribution of thermal neutrons around the core of Saphir.

——— S-bank 50,8cm source removed
——— '' 36,2 '' ''
— — — '' 50,8 '' unloaded
— — — '' '' '' loaded
— - — '' 36,2 '' ''
— - — '' '' '' unloaded

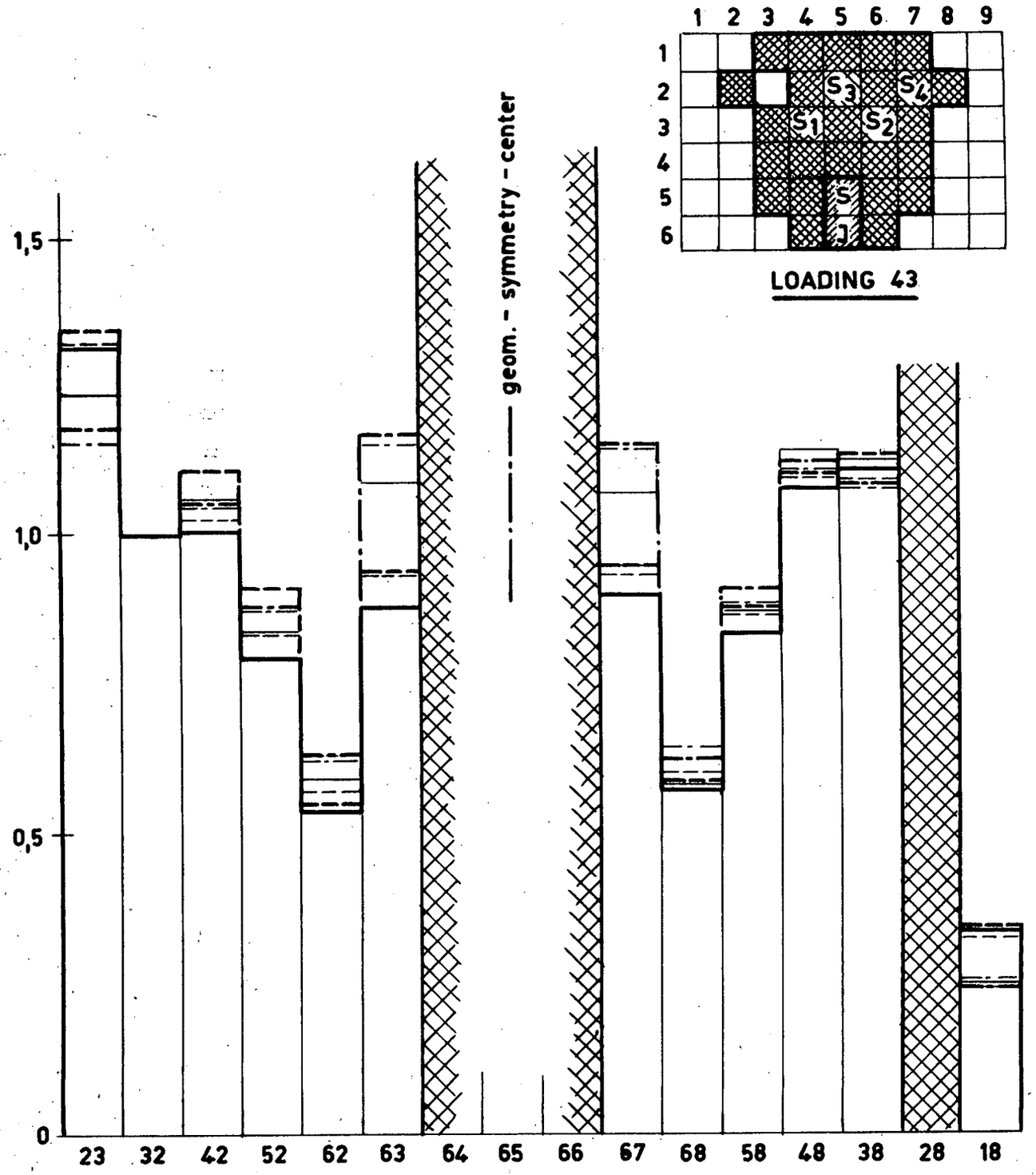

Fig. 10

Distribution of thermal neutrons around the core of Saphir.

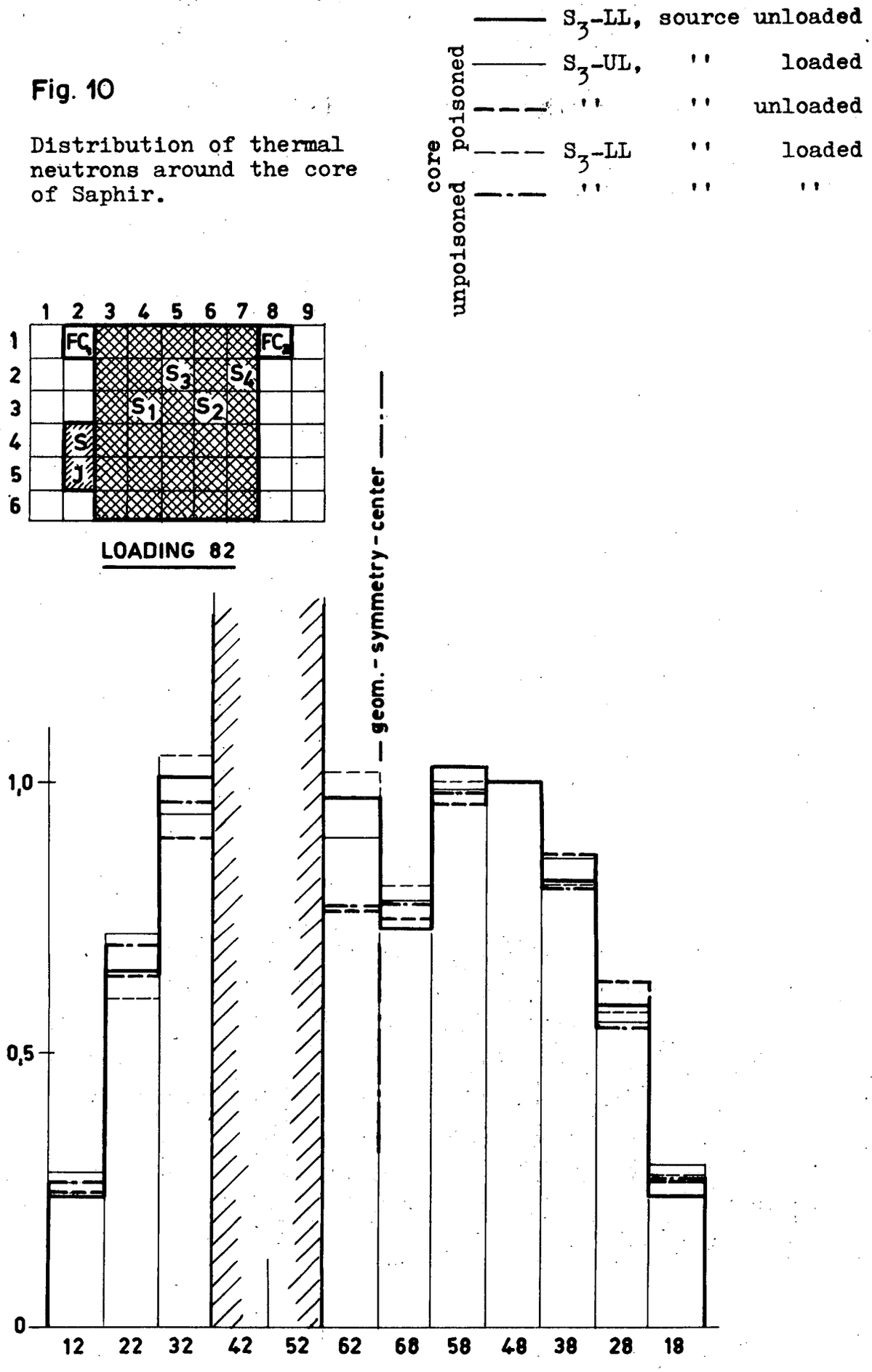

For the background normalization procedure, the ratio S, Eq.16, was determined with the configuration: S_1, S_2, S_3-UL, S_4-LL $-\rho \sim 0{,}5$ $. It was found to be indeed independent of position except at pos.58, which gave a value about 10 % higher than the others.

From the table above one sees on the one hand the improvement introduced by the background normalization, and on the other hand its inherent limitations due to the residual point source.

6. MODIFIED ROD-DROP MEASUREMENTS

6.1 General description

As explained in Chap.II, the rod drop technique is based on a measurement of the reactor response to a rapid insertion of absorber, e.g. a control-rod. This technique offers some advantages over the S.J. method but introduces some serious difficulties. The main advantages can be summarized as follows:

a) Since the reactor is usually critical in the initial state before dropping the rod, the initial count-rate can be chosen as high as necessary to render any background negligible.
b) For the same reason, the statistical precision of this technique is considerably higher than that of the S.J. technique.
c) Due to the high statistical accuracy, the "shape-method" can be used to determine a reactivity free from harmonics in a reasonable number of measurements.
d) No additional equipment is necessary for the rod-drop mechanism, and by means of the "shape-method" the permanent counters of the reactor control circuit may give a reasonably accurate value of reactivity, even if they are located in a harmonics-contaminated zone.

The main limitations of the method are:

a) It is impossible to calibrate a control rod without the help of some compensation of other rods. Thus the method is mainly practical for total worth measurements.
b) The harmonics content involved in such a technique is appreciably larger than that of the S.J. technique (see Chap.II, Sec.4, and A-I and A-III).
   This is so, because of the strong deformation of the neutron distribution near the inserted rod.

c) Dropping of the rod is not instantaneous. This involves, in principle, a separate analysis for each rod that is measured.

d) The R.D. experiment is much more time consuming than the S.J. experiment, since each time the rods must be withdrawn and a constant power at criticality is to be established.

In view of these advantages and limitations, the rod drop technique finds its main application in hot, heavy water or Be moderated reactors, where the external sources available for S.J. or P.S. techniques cannot compete with the inherent photoneutron background, even after relatively long shut-down periods.

The strong contamination with harmonics, and the availability of very high count-rates suggests the use of the shape method, which in addition is less sensitive to counting losses than the integral count method.

Dropping the control-rods causes a non-negligible change in generation time (see IV, Sec.7). However, it can be shown (**ref.43**) that the generation time may be neglected altogether in the theoretical treatment. Using the measured $\rho(t)$ of C.R. S_2 of reactor SAPHIR (Curve 1, **ref.40** ; see also Fig.12) the shape and amplitude indices f_{sh} (for R.D.) f_A (for R.D.) were calculated (**ref.84**) using the previously given delayed neutron parameters. The indices as a function of reactivity are plotted in Figs. 11 and 12.

6.2 Experimental checks

The rod-drop measurement was applied to loading No.61 of SAPHIR.

Loading 61

	1	2	3	4	5	6	7	8	9
1		FC1	X	X	X	X	X	FC2	
2			X	X	S_3	X	S_4		
3			X	S_1	X	S_2	X		
4		S	X	X	FC3	X	X		
5		J	X	X	X	X	X		
6			X	X	X	X	X		

The total worth of each safety rod, S_1, S_2, S_3 and of the banks $S_2 + S_3$ and $S_1 + S_2 + S_3$ were first measured by the S.J. amplitude method (with and without background normalization) at the following three loca-

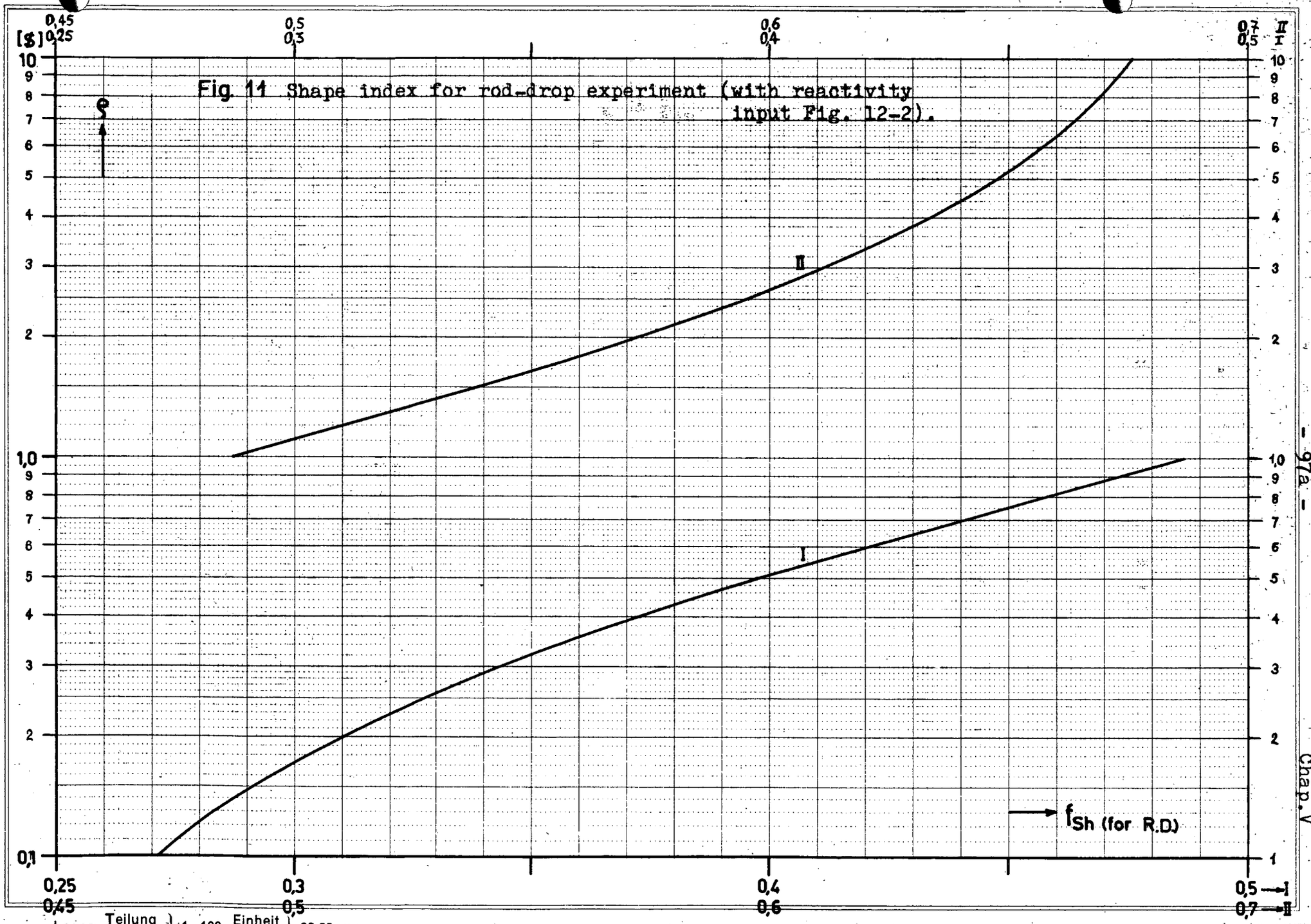

Fig. 11 Shape index for rod-drop experiment (with reactivity input Fig. 12-2).

Logar: Teilung } 1 - 100, Einheit } 83,33 mm
Division
Unité

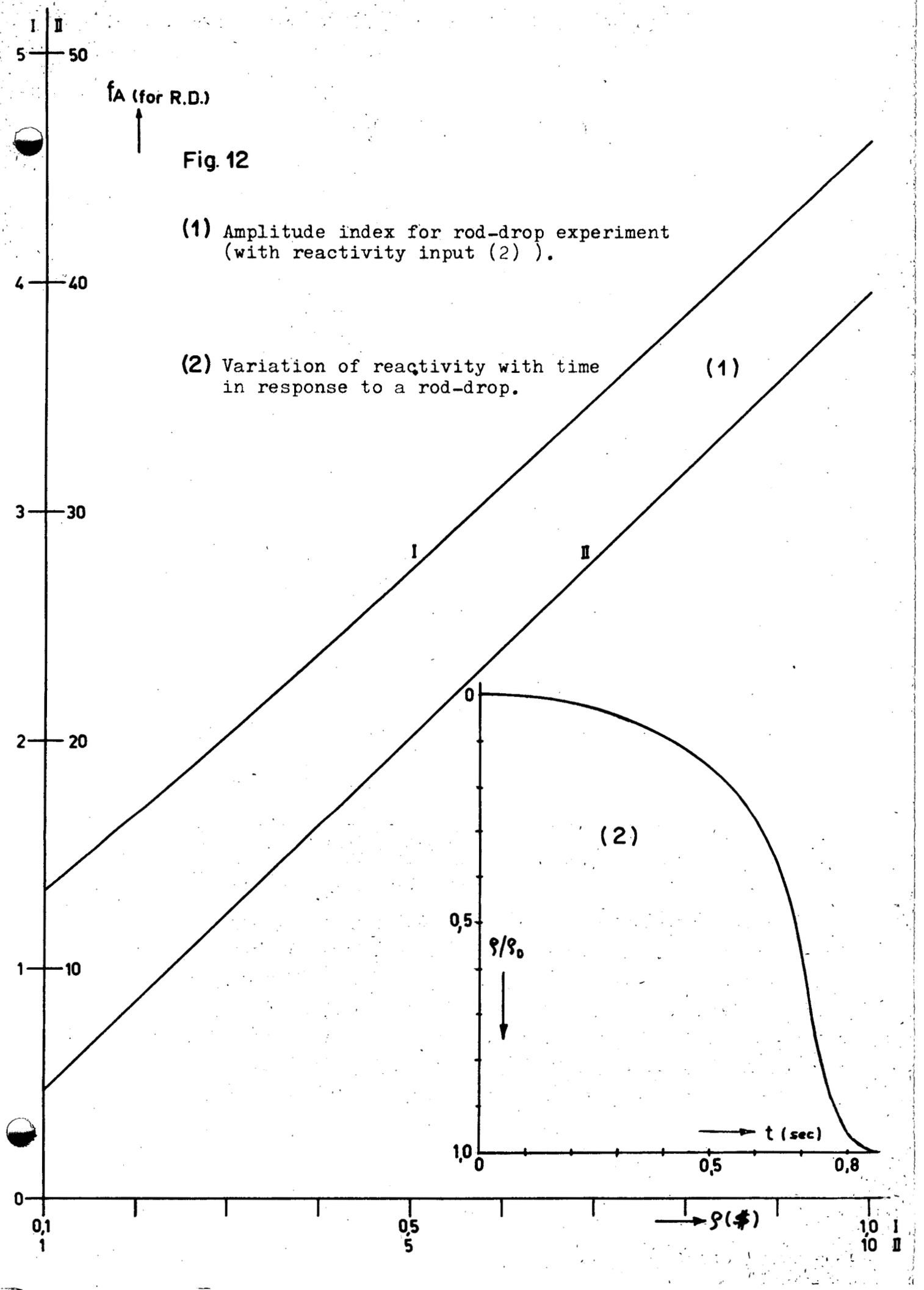

Fig. 12

(1) Amplitude index for rod-drop experiment (with reactivity input (2)).

(2) Variation of reactivity with time in response to a rod-drop.

tions: pos.12(FC1), pos.45(FC3) and pos.18(FC2).Due to the relatively low count-rates, the shape method could not be applied. The ratio S, Eq.16, was determined at $\rho \sim -0,4$ $, obtained by withdrawing the S-rods almost to their UL, while S_4 was kept at LL. The results of these measurements are summarized in Tables 7 and 8

TABLE 7: Amplitude indices in Loading 61.

C.R. pos.			Uncorrected: f_{AU}			bg. normalized: f_{AB}		
S_1	S_2	S_3	FC1 pos.12	FC2 pos.18	FC3 pos.45	FC1	FC2	FC3
LL	UL	UL	11,4 ±0,3	10,6 ±0,3	---	11,7 ±0,3	11,4 ±0,3	---
UL	LL	UL	10,44±0,15	10,26±0,13	11,10±0,60	10,70±0,20	10,24±0,15	10,53±0,10
UL	UL	LL	9,20±0,06	8,83±0,23	---	9,27±0,06	8,68±0,23	---
UL	LL	LL	18,4 ±0,5	17,3 ±0,7	20,0 ±0,1	19,2 ±0,4	17,7 ±0,7	18,1 ±0,2
LL	LL	LL	27,9 ±0,7	24,2 ±0,9	30,6 ±0,2	30,6 ±1,0	25,7 ±1,1	28,0 ±0,2

TABLE 8: Total worth of C.R. in loading 61 (by S.J.).

C.R. pos.			$\langle f_{AU} \rangle$	$\langle f_{AB} \rangle \rightarrow -\rho($$)$		$\langle f_{AU}+f_{AB} \rangle \rightarrow -\rho($$)$	
S_1	S_2	S_3					
LL	UL	UL	11,0 ± 0,4	11,55±0,2	2,85±0.07	11,4 ±0,3	2,75±0.10
UL	LL	UL	10,60±0,25	10,49±0,14	2,62±0.04	10,52±0,17	2,62±0.05
UL	UL	LL	9,01±0,20	8,98±0,30	2,2 ±0.07	9,00±0,25	2,20±0.06
UL	LL	LL	18,6 ± 0,7	18,3 ±0,4	4,75±0.10	18,4 ±0,5	4,74±0.13
LL	LL	LL	27,6 ± 1,8	28,1 ± 1,4	7,33±0.70	27,9 ±1,0	7,30±0.50

The averages listed in Table 8 were done with the appropriate statistical weight given by the statistical error at each measurement. Table 7 shows that the background normalization, though not eliminating the harmonics effect entirely, nevertheless results in some improvement. This is seen clearly in the smaller statistical fluctuations in most values of $\langle f_{AB} \rangle$ compared to those of $\langle f_{AU} \rangle$. Because of the symmetrical location of FC1, FC2 and the close proximity of the source to FC1, one could expect the result of FC1 to be higher than the true value, and that of FC2 to be lower. Actually, the averages of the

background corrected results of FC1 and FC2 are very close to that of FC3. Those facts indicate that the averaging process is meaningful here. However, in general the magnitude of the reactivity derived from the averaged background corrected indices should be accepted as the most reliable of all.

A first check on the feasibility of applying the shape method to the rod-drop technique was carried out on Loading No.61, without source equipment or FC3 counter. The measurements were confined to FC1 and FC2, fixed above the core. The pulse to actuate the scaling system was given by the seat-switch of C.R. S_2. For measuring the total worth of S_2, an initial power of about 250 watts was used, while for the total worth of the bank S_1, S_2 and S_3 the initial power was about 1 kW. In both cases S_4 was at height C-60 (see Fig.7) before the drop. In the last case the amplifier was rather heavily overloaded, so that the high tension was switched on only after the drop, when the power was reduced by virtue of the prompt decay. Such a procedure invalidates the integral count from zero to one second. The results of these measurements are listed in Table 9.

TABLE 9: Shape and amplitude indices in loading 61 (by R.D.).

pos.*	C.R. dropped	$f_{0sh} \pm \%$	$\rightarrow -\rho$ (¢)	$f_{1sh} \pm \%$	$f_{0A} \pm \%$	$\rightarrow -\rho$ (¢)
ax:92 FC1	S_2	0,6060±0,4	2,83±0,06	0,4506±0,5	11,557±0,3	2,80±0,4
rad: (12)	$S_1+S_2+S_3$	(0,6705±1,0)	(8,1)	0,4902±0,3	38,81 ±0,5	9,75±0,05
ax:92 FC2	S_2	0,6049±0,4	2,80±0,06	0,4494±0,5	12,473±0,3	3,05±0,4
rad: (18)	$S_1+S_2+S_3$	---	---	0,4920±0,4	36,612±0,5	9,20±0,05

*) ax=axial position, rad=radial position.

The table shows that the shape indices and their corresponding reactivities are much less sensitive to location of the counter than the amplitude indices and their resultant reactivities. In fact, the "shape" results in each configuration are the same within the statistical precision.

The second step was to conduct rod-drop measurements under the same conditions under which the source-jerk reactivity had been determined previously (Table 7). For this purpose the source equipment

was placed at positions 42-52, and the moveable fission-counter was placed at position 45. Again the measurement was initiated by the end-switch ("seat-switch"), which was actuated when S_2 reached its lower limit (LL). The initial power level was adjusted, whenever possible, by the automatic control system, which attempted to keep the same fine control rod (S_4) position before each drop. Just before the drop, the automatic control was disconnected. Difficulties were encountered when measuring with the FC_3 counter. In order to have the same count rate as the other counters, i.e. FC1 and FC2, the power had to be reduced below the minimum possible power for automatic control. Thus one was obliged to maintain the desired power at a constant level by means of manual operation. In addition, counter FC3 was subjected to intense gamma radiation. The results of the measurements are summarized in Table 10.

TABLE 10: Total worth of C.R. in loading 61, as determined by R.D. technique

pos.	C.R. dropped	S_4 pos. *)	$f_{0sh} \rightarrow -\rho$ (¢)		f_{1sh}	$f_A \rightarrow -\rho$(¢) ±<1 %
ax:40 FC1 rad: (12)	S_2	D-180°	0,5961 ±0,0040	2,55±0,1	0,4467 ±0,0010	10,59 / 2,55
	S_2+S_3	D-200°	0,6417 ±0,0019	4,50±0,12	0,4741 ±0,0013	22,04 / 5,50
	$S_1+S_2+S_3$	D-208°	0,6639 ±0,0010	7,20±0,15	0,4879 ±0,0004	37,02 / 9,35
ax:40 FC2 rad: (18)	S_2	D-180°	0,6042 ±0,0020	2,75±0,1	0,4488 ±0,0013	11,56 / 2,81
	S_2+S_3	D-213°	0,6464 ±0,0014	4,85±0,2	0,4786 ±0,0006	23,35 / 6,85
	$S_1+S_2+S_3$	D-166°	0,6623 ±0,0019	6,85±0,25	0,4856 ±0,0012	36,42 / 9,20
FC3 rad: (45)	S_2	D-180°	0,5947 ±0,0017	2,50±0,05	0,4449 ±0,0017	10,56 / 2,53
	S_2+S_3	D-220°	0,6424 ±0,0015	4,58±0,12	0,4759 ±0,0008	19,23 / 4,80
	$S_1+S_2+S_3$	D-245°	0,6620 ±0,0027	6,80±0,5	0,4875 ±0,0020	31,17 / 7,35

*) see Fig.7

This table shows again that reliable results can be achieved by application of the shape method to the rod-drop technique. While the normal rod-drop technique gives a reactivity at pos. FC1 and FC2 which is about 25 % higher than the true value, the modified technique gives the correct result at pos. FC1 with a statistical scattering of about 2,1 % . At position FC2 the largest negative reacti-

vity (dropping of all S-rods) found is somewhat lower with larger statistical fluctuation.

One usually expects to strongly overestimate the reactivity when measuring close to the dropped rod. But in the described experiment the water hole at position 45 and the introduction of some vacuum, i.e. the counter, radically change this picture. Curiously enough, the amplitude indices at this point turn out to give the correct reactivity of the configuration. However, it is evident that if the counter would not replace fuel and moderator, a large overestimate of reactivity would usually result.

7. CONCLUSIONS

In the preceding sections a stringent series of experimental checks on modified source-jerk and rod-drop technique has been described. It was demonstrated that an appreciable improvement may be gained from these techniques if properly applied to the measurement of reactivity. With the present limitation on count-rates due to conventional electronics and counters the shape method is not amenable to routine determinations of large negative reactivities. However, it may be useful to apply the accurate "shape" method occasionally, in order to make sure that the region where one measures reactivity with the help of the amplitude method is more or less free from harmonics. This can be done in the start-up phase of the reactor to show that there exists a region where the persisting modes of different configurations coincide.

In the amplitude method with background normalization one obtains an improvement almost without additional effort. The magnitude of the improvement depends on the origin and type of the background sources.

In heavy water reactors the elimination of background is rather important. When such a reactor has experienced some power-runs, the only possible way of measuring large amounts of reactivity is by means of the rod-drop technique. Here the shape-method will be more practical, due to the high count rates available. But still one should keep these count-rates low enough, so that counting losses will be confined to the linear region. Considerable improvement could be gained by using faster electronics and faster counters. At the same time, for in-core measurements the counters should be sufficiently insensitive to the gamma background.

Appendices

Appendix I: A bare homogeneous reactor with a time dependent source. One-group treatment.

The kinetic equations describing this case are:

$$v(D\nabla^2 - \Sigma)n(x,t) + vk(1-\beta)\Sigma n(x,t) + \sum_{i=1}^{\ell} \lambda_i c_i(x,t) + Q(x,t) = \frac{\partial n(x,t)}{\partial t} , \quad (1)$$

$$v\beta_i k\Sigma n(x,t) - \lambda_i c_i(x,t) = \frac{\partial c_i(x,t)}{\partial t} , \quad (2)$$

with boundary conditions (at the extrapolated boundaries $\tilde{x}$):

$n(\tilde{x},t) = c_i(\tilde{x},t) = 0$, and initial conditions $\partial n/\partial t = \partial c_i/\partial t = 0$.

The densities are expanded in terms of the geometrical eigenfunctions:

$n_q(x)$, $\qquad \nabla^2 n_q(x) = - B_q^2 n_q(x)$:

$$n(x,t) = \sum_{q=o}^{\infty} n_q(x)T_q(t); \qquad c_i(x,t) = \sum_{q=o}^{\infty} n_q(x)T_q^i(t).$$

After substituting the expansions and using the orthogonality property, the precursors are eliminated from the Laplace-transformed equations, yielding:

$$\bar{T}_p(s) = T_p(0)[\Lambda^* + \bar{W}(s)]g_p(s) + \Lambda^* Q_p(s), \quad (3)$$

where:

$$g_p(s) = \left\{ s[\Lambda^* + \bar{W}(s)] - \rho_p \right\}^{-1} = \mathcal{L}\left\{ G_p(t) \right\}, \quad (4)$$

$$\rho_p = (1/\beta k) \left\{ (k-1) - M^2 B_p^2 \right\},$$

modal reactivity in dollar units, in the modified one group theory,

M^2 = the migration area,

$$\Lambda^* = (v\Sigma k\beta)^{-1} , \quad (5)$$

reduced generation time, which is independent of the mode in the present model,

$$\bar{W}(s) = \sum_{i=1}^{\ell} b_i/(s + \lambda_i),$$

$$b_i = \beta_{i\,eff}/\beta_{eff},$$

$$\bar{Q}_p(s) = \int \bar{Q}(x,s)n_p(x)dx \;/\; \int n_p^2(x)dx.$$

By the above expansion one obtains complete separability of modes. In each mode the time-dependence is formally the same as that of

the space independent model, II-Sec.-2, namely:

In the S.J. experiment:

$$T_p(t)/T_p(0) = 1 + \rho_p(1-A)\int_0^t G_p(t)d\tau, \tag{6}$$

$$T_p(0) = -\Lambda^* Q_p(0)/\rho_p. \tag{7}$$

In a P.S. experiment:

$$T_p(t) = T_p(0) + P_p\Lambda^* G_p(t), \tag{8}$$

where: $P_p = \int P(x)n_p(x)dx \;/\; \int n_p^2(x)dx.$

The delayed neutron density, $n_d(x,0)$, just after the prompt jump, is essential to S.J. and R.D. experiments based on the prompt decay. It can be found from $n(x,t)$ by the following procedure:

$$\lim_{t\to 0} n_d(x,t) = \sum_{q=0}^{\infty} n_q(x)\lim_{t\to 0}[T_q(t)]_{\Lambda^*=0} = \sum_{q=0}^{\infty}[T_q(0)/(1-\rho_q)]\left[1+\frac{A}{T_q(0)}\right],$$

$$= \sum_{q=0}^{\infty}\Lambda^*[Q_q(0)/\rho_q(1-\rho_q)][1+A\rho_q/\Lambda^* Q_q(0)]. \tag{9}$$

The time integrated density, in S.J. with no residual source (A=0) or with substracted background is:

$$\lim_{t\to\infty}\int_0^t n(x,\tau)d\tau = \sum_{q=0}^{\infty} n_q(x)\lim_{s\to 0}\bar{T}_q(s) = (\Lambda^*+\bar{W}(0))\sum_{q=0}(T_q(0)/\rho_q)n_q(x),$$

$$= \Lambda^*(\Lambda^*+\bar{W}(0))\sum_{q=0}^{\infty}(1/\rho_q^2)Q_q(0)n_q(x). \tag{10}$$

The time integrated density in a P.S. experiment, where $Q(0) = 0$, will be:

$$\int_0^{\infty} n(x,t)dt = -\Lambda^*\sum_{q=0}^{\infty}(1/\rho_q)P_q n_q(x). \tag{11}$$

In a slab reactor of extrapolated thickness d cf., Fig.II-2, the geometric eigenfunctions are: $n_q(x) = \sin q(\pi/d)x$, with $B_q^2 = q^2(\pi/d)^2$. In the presence of an infinite plane source at a point x_o of intensity Q neutrons per second per cm^2, the density, $n(x,0)$ is maintained in a steady state with the following distribution (see Eq. 7):

$$n(x,0) = \frac{2Q}{d}\frac{1}{vDB_1^2}\sum_{p=0}^{\infty}\sin p\,B_1 x_o \sin p\,B_1 x \;/\; (p^2 - B^2/B_1^2), \tag{12}$$

where: $B_1^2 = (\pi/d)^2$ and $B^2 = (k-1)/M^2$, the material buckling.

The sum in Eq. 12 is summable (ref. 85)

$$\sum_{p=0}^{\infty} \frac{\sin p B_1 x_0 \sin p B_1 x}{p^2 - B^2/B_1^2} = \frac{d \cdot B_1^2}{4B} \left[\sin B(x+x_0) - \sin B|x-x_0| + \right. \quad (13)$$

$$\left. - 2\cot Bd \sin Bx_0 \sin Bx \right] .$$

The time integrated density in S.J. experiments, Eq.10, in the slab-case will be:

$$\int_0^{\infty} n(x,t)dt = \frac{2Q}{d} \frac{1}{(vDB_1^2)^2} \left[1 + \frac{\bar{W}(0)}{\Lambda^*} \right] \sum_{p=0}^{\infty} \frac{\sin p B_1 x_0 \cdot \sin p B_1 x}{[p^2 - B^2/B_1^2]^2} . \quad (14)$$

The last sum can be expressed in closed form by differentiating Eq.13 with respect to B.

$$\sum_{p=0}^{\infty} \frac{\sin p B_1 x_0 \sin p B_1 x}{[p^2 - B^2/B_1^2]^2} = \frac{d^2 \cdot B_1^4}{8B^2} \left\{ \frac{x+x_0}{d} \cos B(x+x_0) + \right.$$

$$- \frac{|x-x_0|}{d} \cos B|x-x_0| + 2 \sin^{-2} Bd \sin Bx_0 \sin Bx +$$

$$- 2(x_0/d)\cot Bd \cos Bx_0 \sin Bx - 2(x/d)\cot Bd \sin Bx_0 \cos Bx +$$

$$\left. - \left(\frac{1}{Bd}\right) \left[\sin B(x+x_0) - \sin B|x-x_0| - 2 \cot Bd \sin Bx_0 \sin Bx \right] \right\} . \quad (15)$$

In order to find the correct relative amount of harmonics in the initial distribution n(x,0) and of the time integrated flux, Eq.14, the expressions, normalized according to A-III, are compared with the persisting mode, $\sin B_1 x$ (Figs. II-2,3,4). The normalized expressions are:

$$[n(x,0)]_{nor} = \left[\frac{1-(B/B_1)^2}{\sin B_1 x_0} \right] \left(\frac{d \cdot B_1^2}{4B} \right) [\ldots] , \text{ (see Eq.13)} \quad (12a)$$

$$\left[\int_0^{\infty} n(x,t)dt \right]_{nor} = \frac{\left[1-(B/B_1)^2 \right]^2}{\sin B_1 x_0} \left(\frac{d^2 \cdot B_1^4}{8B^2} \right) [\ldots] , \text{ (see Eq.15).} \quad (14a)$$

Appendix II: A bare homogeneous reactor with time dependent fast source. Two-group treatment.

The time dependent diffusion equations describing this situation are:

$$v_1(D_1\nabla^2-\Sigma_1)n_1 + v_2(k/p)(1-\beta)\Sigma_2 n_2 + \sum_{i=1}^{\ell}\lambda_i c_i + Q(x,t) = \frac{\partial n_1}{\partial t}, \quad (1)$$

$$v_1 p\Sigma_1 n_1 + v_2(D_2\nabla^2-\Sigma_2)n_2 = \frac{\partial n_2}{\partial t}, \quad (2)$$

$$v_2(k/p)\beta_i\Sigma_2 n_2 - \lambda_i c_i = \frac{\partial c_i}{\partial t} \qquad i = 1,2,\ldots,\ell, \quad (3)$$

where: $n_1 = n_1(x,t)$, $n_2 = n_2(x,t)$, $c_i = c_i(x,t)$ are the time and space dependent fast, thermal and precursor densities, respectively.
In addition there are the conditions at the extrapolated boundaries: $n_1(\tilde{x},t) = n_2(\tilde{x},t) = c_i(\tilde{x},t) = 0$ and the steady state initial conditions: $\dot{n}_1(x,0) = \dot{n}_2(x,0)\ \dot{c}_i(x,0) = 0$.

The densities are again expanded in terms of the geometrical eigenfunctions $n_q(x)$, which have as geometrical eigenvalues the buckling B_q^2. Substituting these expansions, making use of the orthogonality property of the n_q's, Laplace transforming and eliminating the delayed precursors finally lead to a set of 2 coupled algebraic equations for each mode:

$$\left[-v_1(D_1B_p^2+\Sigma_1)-s\right]\bar{T}_{p1}(s)+v_2\Sigma_2\left(k(s)/p\right)\bar{T}_{p2}(s) + \bar{Q}_p(s) = -T_{p1}(0) - \sum_{i=1}^{\ell}\frac{T_p^i(0)\lambda_i}{s+\lambda_i}, \quad (4)$$

$$v_1 p\Sigma_1\bar{T}_{p1}(s) + \left[-v_2(D_2B_p^2+\Sigma_2)-s\right]\bar{T}_{p2}(s) = -T_{p2}(0), \quad (5)$$

where: $$k(s) = k\left[1-\sum_{i=1}^{\ell}s\beta_i/(s+\lambda_i)\right] = k[1-s\beta\bar{W}(s)], \quad (6)$$

$$\bar{Q}_p(s) = \int\bar{Q}(x,s)n_p(x)dx \Big/ \int n_p^2(x)dx.$$

The solution for the transformed thermal coefficient is:

$$\bar{T}_{p2}(s) = T_{p_1}(0)[\Lambda^*_{p1} + \bar{W}(s) + skp\Lambda^*_{\infty 1}\Lambda^*_{\infty 2}]g_p(s) + T_{p1}(0)p\Lambda^*_{\infty 1}g_p(s) + p\Lambda^*_{\infty 2}\bar{Q}_p(s)g_p(s), \quad (7)$$

where: $$g_p(s) = \{s^2\beta k\Lambda^*_{\infty 1}\Lambda^*_{\infty 2} + s[\Lambda^*_{p_1} + \Lambda^*_{p_2} + \bar{W}(s)] - \rho_p\}^{-1}, \quad (8)$$

$\rho_p = (k_{effp}^{-1}) / \beta k_{effp}$, the modal reactivity in $ (9)

$$k_{effp} = k / (1+\tau B_p^2)(1+L^2 B_p^2) \quad . \tag{10}$$

$$\left.\begin{aligned} \Lambda^*_{p1} &= \{v_1 \Sigma_1 \beta k_{effp}(1+\tau B_p^2)\}^{-1} = (1+L^2 B_p^2) / v_1 \Sigma_1 \beta k \\ \Lambda^*_{p2} &= (1+\tau B_p^2) / v_2 \Sigma_2 \beta k \end{aligned}\right\} , \tag{11}$$

$\Lambda^*_{p1} + \Lambda^*_{p2} = \Lambda^*_p$, the reduced two-group neutron generation time

$$\Lambda^*_{\infty 1} = (v_1 \Sigma_1 \beta k)^{-1} ; \quad \Lambda^*_{\infty 2} = (v_2 \Sigma_2 \beta k)^{-1} , \tag{12}$$

$\Lambda^*_{\infty 1} + \Lambda^*_{\infty 2} = \Lambda^*_\infty$, the reduced two-group neutron generation time for infinite systems.

Using the initial conditions one finds:

$$T_{p1}(0) = - \Lambda^*_{\infty 1} Q_p(0)(1+L^2 B_p^2) / \rho_p ; \quad T_{p2}(0) = - \mathbf{p} \Lambda^*_{\infty 2} Q_p(0) / \rho_p .$$

Substituting this into Eq. 7 results in the expression:

$$\bar{T}_{p2}(s) = -\mathbf{p}\Lambda^*_{\infty 2}[Q_p(0)/\rho_p][\Lambda^*_p + \bar{W}(s) + s^2 k\beta \Lambda^*_{\infty 1}\Lambda^*_{\infty 2}] g_p(s) + \tag{13}$$

$$+ \mathbf{p}\Lambda^*_{\infty 2} Q_p(s) g_p(s).$$

If one uses only one averaged delayed neutron group, the three solutions of the two-group inhour equation $g_p^{-1}(s) = 0$, may be found rather easily to a good degree of approximation. This is done by noting that these solutions describe three different time scales: the very slow decay of delayed neutrons, γ_1, the rapid prompt thermal neutron decay, γ_2, and the extremely rapid decay of the fast prompt neutrons, γ_3. Thus: $\gamma_1 << \gamma_2 << \gamma_3$, then:

$$\gamma_{p1} \cong \lambda\rho_p/(1-\rho_p); \quad \gamma_{p2} \cong -(1-\rho_p)/\Lambda^*_p; \quad \gamma_{p3} \cong -\Lambda^*_p/\beta k \Lambda^*_{\infty 1}\Lambda^*_{\infty 2}. \tag{14}$$

For example, in the DI-1 configuration (A-V) $|\gamma_{o3}| \approx 2 \cdot 10^4 \text{sec}^{-1}$, $\gamma_{o2} \approx -124$ sec^{-1} (for $\rho_o = -10$ $) and $\gamma_{o1} \approx -0{,}063$ sec^{-1} (for $\rho_o = -10$ $). In the SR-1 configuration $\gamma_{o3} \approx -9 \cdot 10^4 \text{sec}^{-1}$, $\gamma_{o2}(\rho_o = -10$ $) $= 1{,}3 \cdot 10^3 \text{sec}^{-1}$, $\gamma_{o1}(\rho_o = -10$ $) \approx -0{,}071$ sec^{-1}.

Conducting measurements at times $t >> 10^{-4}$ sec then permits neglecting the s^2 term in Eq. 13, and this expression, with $\mathbf{p}=1$, reduces to the corresponding expression in a one-energy group model. With $\mathbf{p}=1$, the time integrated thermal density coincides exactly with the corresponding quantity in one group theory.

Appendix III: The normalization of densities in different states.

The problem of consistent normalization is encountered when two neutron densities belonging to two different states of the reactor, e.g. the densities in critical and subcritical states, are compared with one another. A physical procedure, which also maintains mathematical consistency is to normalize both densities to the same weighted total population of chain carriers (i.e. neutrons and precursors). The choice of the weight function depends on the state which is considered as reference state.

If in the reference state the persisting mode prevails, then the appropriate weight function will be the adjoint density vector of this state. This means that one weights the carriers in the perturbed state by the importance of the reference state, in order to get the same total population.

$\vec{n}(x,t)$ is the density vector of the perturbed state in the two-group model:

$$\vec{n}(x,t) = \{n_1(x,t),\ n_2(x,t),\ c_1(x,t),\ \ldots,\ c_\ell(x,t)\}. \tag{1}$$

The reference state, if assumed stable, is characterized by the density vector $\vec{An}(x)$, and the importance vector $\vec{n}^+(x)$:

$$\begin{aligned} \vec{n}(x) &= \{n_1(x),\ n_2(x),\ c_1(x),\ \ldots,\ c_\ell(x)\}, \\ \vec{n}^+(x) &= \{n_1^+(x),\ n_2^+(x),\ c_1^+(x),\ \ldots,\ c_\ell^+(x)\}. \end{aligned} \tag{2}$$

The total weighted population of chain carriers in the perturbed state will therefore be (scalar product is denoted by round brackets and comma),

$$\left(\vec{n}(x,t),\vec{n}^+(x)\right) = \left(n_1(x,t),n_1^+(x)\right) + \left(n_2(x,t),n_2^+(x)\right) + \sum_{i=1}^{\ell}\left(c_i(x,t),c_i^+(x)\right). \tag{3}$$

Taking the Laplace transform of the last equation and using the relations (see Chap-IV):

$$\bar{c}_i(x,s) = \left[\beta_i \nu k\Sigma\ /\ (\lambda_i + s)\right]\bar{n}_2(x,s), \qquad c_i^+(x) = n_1^+(x),$$

one gets:

$$\left(\vec{\bar{n}}(x,s),\vec{n}^+(x)\right) = \left(\bar{n}_1(x,s),n_1^+(x)\right) + \left(\bar{n}_2(x,s),n_2^+(x)\right) + \frac{\bar{W}(s)}{\Lambda^*_{\infty 2}}\left((\bar{n}_2(x,s),n_1^+(x)\right)_c,$$

c - denotes integration on the core alone. (4)

The scalar products are of the same order of magnitude, however $\bar{W}(s)/\Lambda^*_{\infty 2}$ is of order 10^2 (for $t>\gamma_2^{-1}$, A-II) thus the contribution of the precursors to the total population predominates:

$$\left(\vec{\bar{n}}(x,s),\vec{n}^+(x)\right) \cong \left(\bar{n}_2(x,s),n_1^+(x)\right)_c \bar{W}(s) \,/\, \Lambda^*_{\infty 2} \,. \tag{5}$$

Equating this total population to that of the reference reactor determines the normalization factor, A:

$$A \cong \frac{\left(\bar{n}_2(x,s),n_1^+(x)\right)_c}{\left(n_2(x),\, n_1^+(x)\right)_c} \left(\frac{\bar{W}(s)}{\bar{W}(0)}\right) . \tag{6}$$

In normal two-group theory the source consists of fast neutrons due to thermal fissions. Since the importance of a neutron at a certain point in phase space is proportional to the change of the power resulting from the injection of that neutron, the ratio of the products in Eq.6 may be replaced by the ratio of the powers:

$$A \approx \left(\frac{\int \bar{n}_2(x,s)dx}{\int n_2(x)\, dx}\right)_c \left(\frac{\bar{W}(s)}{\bar{W}(0)}\right). \tag{7}$$

Both integrals are extended over the core alone.
From the formal point view the normalization described above is equivalent to the determination of the coefficient of $\vec{n}(x)$ in the expansion of the density vector $\vec{\bar{n}}(x,s)$ in terms of the eigenfunctions of the reference reactor.

In one group theory $n_1(x) = n_2(x) \equiv n(x) = n^+(x)$, thus the exact normalization factor A, in a bare system is:

$$A = \frac{\left(\bar{n}(x,s),n(x)\right)}{\left(n(x)\ ,\ n(x)\right)} \frac{\left[1+\bar{W}(0)\,/\,\Lambda^*\right]}{\left[1+\bar{W}(0)\,/\,\Lambda^*\right]} . \tag{8}$$

In reflected system the last equation is approximately valid (it involves the same approximation as in Eq.6) if the integration extends only on the core volume.

Appendix IV: A bare homogeneous reactor with time dependent sink. One-group treatment.

The time dependent diffusion equations governing this case are:

$$\left[v(D\nabla^2-\Sigma)+vk\Sigma(1-\beta)\right]n(x,t)+\sum_{i=1}^{\ell}\lambda_i c_i(x,t)-\gamma(x,t)n(x,t)=\frac{\partial n(x,t)}{\partial t}, \quad (1)$$

$$v\beta_i k\Sigma n(x,t)-\lambda_i c_i(x,t)=\frac{\partial c_i(x,t)}{\partial t}, \quad (2)$$

with the steady-state as initial condition, and vanishing of the densities at the extrapolated boundaries.

$$\gamma(x,t)=\begin{cases}0 & t<0,\\ \gamma\delta(x-x_0) & t>0\end{cases} \quad (3)$$

(the sink is at the point x_0)

$\gamma(x,t)$ is the number of absorptions per second by the external absorber.

Expanding the densities in terms of the geometrical eigenfunctions and repeating the procedure described in A-I and A-II, one gets for the Laplace-transformed coefficient of the p-th mode:

$$\bar{T}_p(s)g_p^{-1}(s)+\gamma^*\Lambda^* n_p(x_0)F(s)=T_p(0)[\bar{W}(s)+\Lambda^*], \quad (4)$$

where: $\gamma^*=\gamma/\int n_p^2(x)dx$ (independent of the mode in slab geometry),

$F(s)=\sum_q \bar{T}_q(s)n_q(x_0)$ the Laplace transformed density at the sink.

Multiplying Eq.4 by $n_p(x_0)$ and summing on p furnishes an expression for F(s) in terms of known quantities:

$$F(s)=[\Lambda^*+\bar{W}(s)]\frac{\sum_{p=0}^{\infty} g_p(s)T_p(0)n_p(x_0)}{1+\gamma^*\Lambda^*\sum_{p=0}^{\infty} n_p^2(x_0)g_p(s)}. \quad (5)$$

Since the reactor is initially critical $T_0(0)\neq 0$ while $T_p(0)=0$ for $p\geq 1$, therefore:

$$\bar{T}_0(s)=-\gamma^*\Lambda^* n_0(x_0)g_0(s)F(s)+[\Lambda^*+\bar{W}(s)]g_0(s)T_0(0), \quad (6)$$

$$\bar{T}_p(s)=-\gamma^*\Lambda^* n_p(x_0)g_p(s)F(s) \qquad p\geq 1, \quad (7)$$

$$F(s) = [\Lambda^* + \bar{W}(s)] \frac{g_o(s) n_o(x_o) T_o(0)}{1+\gamma^*\Lambda^* \sum_{p=0} n_p^2(x_o) g_p(s)} . \qquad (5a)$$

Substituting $F(s)$ in $\bar{T}_p(s)$, one obtains

$$\bar{T}_o(s) = \frac{T_o(0)[\Lambda^* + \bar{W}(s)][1+\gamma^*\Lambda^* \sum_{p=1} n_p^2(x_o) g_p(s)]}{g_o^{-1}(s)+\gamma^*\Lambda^* n_o^2(x_o)+\gamma^*\Lambda^* g_o^{-1}(s) \sum_{p=1}^{\infty} n_p^2(x_o) g_p(s)} , \qquad (6a)$$

$$\bar{T}_p(s) = \frac{-T_o(0) n_o(x_o)[\Lambda^*+\bar{W}(s)]\gamma^*\Lambda^* n_p(x_o) g_p(s)}{g_o^{-1}(s)+\gamma^*\Lambda^* n_o^2(x_o)+\gamma^*\Lambda^* g_o^{-1}(s) \sum_{p=1}^{\infty} n_p^2(x_o) g_p(s)} , \quad p \geq 1 . \qquad (7a)$$

The time integrated density may be obtained, as before, by letting s tend to zero:

$$\bar{T}_o(s \to 0) = T_o(0)[\Lambda^*+\bar{W}(0)] \frac{1-\gamma^*\Lambda^* \sum_{p=1}^{\infty} n_p^2(x_o)/\rho_p}{\Lambda^*\gamma^* n_o^2(x_o)} , \qquad (8)$$

$$\bar{T}_p(s \to 0) = T_o(0)[\Lambda^*+\bar{W}(0)] \frac{n_p(x_o)/\rho_p}{n_o(x_o)} , \quad p \geq 1 . \qquad (9)$$

Thus:

$$\int_0^{\infty} n(x,t)dt = T_o(0)[\Lambda^*+\bar{W}(0)] \left\{ \frac{1-\gamma^*\Lambda^* \sum_{p=1}^{\infty} n_p^2(x)/\rho_p}{\gamma^*\Lambda^* n_o^2(x_o)} n_o(x) + \right.$$

$$\left. + \frac{\sum_{p=1}^{\infty} n_p(x_o) n_p(x)/\rho_p}{n_o(x_o)} \right\}, \quad p \geq 1 . \qquad (10)$$

The persisting distribution, $n(x,\infty)$ of the reactor with a sink, is established after all higher modes, which are due to the initial conditions, have died out. It can be calculated by making the reactor fictitiously critical, i.e. changing k to k_f, thus:

$$v[D\nabla^2+(k_f-1)\Sigma]n(x,\infty)-\gamma\delta(x-x_o)n(x,\infty) = 0. \qquad (11)$$

Expanding the density as usual in terms of the geometrical eigenfunctions of the system:

$$n(x,\infty) = \sum_{q=0}^{\infty} T_q(\infty) n_q(x),$$

and repeating again the procedure of isolating the coefficient of expansion $T_q(\infty)$ and the density at the sink, $F(\infty) = n(x_0,\infty)$ leads to the following expressions:

$$\gamma^* = \left\{\Lambda^* \sum_{p=0}^{\infty} n_p^2(x_0)/\rho_p\right\}^{-1}, \tag{12}$$

and

$$\frac{n(x,\infty)}{F(\infty)} = \gamma^*\Lambda^* \sum_{p=0}^{\infty} n_p(x_0)n_p(x)/\rho_p. \tag{13}$$

In slab geometry:

$$-\frac{\rho_p}{\Lambda^*} = \frac{1}{B_1^2 vD}\,\frac{1}{p^2 - B_f^2/B_1^2},$$

where:

$$B_f^2 = \frac{k_f - 1}{M^2}, \qquad B_1^2 = (\pi/d)^2,$$

$$n_p(x) = \sin pB_1 x.$$

The sums which appear in Eqs. 12 and 13 are of the form of Eq. A-I-13, which leads to:

$$\gamma^* = -(2vDB_f/d)\sin B_f d \;/\; \sin B_f x_0 \sin B_f(d-x_0), \tag{14}$$

$$\frac{n(x,\infty)}{n(x_0,\infty)} = \frac{\gamma^* d}{4vDB_f}\left\{\sin B_f|x-x_0| - \sin B_f(x+x_0) + \right.$$
$$\left. - 2\cot B_f d \sin B_f x_0 \sin B_f x\right\}. \tag{15}$$

The sums which appear in Eq. 10 are of the form

$$\sum_{p=1}^{\infty} \frac{n_p(x_0)n_p(x)}{\rho_p} = -\frac{1}{\Lambda^*}\left\{-\frac{1}{B_1 vD}\sum_{p=2}^{\infty}\frac{\sin pB_1 x_0 \sin pB_1 x}{p^2-1}\right\}, \tag{16}$$

since in the real reactor $B = B_1 = \pi/d$.

From Eq. 13 one finds:

$$\sum_{p=2}^{\infty} \frac{\sin pB_1 x_0 \sin pB_1 x}{p^2-1} = \lim_{B\to B_1} \frac{d\cdot B_1^2}{4B}\left\{\sin B(x+x_0)-\sin B|x-x_0|\right\} +$$

$$- \lim_{B\to B_1}\left\{\frac{d\cdot B_1^2}{2B}\cot B d \sin Bx_0 \sin Bx + \right.$$

$$\left. + \frac{\sin B_1 x_0 \sin B_1 x}{1-B^2/B_1^2}\right\} \qquad (17)$$

$$= \frac{\pi}{4}\left\{\sin B_1(x+x_0)-\sin B_1|x-x_0| + \right.$$

$$\left. - \frac{2x}{d}\sin B_1 x_0 \cos B_1 x - \frac{2x}{d}\sin B_1 x \cos B_1 x_0\right\},$$

and

$$\sum_{p=2}^{\infty} \frac{\sin^2 pB_1 x_0}{p^2-1} = \frac{\pi}{4}\sin 2B_1 x_0\left[1-\frac{2x_0}{d}\right]. \qquad (18)$$

Assembling all expressions one gets the following equation for the time integrated density in the R.D. experiment:

$$\int_0^{\infty} n(x,t)dt = T_0(0)\left[1+\frac{\bar{W}(0)}{\Lambda^*}\right]\frac{\pi}{4\nu D B_1^2}\frac{1}{\sin^2 B_1 x_0}\left\{\left[\frac{4\nu D B_1^2}{\pi\gamma^*} + \right.\right.$$

$$+ \sin 2B_1 x_0\left(1-\frac{2x_0}{d}\right)\left]\sin B_1 x - \sin B_1 x_0\right[\sin B_1(x+x_0) +$$

$$- \sin B_1|x-x_0| - 2(x/d)\sin B_1 x_0 \cos B_1 x -$$

$$\left.\left. - 2(x_0/d)\cos B_1 x_0 \sin B_1 x\right]\right\}. \qquad (19)$$

Appendix V: Various DI-configurations (typical heavy water reactor)

DI-1: Critical axial buckling: $1.470161 \cdot 10^{-4}\,cm^{-2}$;
critical $k_\infty = 1.100567$

Radial-parameters (two groups):

zone	outer-radius cm	τ cm^2	L^2 cm^2	p	D_1 cm	D_2 cm
C-ref	187.0	370.0	2025.0	1.0	0.9733	0.8433
Al-tank	114.4	5000.0	300.0	1.0	3.59	3.59
D_2O-ref	114.0	129.1	4582.44	1.0	1.256975	0.845405
core	111.03251	130.50	113.28	0.908152	1.243930	0.835380

Delayed-neutron parameters:

i	1	2	3	4	5	6
λ_i sec^{-1}	3.164	1.183	$3.069 \cdot 10^{-1}$	$2.773 \cdot 10^{-1}$	$1.136 \cdot 10^{-1}$	$3.062 \cdot 10^{-2}$
β_i eff $\cdot 10^{-4}$	3.176	8.846	27.331	2.389	13.316	14.538

i	7	8	9	10
λ_i sec^{-1}	$1.691 \cdot 10^{-2}$	$1.247 \cdot 10^{-2}$	$4.814 \cdot 10^{-3}$	$1.5 \cdot 10^{-3}$
β_i eff $\cdot 10^{-4}$	0.748	2.127	0.256	0.123

$$\sum_{i=1}^{10} \beta_i \text{ eff} = \beta_{eff} = 7.285 \cdot 10^{-3}.$$

$v_1 = 1.833 \cdot 10^6$ cm/sec; $v_2 = 2.2 \cdot 10^5$ cm/sec.

DI-2: Critical axial buckling: $3.6 \cdot 10^{-4}\,cm^{-2}$; critical
$k_\infty = 1.159399$.
The other parameters are as in DI-1.

DI-3: Critical axial buckling: $3.87837 \cdot 10^{-4}\,cm^{-2}$,
critical $k_\infty = 1.2016$.

Radial parameters (two groups):

zone	outer-radius cm	τ cm^2	L^2 cm^2	p	D_1 cm	D_2 cm
D_2O-ref.	187.0	129.1	4582.44	1.0	1.25697	0.845405
core	79.72915	130.5	113.28	0.908152	1.24393	0.835380

The delayed neutron parameters are those of DI-1.

DI-4: This configuration is - 3.23% subcritical, which is achieved by introducing a central control rod of 5 cm radius into the critical configuration DI-3.

The control rod is treated as a non-multiplicative zone, and its absorbing properties are taken into account by special boundary conditions at the rod surface. They give the effective distance $d = n\,(C.R.) \,/\, n'(C.R.)$ from the control rod surface to the point inside the rod where the density virtually vanishes. This boundary condition enables one to use diffusion theory for deriving the neutron density beyond a distance of about a transport mean free path from the control rod (e.g. ref. 86).

In the DI-4:

$d_1 = 10^3$ cm, the control rod has almost no effect on the fast neutrons except through the absence of production and moderation in it (from r = 0 to r = 5 cm),

$d_2 = 2.107$ cm.

The insertion of the control rod introduces a static negative reactivity of 3.23% or 4.43 $.

Examples of w for delayed iterations:

$\rho_o = -4.43$ $.

The fastest delayed eigenvalue of the zeroth main mode - $w_{o.1}$

$k^{(o)} = 1.24041223$; $w_1^{(o)} = -\lambda_1 = -3.164\ sec^{-1} \rightarrow k^{(1)} = 1.23711345 \rightarrow$
$\rightarrow w_1^{(1)} = -3.13759216\ sec^{-1} \rightarrow k^{(2)} = 1.23714106 - w_1^{(2)} =$
$= -3.13761564\ sec^{-1} \equiv w_{o.1}$
$\rightarrow k^{(3)} = 1.237141102.$

The fourth delayed eigenvalue - $w_{o.4}$

$k^{(o)} = 1.24041223$; $w_4^{(o)} = -\lambda_4 = -0.2773\ sec^{-1} \rightarrow k^{(1)} = 1.24012383 \rightarrow$
$\rightarrow w_4^{(1)} = -0.271247517\ sec^{-1} \rightarrow k^{(2)} = 1.24013013 \rightarrow w_4^{(2)} =$
$= -0.273110109\ sec^{-1} \equiv w_{o.4}$
$\rightarrow k^{(3)} = 1.24012830.$

Comparison of one group inhour solutions (ref. 78 with $\Lambda^* = 0.1$ sec) with kinetic solutions for the zeroth main mode (10 groups of delayed neutrons in a heavy water reactor, ref. 80).

$\rho = -3.23$ % .

i	1	2	3	4	5
λ_i sec^{-1}	3.164	1.183	$3.069 \cdot 10^{-1}$	$2.773 \cdot 10^{-1}$	$1.136 \cdot 10^{-1}$
w_{inhour} sec^{-1}	3.13793	1.15672	$2.8835 \cdot 10^{-1}$	$2.7281 \cdot 10^{-1}$	$1.0921 \cdot 10^{-1}$
$w_{\text{two groups}}$ sec^{-1}	3.13762			2.7125	

i	6	7	8	9	10
λ_i sec^{-1}	$3.062 \cdot 10^{-2}$	$1.691 \cdot 10^{-2}$	$1.247 \cdot 10^{-2}$	$4.814 \cdot 10^{-3}$	$1.5 \cdot 10^{-3}$
w_{inhour} sec^{-1}	$2.9301 \cdot 10^{-2}$	$1.6870 \cdot 10^{-2}$	$1.2385 \cdot 10^{-2}$	$4.8102 \cdot 10^{-3}$	$1.4994 \cdot 10^{-3}$
$w_{\text{two groups}}$ sec^{-1}	$2.9302 \cdot 10^{-2}$				

Results of iteration for higher main modes:

First main mode:

$\rho_1 = -103.663$ ¢ $\quad w_{1.1} = -3.16268$ sec^{-1} $\quad w_{1.6} = -3.05611 \cdot 10^{-2}$ sec^{-1}

$(w_{1.p})_2 = -278.240$ sec^{-1} .

Second main mode:

$\rho_2 = -393.313$ ¢ $\quad w_{2.1} = -3.16365$ sec^{-1} $\quad w_{2.6} = -3.06045 \cdot 10^{-2}$ sec^{-1}

$(w_{2.p})_2 = -583.764$ sec^{-1} .

Appendix VI: Various SR-configurations (typical light water reactor).

SR-1: critical axial buckling: $2.055101 \cdot 10^{-3}\,cm^{-2}$; $k_\infty = 1.60708$.
Radial-parameters (two groups)

zone	outer-radius cm	τ cm^2	L^2 cm^2	p	D_1 cm	D_2 cm
H_2O ref.	∞	31.40	8.13	1.0	1.111	0.1585
core	18.659	56.60	2.64	0.9651	1.232	0.2438

Delayed neutron parameters (ref. 87)

i	1	2	3	4	5	6
λ_i sec^{-1}	3.87	1.40	$3.110 \cdot 10^{-1}$	$1.155 \cdot 10^{-1}$	$3.170 \cdot 10^{-2}$	$1.27 \cdot 10^{-2}$
β_i $_{eff}$ $^{-10^{-4}}$	2.080	10.240	32.560	15.040	17.040	3.04

$$\sum_{i=1}^{6} \beta_i \text{ eff} = \beta_{eff} = 8.0 \cdot 10^{-3}$$

$v_1 = 1.833 \cdot 10^{6}$ cm/sec; $v_2 = 2.2 \cdot 10^{5}$ cm/sec.

SR-1* has the same parameters as SR-1, except for the reflector, which has a finite outer radius of 40 cm. This configuration is made about -4% subcritical by reducing the core radius to 17.11 cm.

SR-2: critical axial buckling: $2.055101 \cdot 10^{-3}\,cm^{-2}$ critical $k_\infty = 1.539213$
Radial Parameters (two groups)

zone	outer-radius cm	τ cm^2	L^2 cm^2	p	D_1 cm	D_2 cm
H_2O ref.	∞	31.40	8.13	1.0	1.111	0.1585
core	22.2601	56.50	2.64	0.96510	1.232	0.2438
H_2O ref.	4.27	31.40	8.13	1.0	1.111	0.1585

The delayed neutron parameters are those of SR-1.

Radial parameters (two groups)

zone	outer-radius cm	τ cm^2	L^2 cm^2	p	D_1 cm	D_2 cm
H_2O ref.	∞	31.40	8.13	1.0	1.111	0.1585
C-ref.	23.988	345.00	2809.0	1.0	1.125	0.816
core	15.988	56.50	2.64	0.9651	1.232	0.2438

The delayed neutron parameters are those of SR-1.

REFERENCES

1) P. Liewers
Reaktivitätsmessungen - Probleme, Methoden und Anwendungsmöglichkeiten.
Kernenergie, 4, 593-518, (8/61).

2) E.G. Silver and K.M. Henry, Jr.
Bulk Shielding Reactor II: Status report, including SPERT tests.
ORNL-3016 (9.1960).

3) H.W. Glauner and M. Küchle
Reaktivitätsmessungen am FR-2.
Private communication.

4) M. Bernardine et al.
Experiments and Calculation on a D_2O 20% Enriched Reactor.
CNEN-100 (11.1961).

5) D.H. Shaftman
Zero-Power Experiments on the Argonne Low Power Reactor (ALPR).
ANL-6078 (5.1961).

6) G.R. Hopkins and C.P. Jamieson
Techniques of Reactivity Measurements.
WAPD-BT-8, 90-103, (6.1958).

7) P.F. Gast
Experimental Checks of Control Rod Theory.
Proc. 1st Geneva Conf., 5, (389-392), (1956).

8) Martin Co. - Nuclear Div.
Nuclear Studies on the MPR Zero Test Core.
MND-MPR-1646 (12.1958).

9) J. Bernot and V. Raievski
Mesure des réactivités dans une pile.
CEA-Report No.310 (1954).

10) R.M. Absalom et al.
A Report of the First Loading of Zenith.
AEEW-R 50 (12.1960).

11) Reactor Physics Constants
ANL-5800 (1.7.1958).

12) E. Fast and D.A. Millsap
Calibration of RMF Control Elements.
IDO-16610: Pt.1 (1957), Pt.2 (1959), Pt.3 (1959).

13) G. Röbert
Eine Kalibrierung der Regelstäbe des Forschungsreaktors Geesthacht.
Kerntechnik, 1, 140-145, (1959).

14) B.J. Toppel
Sources of Error in Reactivity Determination by Means of Asymptotic Period Measurement.
Nucl.Sci.Engn.5, 88-98 (1959).

15) C.E. Cohn
Errors in Reactivity Measurements due to Photoneutron Effects.
Nucl.Sci.Engn.6, 284-287 (1959).

16) B.S. Finn
Relationships between Reactivity Changes, Buckling Changes and Periods in Heavy Water Reactor.
Nucl.Sci.Engn.7, 396-397 (1960).

17) V. Raievski and B. Lerouge - Editors
Etude experimentale de la pile EL 3.
CEA-Report No.794 (1958).

18) V. Raievski
Etude de transport des neutrons par la méthode de modulation.
CEA-Report no.1095 (1959).

19) H. Winkler et al.
Transfer Function Measurements with SAPHIR.
To be published.

20) F.J. Jankowski, D. Klein and T.M. Miller
Calibration of Control Rods.
Nucl.Sci.Engn.2, 288-302 (1957).

21) M.N. John
The Response of the Reactor Kinetic Equations to Square Wave Oscillations of Reactivity.
AEEW-M 193 (1.1962).

22) H.D. Brown and W.E. Loewe
Analysis of Reactor Oscillation for Coefficients of Reactivity.
Nucl.Sci.Engn.5, 376-381 (1959).

23) C.A. Sastre
The Measurements of Reactivity.
Nucl.Sci.Engn.8, 443-447 (1960).

24) F. Schroeder - Editor
Quarterly Technical Report, SPERT Project.
IDO-16640 (4.1961).

25) T.F. Wimett et al.
Godiva II - An Unmoderated Pulse-Irradiation Reactor.
Nucl.Sci.Engn.8, 691-708 (1960).

26) G.S. Brunson et al.
Measuring the Prompt Period of a Reactor.
Nucleonics 15, 132-141 (11.1957).

27) J. Bengston et al.
Determination of Prompt Neutron Constants of Multiplying Systems.
Proc. 2nd Geneva Conf. A/Conf. 15/P/1783. (1958).

28) Experiments on Zenith Reactor
Dragon Project, private communication.

29) P. Schmid
Absolute Reactivity Measurement from the Transient Behavior of a Subcritical Nuclear Reactor.
RAG-Report No.1 (6.1957).

30) K.H. Beckurts
Reactor Physics Research with Pulsed Neutron Source.
Nucl.Ins.Methods, 11, 144-168 (1961).

31) E.E. Carroll, Jr., N. Hartmann and D. Klein
Pulsed Neutron Measurements in Subcritical Lattices.
WAPD-R(D)-7 (4.1961).

32) D.R. Bach et al.
Prompt Neutron Decay Constants in Multiplying Hydrogenous Media.
Nucl.Sci.Engn. 11, 199-210 (1961).

33) A.M. Weinberg and E.P. Wigner
The Physical Theory of Neutron Chain Reactors.
The University of Chicago Press, (1958).

34) M. Ash
Solutions of the Reactor Kinetics Equations for Time Varying Functions.
Jour. of App. Phys. 27, 9 (1956).

35) P. Schmid
Basic Integral Equation of Reactor Kinetics.
Proc. 2nd Geneva Conf., 11, 277-288 (1958).

36) W.S. Hogan
Negative Reactivity Measurement.
Nucl.Sci.Engn. 8, 518-522 (1960).

37) E.A. Burrill and M.H. MacGregor
Using Accelerator Neutrons.
Nucleonics 18, 12 (1960).

38) W. Francioni
Konstruktion, Einbau und Bedienung der Langsamen Sprungquelle.
Internal E.I.R.-Report (1960).

39) T. Gozani et al.
Reactivity Measurement in Subcritical Nuclear Reactors by Means of Source Step Techniques.
RAG-Report No.17 (1960).

40) P. Schmid and H. Winkler
Experimentelle Untersuchungen am SAPHIR zur Entwicklung der Reaktivitätsmessung durch Stabfall.
Internal E.I.R.-Report (1960).

41) J. Patry
La détermination numérique du comportement dynamique d'une pile à l'aide d'une calculatrice électronique.
Codes for Reactor Computations - Inter. Atomic Energy Agency, Vienna (1961).

42) W. Hage and I.R. Cameron
An Iterative Solution of the Reactor Kinetic Equation for the Rod-Drop and Source-Jerk Experiments.
Dragon-Project Report No.39 also Nucleonik 3,2,76-80 (1961).

43) T. Gozani and P. Schmid
Anpassung der "Shape"-Methode an Stabfall-Experimente zur Messung der Reaktivität von Unterkritischen Zuständen.
Internal E.I.R.-Report (1960).

44) Th. Auerbach
Multigroup Treatment of Complex Reactors.
Internal E.I.R.-Report (1960);
Control Rod Theory Pt.1.
Internal E.I.R. Report (1962).

45) B. Davison
Neutron Transport Theory.
Oxford at the Clarendon Press (1957).

46) R.V. Meghreblian and D.K. Holmes
Reactor Analysis.
McGraw-Hill Book Company Inc. (1960).

47) G. Birkhoff and R.S. Varga
Reactor Criticality and Non-Negative Matrices.
WAPD-166 (1957).

48) G. Birkoff and E.P. Wigner - Editors
a) G. Birkoff
Positivity and Criticality
b) G.J. Habetler and M.A. Martino
Existence Theorems and Spectral Theory for the Multigroup Diffusion Model.
Proc. of Symposia in Applied Mathematics - Nuclear Reactor Theory.
American Mathematical Society (1961).

49) B. Davison
Simplified Derivation of the Spherical Harmonics Moments for Cylindrical and other Geometries.
AECL-1068 (1959).

50) K. Zumbrunn
Derivation of Time Dependent Adjoint Transport Equation.
Unpublished (1961).

51) E.R. Cohen
Some Topics in Reactor Kinetics.
Proc. 2nd Geneva Conf. A/Conf.15/P/629 (1958).

52) J. Lewins
The Time Dependent Importance of Neutrons and Precursors.
Nucl.Sci.Engn.7, 268-274 (1960).

53) J. Lewins
Variational Representations in Reactor Physics Derived from a Physical Principle.
Nucl.Sci.Engn. 8, 95-104 (1960).

54) J. Lewins
A.Derivation of the Time-Dependent Adjoint Equations for Neutron Importance in the Transport, Continous Slowing-Down and Diffusion Models.
J. Nucl. Energy. Part A. 13, 1-5 (1960).

55) J. Lewins
The Use of Generation Time in Reactor Kinetics.
Nucl. Sci. Engn. 7, 122 (1960).

56) A.F. Henry
Computation of Parameters Appearing in the Reactor Kinetics Equation.
WAPD-142 (Navy) (1955).

57) A.F. Henry
The Application of Reactor Kinetics to Analysis of Experiments.
Nucl. Sci. Engn. 3, 52-70 (1958).

58) E.E. Gross and J.H. Marable
Static and Dynamic Multiplication Factors and their Relation to Inhour Equation.
Nucl.Sci.Engn. 7, 281-291 (1960).

59) S. Glasstone and M.C. Edlund
The Elements of Nuclear Reactor Theory.
Van Nostrand, Princeton, N.J. (1957).

60) J. Lewins
The Reduction of the Time Dependent Equations for Nuclear Reactors to a Set of Ordinary Differential Equations.
Nucl. Sci. Engn. 9, 399-407 (1961).

61) L. Schiff
Quantum Mechanics.
McGraw Hill Book Co. N.Y. (2nd Ed. 1955).

62) P.M. Morse and H. Feshbach
Methods of Theoretical Physics
McGraw Hill Book Co. N.Y. (1953).

63) E. Blue and J.W. Zink
Perturbation Theory and Reactor Analysis.
NAA-SR-4351 (1959).

64) L.H. Holway
Perturbation Methods for Reactor Diffusion Equations.
Nucl. Sci. Engn. 6, 191-201 (1959).

65) A.Foderaro and H.L. Garabedian
A New Method for Solution of Group-Diffusion Equations.
Nucl.Sci.Engn. 8, 44-52 (1959).

66) K. Zumbrunn
Der RIFIFI Code.
Internal E.I.R.-Report (1961).

67) K. Zumbrunn
Bedienungsanleitung für das Programm RIFIFI.
Internal E.I.R.-Report (1961).

68) R.L. Murray
Nuclear Reactor Physics.
Prentice-Hall Inc. (1957).

69) S. Kaplan and A.F. Henry
An Experiment to Measure Effective Delayed Neutron Fractions.
WAPD-TM-209 (12.1960).

70) J.D. Kington, R. Perez-Belles and G. de Saussure.
The Measurement of the Effective Delayed-Neutron Fraction for the Bulk Shielding Reactor I.
ORNL-3016, (12.1960).

71) H. Sandmeier
Multigroup Calculations of Effective Neutron Fraction β_{eff}. Prompt Neutron Lifetime l_p etc.
ANL-6423 (1961).

72) D.H. Frederich et al.
A PI and SN Theory Code for Static and Dynamic Synthesis of Two Dimensional Flux and Reactivity.
Trans. ANS 4, No.1 (6.1961).

73) D.C. Kolar and F.A. Kloverstrom
Pulsed Neutron Measurement of Control Rod Worths.
Nucl.Sci.Engn. 10, 45-52 (1961).

74) G. De Saussure, K. Henry and Perez-Belles
Reactivity Worth of the Central Fuel Element in the Bulk Shielding Reactor I.
Nucl.Sci.Engn. 9, 291-298 (1961).

75) F. Holzer and M. Crouch
Interpretation of Thermal Neutron Mean Lifetime Experiments.
Nucl.Sci.Engn. 6, 545-553 (1959).

76) C.J. Emert and S. Milani
Modified Rod-Drop Experiments.
WAPD-T-989 (1959).

77) H.I. Garabedian
Determination of Shutdown with the Aid of a Source.
WAPD-RM-207 (1953).

78) J. Patry
AGAMA and GFUNK
Internal E.I.R.-Report (3.1961).

79) W. Zünti
Reaktivitätsmessungen am Stationären Reaktor. Korrekturen wegen der verzögerten Neutronen.
Internal E.I.R.-Report (1.1962).

80) R. Meier
Daten der verzögerten und Photoneutronen-Gruppen für DIORIT.
Internal E.I.R.-Report (6.1961).

81) W. Francioni
Die schnelle Sprungquelle.
Unpublished.

82) T. Gozani
Reactivity Measurements by the Step-Source Technique in the 132-Core of DIORIT.
Internal E.I.R.-Report (11.1960)

83) H. Albers
Startexperimente DIORIT.
Unpublished (1960).

84) J. Patry
DYNAU Programm
Internal E.I.R.-Report (3.1961).

85) I.M. Ryshik and I.S. Gradstein
Tables of Series, Products and Integrals.
Deutscher Verlag der Wissenschaften, Berlin (1957).

86) C.D. McKay
The Extrapolation Length of Black and Gray Cylinders in a Purely Scattering Medium.
NEI-143 (1960).

87) P. Schmid
Vergleich der alten und neuen Gruppenparameter verzögerter Neutronen.
Internal E.I.R.-Report (3.1960).

ACKNOWLEDGEMENTS

I would like to express my deep gratitude to the people of the Eidg. Institut für Reaktorforschung for the kind hospitality granted to me during my stay here.

Especially I am indebted to the director of the institute Dr.W.Zünti, to Prof.W.Hälg, Dr.H.Albers, Dr.T.Auerbach, Dr.T. Hürlimann, Dr.R.Meier, Dr.P.Schmid, Mr.H.Winkler and to Mr.K.Zumbrunn.

In carrying out the experimental part of the work, the personnel of SAPHIR played a desicive role, in particular Dr.Th.Hürlimann and Mr.H.Winkler. I should like to express my gratitude to them for their kind help.

Thanks are due to the computing center, and especially to Dr.J. Patry, for many numerical calculations done on my behalf.

Special thanks are due to Mr.K.Zumbrunn for many helpful discussions and in particular for modifying the RIFIFI program to include kinetic iteration and for using it in a series of computations.

My sincere thanks are due to Dr.T.Auerbach for his permanent readiness to discuss problems concerning the work and related subjects. In particular I should like to thank him for showing me his control rod calculations and above all for critically reading the manuscript.

I am deeply indebted to Dr.P.Schmid. His friendly guidance and cooperation from the very first were a source of scientific inspiration. This work would not have cometo a conclusion without his close attention to its development and his readiness to help in the scientific and administrative areas.

I am very grateful to Miss Regolati for undertaking the tedious job of typewriting the work, and for her excellent accomplishment.

Finally, I should like to thank the Israel Atomic Energy Commission for enabling me to carry out this work.